

The Control of Chaos

by

C M Bird

1996

This Thesis is Submitted for the Degree of
Doctor of Philosophy
at the University of Surrey

Department of Mathematical
and Computing Sciences,
Guildford,
Surrey,
GU2 5XH.

Abstract

The complicated behaviours seen in chaotic dynamical systems can be tamed in extremely subtle ways. The application of miniscule bounded parameter perturbations can transform chaos into order, provided those perturbations are appropriately chosen. Many methods have been derived to control chaotic behaviour in a wide range of systems. Moreover, they often require no knowledge of the underlying dynamical equations describing the system. A simple estimate of the dynamics at particular points on the chaotic attractor suffices in order to effect control.

In this thesis a well known method for the control of chaos is reviewed and its convergence properties analysed. From this analysis, several more powerful methods are proposed. Robust methods are considered which are less sensitive to errors in the estimation of system dynamics and in the presence of noise.

Before systems can be brought under control a chaotic transient is observed. The length of this transient depends sensitively upon initial conditions and on the size of the permitted maximum perturbation. By extending the region within which parameter perturbations can be activated, transient times can be reduced. The adverse effects of noise can also be combatted. Targeting, that is, rapidly changing the state of a system from a given initial condition to some desired state, can also reduce transient times. Both of these avenues for the reduction of transient times are explored here.

Synchronising the dynamics of two independent chaotic oscillators can often be achieved by coupling the systems in a particular way. If the coupling is not strong enough, synchronised behaviour will not result. In such a case, it is shown that control methods can be used to induce a synchronous behaviour in systems and to maintain synchronous behaviour as desired.

Acknowledgements

Firstly and foremostly I am indebted to my Supervisor Dr. P. J. Aston for suggesting the topic for my research and for the guidance he gave me. Without his help and encouragement I would have never completed my thesis.

I would like to thank the staff of the Department of Mathematical and Computing Sciences who have helped and supported me throughout my stay there.

Thanks also go to Dr. D. A. Agg of Smith System Engineering, Guildford, for without him, the topic of controlling chaos may not have been brought to my attention.

Finally, I would like to express my gratitude to my Mum and Dad for their advice and stalwart support.

Contents

0	Introduction	10
0.1	Background	12
0.2	Preliminaries	14
0.3	The Eradication of Chaotic Behaviour	16
0.3.1	Simple Methods for Taming Chaos	17
0.3.2	The OGY Method	20
0.3.3	Calculation of \mathbf{x}^* , M and \mathbf{w}	23
0.3.4	Continuous Systems and Time Delays	27
0.3.5	Higher Period Orbits	30
0.3.6	Higher Dimensional Systems	31
1	Controlling Chaos – Rates of Convergence	33
1.1	Convergence Analysis of the OGY Method	33
1.2	Related methods	35
1.2.1	The Shortest Distance Method	35

1.2.2	Reducing the Spectral Radius of J	37
1.2.3	Quadratic Methods	44
1.3	Higher Dimensional Systems	46
1.4	Numerical Example	49
2	Robust Methods and Tolerance	54
2.1	Robust Methods	55
2.1.1	Inaccuracies in \mathbf{x}^*	56
2.1.2	Inaccuracies in \mathbf{w}	60
2.1.3	Inaccuracies in M	62
2.2	Tolerance	64
2.2.1	The OGY Method	65
2.2.2	The Zero Spectral Radius Method	80
2.3	Numerical Example	85
3	Basins of Attraction	90
3.1	Extending the Basin of Attraction	91
3.1.1	The OGY Method	91
3.1.2	The General Result	97
3.1.3	Immediate Basin of Attraction for the ZSR Method	99

3.2	Capping The Basin of Attraction	101
3.2.1	The OGY Criterion	102
3.2.2	Basin of Attraction for the One-dimensional Map	102
3.2.3	Curvature of the Stable Manifold	105
3.2.4	Choosing a Basin of Attraction	106
3.3	The Time Until Control is Achieved	109
3.4	Numerical Example	113
4	Targeting	116
4.1	Targeting in Systems Where \mathbf{F} is Known	117
4.2	Targeting in Systems With \mathbf{F} Unknown	119
4.3	The Effect of Noise	122
4.4	Numerical Example	125
5	Synchronisation	128
5.1	Coupled One-dimensional Systems	132
5.1.1	Simultaneously Perturbing Both Equations	133
5.1.2	Perturbing One Equation	139
5.2	Higher Dimensional Systems	141
5.2.1	Iterated Maps	142

5.2.2 Continuous Time Systems 147

5.2.3 Calculating the Required Quantities 149

5.3 Numerical Example 150

5.4 Summary 154

List of Figures

0.1	Effect of the OGY control algorithm when parameter perturbations are activated at the n th step. The dashed line indicates the direction parallel to \mathbf{w}	23
0.2	Iterates approach the fixed point approximately along the stable manifold and then get pushed away again roughly in the direction of the unstable manifold.	24
1.1	$\mathbf{x}_{n+1}(p_n)$ is placed as close to \mathbf{x}^* as possible in a linear sense.	36
1.2	The linear approximation for λ_ρ plotted against ϵ for (a) $d_l < 0$ and (b) $d_l > 0$	39
1.3	The Hénon attractor at the parameter values $A = 1.4$ and $B = 0.3$. A saddle fixed point of the mapping lies at $\mathbf{x}^{*T} = (0.631354, 0.189806)$	49
1.4	The fixed point is at the centre of an ensemble of 136 evenly spaced initial conditions within an distance of 0.1 of \mathbf{x}^* . Also shown here are the linearised stable and unstable manifolds of \mathbf{x}^* . The vector \mathbf{w} lies parallel to the x -axis.	51
1.5	Small scale structure of the Hénon map (a) in the absence of noise, and (b) with noise distributed as $\text{Normal}(0, 1.8 \times 10^{-7})$	53

1.6	The Hénon map proves impossible to fully control in the presence of small amplitude noise with the OGY method. Only ‘windows’ of controlled behaviour are observed.	53
2.1	A family of fixed points of the Hénon map created using different forms for the projection P	60
2.2	Plot of $f(\alpha) = \left \frac{\alpha}{\alpha-1} \right $	69
2.3	Possible bifurcations and stabilities for (a) $\lambda_u < 0$ and (b) $\lambda_u > 0$. .	74
2.4	Bifurcation diagram for $\ \mathbf{x}\ $	75
2.5	Bifurcation diagram for δp	75
3.1	The region suitable for control activation.	92
3.2	Example of an extended basin of attraction. The circle centred at \mathbf{x}^* denotes the region within which the linear dynamics are valid. The regions B_{n+1} are mapped into the regions B_n when parameter perturbations are set to their maximum value.	97
3.3	Example of a typical immediate basin of attraction for the ZSR method.	101
3.4	Spurious fixed points created when implementing a fully extended basin of attraction. In this case, λ_u and ξ are of opposite sign and $\eta > 0$	107
3.5	Situations where the local stable manifold leaves the strip (a) along its width and (b) along its length.	108
3.6	The actual basin of attraction for the OGY method with $\delta p_{\max} = 0.05$ applied to the Hénon map.	114

4.1	Targeting in the Hénon map with added noise.	126
4.2	Switching between controlled states without (left) and with (right) the targeting process.	127
5.1	Schematic representation of the coupling of the \mathbf{Y} , \mathbf{Z} and \mathbf{Z}' sub- systems of the Pecora and Carroll method.	131
5.2	Schematic representation of the coupling between the \mathbf{x} and \mathbf{y} sys- tems considered by Yamada and Fujisaka.	131
5.3	The stuck on attractor of Ashwin.	135
5.4	Keeping the x -coordinate fixed in the vicinity of the fixed point where $\mathbf{x}_k = \mathbf{x}_k(p^*)$ and $\mathbf{x}'_k = \mathbf{x}_k(p^* + \delta p_{k-1})$	138
5.5	The average distance iterates spend from the synchronous subspace for a pair of coupled Duffing oscillators with $K_1 = K_2 = 0.1$, $A = 0.3$ and $\omega = 0.2$	150
5.6	Poincaré section of the coupled Duffing system where $K_1 = K_2 =$ 0.1 , $A = 0.3$, $\omega = 0.2$ and $c = 0.68$	151
5.7	A projection of the dynamics in the invariant subspace when a pe- riodic point with two stable directions is stabilised.	152
5.8	A projection of the transverse dynamics when control is repeatedly applied.	153
5.9	Poincaré section of the coupled Duffing system where $K_1 = K_2 =$ 0.5 , $A = 2.5$, $\omega = 2.6$ and $c = 0.13$	154
5.10	Projection of the controlled transverse dynamics for a periodic point possessing two stable directions.	155

5.11 The corresponding chaotic dynamics within the invariant subspace. 156

Chapter 0

Introduction

The existence of chaotic dynamics has been widely appreciated for quite some time now. One could say that chaos was brought to the attention of the scientific world by the work of Lorenz in the early 1960's. But even as far back as the 1900's, Poincaré observed an apparently random behaviour whilst studying the familiar three body problem of celestial mechanics. We now know that he observed not random behaviour, but rather chaos, the antithesis of order. One of the hallmarks of chaos is the notion of sensitivity to small perturbations, often referred to as the 'butterfly effect'. Traditionally, this has been seen as a very troublesome property. Two solutions of a system, initially very close together, diverge exponentially with time until they become totally uncorrelated. Indeed, long term predictability of a system exhibiting the butterfly effect proves highly intractable.

During the mid 1980's NASA scientists projected the ISEE-3/ICE spacecraft in excess of fifty million miles across the solar system using only tiny amounts of fuel [20, 21, 42, 43]. A remarkable feat one might affirm, but totally attributable to the butterfly effect. Such an achievement would not have been possible in a system that was not chaotic, but the solar system, like many physical systems, is chaotic. This kind of behaviour may lead one to believe that a system exhibiting

sensitivity to small perturbations, rather than being troublesome, is actually quite the opposite. Indeed, much research over the past five to ten years has strengthened this view beyond doubt.

In 1991, Ott, Grebogi and Yorke [53] demonstrated that one can select and observe a particular behaviour from amongst a rich lore of behaviours, some simple, some much more complex, occurring naturally within chaotic systems. By the application of small, discerningly chosen perturbations in an available system parameter, system dynamics can be made to follow that particular behaviour. Their method is now very well known and is referred to as the OGY method in the literature. Perhaps most importantly, one should note that without the presence of chaos this would not be possible. Shinbrot *et al.* [69, 70, 71, 72] exploit the butterfly effect in their method for ‘targeting’ in chaotic systems, that is, changing the state of a system from a given initial state to some desired target state in a very efficient manner. This is also achieved via the application of carefully chosen parameter perturbations.

So it seems as though the presence of chaos is not only useful, but can actually prove invaluable. This, united with the ability to tune an available system parameter, is the starting point for this thesis. We shall review some of the more prominent methods proposed for the control and suppression of chaos shortly and then in Chapter 1 propose other, more efficient control methods. In Chapter 2 we will look for robust methods and investigate how tolerable two particular methods are to inaccuracies. We shall see that the time before a system can be brought under control can be long. Chapters 3 and 4 are devoted to the analysis and reduction of these so-called ‘transient times’. Finally in Chapter 5, we focus our attention on the synchronisation of chaotic oscillators via the application of small parameter perturbations.

Firstly, we shall review some of the applications of chaos and its control and then explore some elementary theory on chaotic dynamical systems and set out the basic terms and definitions used throughout the thesis.

0.1 Background

The presence of chaos may be greatly beneficial in many physical systems, for example in the mixing of fluids [55, 56] and the prevention of heart failures [26, 84] and brain seizures [68]. The presence of chaotic behaviour in a dynamical system endows us with the opportunity to apply control which can change a systems dynamics quite dramatically with only minor modification to the system itself. In a system that does not exhibit chaotic behaviour, this avenue is not available. In such a case, small control signals will typically only affect the system dynamics slightly. To make any significant changes to a systems dynamics, one generally has to apply large controls. The presence of chaos in a system greatly enriches the type and complexity of behaviours we are able to observe. Thus it may be highly advantageous to design chaos into systems, allowing flexibility without the need for large control signals.

Alternatively, one may be presented with a chaotic system in which the effects of chaos are undesirable and the observation of orderly behaviour would be preferable. The application of some form of control can achieve this desired effect. In a very simple sense, the spacecraft example mentioned earlier was a crude form of the control of chaos. The chaotic properties of the solar system were exploited to direct the spacecraft to its desired target in an efficient manner. One can envisage many scenarios where the control of chaos would be desirable. The dynamics of a controlled system are relatively simple (as compared to a chaotic regime) and are predictable. Several obvious applications here then are the influencing of the

behaviour of the weather, the financial markets and even the human brain which operates in a chaotic mode on the micro scale [22, 41, 44]. Although these specific examples are far from being well understood at the moment, many positive steps have been made in the control of dynamics describable by systems involving a limited number of variables. Control of systems such as the weather and high Reynolds number flows, for example, may yet prove intractable due to their complexity.

The use of the OGY method for controlling chaos has figured heavily in the literature. The first successful implementation of the OGY method was in the control of a chaotically oscillating magneto elastic ribbon [15]. This was achieved without knowledge of the underlying dynamical equations describing the system. Since then it has been implemented in many physical systems, for example in the control of spin wave instabilities [6], cardiac chaos in rabbits hearts [24], chemical reactions [61], thermal convection loops [75], chaotic lasers [25, 65], neural information processing [14] and the control of transient chaos [79]. The OGY technique is by no means the only method known for controlling chaos. Many methods, diversely varied in their approach, have recently appeared in the literature. We shall present a review of some of these methods paying particular attention to the OGY method presently.

The chaotic properties of dynamical systems have not only been exploited for control purposes. Recently Hayes, Grebogi and Ott [33] have used the properties of chaos in the transmission of information. Shinbrot *et al.* [69, 70, 71, 72] describe a method to direct trajectories towards specific targets on a chaotic attractor. We shall investigate this further in Chapter 4 where we shall see that the targeting process can be useful in the reduction of the so-called transient times. No doubt, more applications will be found where the properties of chaotic systems will prove invaluable.

0.2 Preliminaries

Much of the theory developed presently is directly applicable to maps of the form

$$\mathbf{x}_{n+1} = \mathbf{F}(\mathbf{x}_n, p_n) \quad (0.2.1)$$

where $\mathbf{F} : \mathbb{R}^N \times \mathbb{R} \mapsto \mathbb{R}^N$ and p_n is a system parameter available for tuning at each iteration of the map. We shall assume that p_n is adjustable about some nominal value p^* and define $\delta p_n \equiv p_n - p^*$. Furthermore, we shall impose the constraint that only small adjustments are permissible such that $|\delta p_n| \leq \delta p_{\max}$ for some suitably small constant $\delta p_{\max} > 0$. Such a constraint ensures that the structure of the map does not alter significantly under the application of parameter perturbations and so only small changes are made to system dynamics. Many systems encountered in practice are continuous, but given an $N+1$ dimensional continuous time dynamical system

$$\frac{d\mathbf{y}}{dt} = \Phi(\mathbf{y}, p) \quad (0.2.2)$$

$\Phi : \mathbb{R}^{N+1} \times \mathbb{R} \mapsto \mathbb{R}^{N+1}$, where Φ may or may not be autonomous, one can obtain a map of the form (0.2.1) via a Poincaré (surface of) section. There are two types:

- (i) The stroboscopic section;
- (ii) The return map.

The former is generally preferred when the system is non-autonomous and depends periodically on time. In such a case, the flow of (0.2.2) is sampled at discrete intervals in time, generally once per period of the forcing (periodic) term. In (ii), one simply samples the state of the system at a particular fixed value of one of the state variables. This is analogous to looking at the dynamics on an N -dimensional hyperplane in phase space.

The theory developed herein assumes that systems are chaotic. A formal definition of chaos will be given shortly. We shall only be concerned with dissipative systems, consequently we shall often speak of the dynamics evolving on some ‘attractor’. A subset $\mathcal{A} \subset \mathbb{R}^N$ is

(i) an *invariant* set if it is invariant under the action of the map \mathbf{F} , i.e.

$$\mathbf{F}(\mathcal{A}) = \mathcal{A};$$

(ii) an *attractor* if it is a compact attracting ω -limit set $\omega(\mathbf{x})$ for some $\mathbf{x} \in \mathbb{R}^N$.

We define the *basin of attraction* of \mathcal{A} , $\mathcal{B}(\mathcal{A})$, as the set of points that asymptote towards the attractor \mathcal{A} in the limit as $n \rightarrow \infty$ (or as $t \rightarrow \infty$ in the continuous time case).

The tool we shall be using to investigate the dynamical behaviour of (0.2.1) is *ergodic theory*, a theory of the statistical properties of dynamical systems. Such theory is particularly useful when the shape of the attractor or the motion on it are not precisely known. Ergodic theory says that a time average equals a space average. The weight with which the space average must be taken is an *invariant measure*. An invariant measure, μ , satisfies

$$\mu(U) = \mu(\mathbf{F}^{-1}(U))$$

where U is a subset of points in \mathbb{R}^N . $\mathbf{F}^{-1}(u)$, $u \in U$ are the set of preimages of the points in U . The invariant measure μ is said to be *ergodic* (indecomposable) if there exists no non-trivial decomposition of μ such that

$$\mu = q\mu_1 + (1 - q)\mu_2 \quad 0 < q < 1$$

where $\mu_1 \neq \mu_2$ are themselves invariant measures. If μ is the same for almost all initial conditions \mathbf{x}_0 , with respect to the ordinary (Lebesgue) measure, we say that μ is the *natural measure*.

Of particular interest will be the *Lyapunov exponents* of (0.2.1) which help quantify the so-called ‘stretching and folding’ characteristics of chaotic attractors [51]. For an N -dimensional system there will be at most N distinct Lyapunov exponents,

$$\lambda_1(\mathbf{x}_0) \geq \lambda_2(\mathbf{x}_0) \geq \cdots \geq \lambda_N(\mathbf{x}_0).$$

For an ergodic measure μ , the Lyapunov exponents are the same for almost all initial conditions \mathbf{x}_0 with respect to the measure μ [19]. Thus we may speak of a Lyapunov exponent of a system without reference to a specific initial condition. A system is said to be *chaotic* if it has a positive Lyapunov exponent, i.e. $\lambda_1 > 0$.

The Lyapunov exponents and quantities derived from them give useful results on the dimensions of attractors and the entropy (production of information) of a system. Lyapunov exponents (and their related quantities) are experimentally accessible for a given system. See for example the papers by Grassberger and Procaccia [28, 29]. We shall be drawing upon some of these results later, but we shall leave any further discussion of the relevant theory until it is needed. Much of the theory discussed above and other interesting related results can be found in the excellent survey paper by Eckmann and Ruelle [19].

0.3 The Eradication of Chaotic Behaviour

We shall begin this section by reviewing several methods proposed recently for eradicating chaotic behaviour, some applicable to systems described by differential equations and others described by maps. The link between the two was discussed previously. By ‘eradicating’ chaos, we mean the application of an algorithm of some description that changes the dynamics of a system from a chaotic regime to an orderly (periodic) one. The brief review given here is by no means exhaustive, but some of the more prominent methods that have appeared in the literature over

the past five years or so are discussed.

0.3.1 Simple Methods for Taming Chaos

Perhaps the simplest way to suppress (or tame) chaos is to change system parameters so as to produce the desired kind of orderly behaviour. The problem with this is that large parameter variations may be needed in order to achieve the required effect. This is often not possible in a particular physical system, since some or all of the system parameters may be fixed or else only adjustable by a small amount. Ogorzalek [47, 48] demonstrates that a large variety of behaviours can be observed for appropriate choices of system parameters for the so-called RC-ladder chaos generator.

Rajasekar and Lakshmanan [64] consider the control of the Bonhoeffer-van der Pol (BVP) oscillator. The BVP oscillator may be written as

$$\begin{aligned}\dot{x} &= x - \frac{x^3}{3} - y + A_0 + A_1 \cos \omega t \\ \dot{y} &= c(x + a - by).\end{aligned}\tag{0.3.3}$$

For typical choices of parameter values $a = 0.7$, $b = 0.8$, $c = 0.1$ and $\omega = 1$ and for $A_0, A_1 > 0$, the BVP oscillator has been shown to behave chaotically [63, 82]. Rajasekar and Lakshmanan add a noise term to the right hand side of (0.3.3) at every tenth of a time step. They show that with the addition of Gaussian random numbers of zero mean and standard deviation $\sigma \geq 0.03$, the BVP oscillator shows irregular behaviour that is damped out in time and thus produces an orderly behaviour. The chaotic behaviour does however persist for $\sigma < 0.03$.

Also investigated in the paper by Rajasekar and Lakshmanan are the adaptive control algorithm (Huberman and Lumer [34]; Sinha *et al.* [76]) and the method of Braiman and Goldhirsch [8]. Huberman and Lumers approach is to consider an equation of the form (0.2.1). Control is achieved via an adaptive control mechanism

whereby feedback signals are used to produce stable outputs from the system, within a range of parameter values. They claim that the dynamics of a large class of adaptive systems can be written in the form of equation (0.2.1). Then the parameter perturbations are defined by

$$p_{n+1} = p_n - \epsilon \mathbf{G} \left(\mathbf{e}_{n+1}, \frac{d\mathbf{e}_{n+1}}{dp_n} \right),$$

$$\mathbf{e}_{n+1} = \mathbf{x}_{n+1} - \mathbf{d}_{n+1}$$

where \mathbf{G} is a continuous function of \mathbf{e}_n and its derivative with respect to p_n , dependent on the particular system to be controlled. The quantity \mathbf{d}_n is the output required from the system, termed the goal output, \mathbf{e}_n is the error signal, the difference between the actual output of the system at the n th step and the goal output and ϵ is a small parameter. This signal is then used to change the control parameter p_n in such a way that the error is reduced to zero. The implementation of the algorithm will not be discussed here, but see [64] for application of the method to the BVP oscillator. It is worth noting, however, that the system exhibits a novel behaviour under control, a behaviour not naturally present in the chaotic attractor.

Braiman and Goldhirsch [8] suggest that the application of a weak external periodic forcing term can help tame chaotic behaviour in a system. In particular, they investigate the equation

$$\ddot{x} + G\dot{x} + \sin x = I + A \sin \omega t + \alpha \sin \beta \omega t \quad (0.3.4)$$

taking $G = 0.7$, $A = 0.4$ and $\omega = 0.25$ for which the behaviour of (0.3.4) has been studied when $\alpha = 0$. Equation (0.3.4) models the dynamics of a damped pendulum driven by ac and dc forces. When $\alpha = 0$ and $I = 0.905$ the solution of (0.3.4) is chaotic. Braiman and Goldhirsch found that by setting $\alpha = 0.01$ and $\beta = 1.11803$, \dot{x} behaved periodically, alternating between $\dot{x} = 0$ and $\dot{x} = 0.25$ so that a period-2 orbit in \dot{x} had been formed.

It is worth examining here a possible reason as to why this method works. It is well known [52] that chaotic attractors are the closure of a set of unstable periodic orbits. That is, there is a countable infinity of unstable orbits embedded within a chaotic attractor. With the addition of the external periodic forcing term, the system possibly finds an appropriate unstable orbit and settles on that orbit.

The algorithms described above are but a handful of the methods appearing in the literature recently for the eradication of chaotic behaviour in dynamical systems. Several interesting reviews of the literature in this area can be found in the papers by Chen and Dong [10], Shinbrot *et. al.* [73] and Ogorzalek [50] amongst others. Many of the results demonstrate how only a diminutive perturbation can drastically affect the behaviour of a dynamical system, turning a chaotic behaviour into a periodic one.

Possibly the most interesting of recently developed methods are for the *control* of chaos. Whilst it seems that there are many ways to suppress chaos in particular experimental situations, there are notably less for its control. By control, we mean the application of algorithms that do not alter the system in any way in the long term, but which also produce behaviour naturally present in the system (though usually unobservable). An elegant method has been recently proposed by Ushio [80] which uses a property of contraction mappings in its implementation. He considers chaotic discrete-time systems with external input described by

$$\mathbf{x}_{n+1} = \mathbf{f}(\mathbf{x}_n) + \mathbf{B}\mathbf{u}_n \quad (0.3.5)$$

where $\mathbf{x}_n \in \mathbb{R}^N$ and $\mathbf{u}_n \in \mathbb{R}^l$ are the state and input of the system, and \mathbf{B} is an $N \times l$ constant matrix. Suppose (0.3.5) has an attractor \mathcal{A} and embedded within that attractor is a periodic orbit $\{\bar{\mathbf{x}}_0, \bar{\mathbf{x}}_1, \dots, \bar{\mathbf{x}}_{k-1}\}$ of period $k - 1$. Write $\bar{\mathbf{x}}_k = \bar{\mathbf{x}}_i$ where $i = n \bmod k$. Then with the input

$$\mathbf{u}_n = \mathbf{D}(\mathbf{x}_k) - \mathbf{D}(\bar{\mathbf{x}}_k)$$

where \mathbf{D} is a mapping from \mathbb{R}^N to \mathbb{R}^l , \mathbf{D} can be chosen such that $\mathbf{f} + \mathbf{B}\mathbf{D}$ is a contraction mapping on a closed set $\Omega \in \mathbb{R}^N$. Stabilisation of the periodic orbit is then possible for an initial state \mathbf{x}_0 in Ω .

Arguably, the most notable of recent research in this area is that of Ott, Grebogi and Yorke [53]. Their approach differs from those discussed previously in that it exploits the chaotic properties (in particular, the structure of saddle periodic orbits) of the dynamical system in order to stabilise one of the many unstable periodic orbits embedded within a chaotic attractor of the system. Most notably, no knowledge of the underlying dynamical equations describing the system is required. This method has spurred much interest in the area of controlling chaos and we shall now examine it here in more detail.

0.3.2 The OGY Method

We shall assume that the system we are attempting to control is two-dimensional and possesses a chaotic attractor which is the support for an ergodic measure μ . The principle upon which the method of Ott, Grebogi and Yorke [53] (the OGY method) works is inherently simple and consists of stabilising a saddle fixed point embedded within the attractor via the application of small, judiciously chosen, parameter perturbations. To begin with, we assume that our system is describable by an equation of the form

$$\mathbf{x}_{n+1} = \mathbf{F}(\mathbf{x}_n, p_n) \quad (0.3.6)$$

where $\mathbf{F} : \mathbb{R}^2 \times \mathbb{R} \mapsto \mathbb{R}^2$ and p_n is our system parameter. Later, the method will be generalised to differential equations of the form (0.2.2). The parameter p_n is available for external adjustment about some nominal value p^* . Only small adjustments will be permitted such that $|\delta p_n| \leq \delta p_{\max}$ for some suitable $\delta p_{\max} > 0$. Suppose equation (0.3.6) has a saddle fixed point at \mathbf{x}^* which we wish to stabilise

for $p = p^*$. Then by a careful choice of p_n it is possible to slightly change the dynamics of (0.3.6) at the n th time step, when \mathbf{x}_n is near \mathbf{x}^* , so that \mathbf{x}_{n+1} , the image of \mathbf{x}_n , is placed on the stable manifold of \mathbf{x}^* . Then successive iterates of (0.3.6) will approach \mathbf{x}^* at a rate governed by the strength of the stable manifold for all time, thus stabilising the fixed point.

Consider an expansion of (0.3.6) about (\mathbf{x}^*, p^*)

$$\begin{aligned}\mathbf{x}_{n+1} &= \mathbf{F}(\mathbf{x}^*, p^*) + \mathbf{F}_{\mathbf{x}}(\mathbf{x}^*, p^*)(\mathbf{x}_n - \mathbf{x}^*) + \mathbf{F}_p(\mathbf{x}^*, p^*)(p_n - p^*) + \cdots \\ &\simeq \mathbf{x}^* + M\delta\mathbf{x}_n + \mathbf{w}\delta p_n\end{aligned}$$

so that

$$\delta\mathbf{x}_{n+1} = M\delta\mathbf{x}_n + \mathbf{w}\delta p_n \quad (0.3.7)$$

to a first order approximation, where $M = \mathbf{F}_{\mathbf{x}}(\mathbf{x}^*, p^*)$ is the Jacobian of (0.3.6) evaluated at (\mathbf{x}^*, p^*) , $\mathbf{w} = \mathbf{F}_p(\mathbf{x}^*, p^*)$, $\delta\mathbf{x}_n = \mathbf{x}_n - \mathbf{x}^*$ and $\delta p_n = p_n - p^*$ is available for adjustment at each iteration of the map. Let λ_s and λ_u ($|\lambda_s| < 1 < |\lambda_u|$) be the eigenvalues of M with corresponding right eigenvectors \mathbf{e}_s and \mathbf{e}_u . Denote the left eigenvectors of M by \mathbf{f}_s^T and \mathbf{f}_u^T , normalised such that $\mathbf{f}_u^T \mathbf{e}_u = \mathbf{f}_s^T \mathbf{e}_s = 1$. We shall also assume that the eigenvectors are normalised to have unit length. Note that $\mathbf{f}_s^T \mathbf{e}_u = \mathbf{f}_u^T \mathbf{e}_s = 0$. We assume that \mathbf{x}_n falls sufficiently close to \mathbf{x}^* for some n so that (0.3.7) gives a good approximation to the dynamics of the system about \mathbf{x}^* . Indeed, by ergodicity, this requirement is necessarily satisfied for \mathbf{x}^* lying within a chaotic attractor of the system and for suitably chosen initial conditions. We attempt to pick p_n so that \mathbf{x}_{n+1} falls on the stable manifold of \mathbf{x}^* , i.e. choose p_n such that $\mathbf{f}_u^T \delta\mathbf{x}_{n+1} = 0$. Then using this condition we see that, from (0.3.7),

$$\mathbf{f}_u^T M \delta\mathbf{x}_n + \mathbf{f}_u^T \mathbf{w} \delta p_n = 0.$$

Hence,

$$\delta p_n = -\frac{\mathbf{f}_u^T M \delta\mathbf{x}_n}{\mathbf{f}_u^T \mathbf{w}}$$

$$= -\frac{\lambda_u \mathbf{f}_u^T \delta \mathbf{x}_n}{\mathbf{f}_u^T \mathbf{w}} \quad (0.3.8)$$

provided $\mathbf{f}_u^T \mathbf{w} \neq 0$. We should then be able to set $\delta p_n = 0$ for all subsequent time and the orbit will approach the fixed point at the geometrical rate λ_s . However, because of nonlinearities not present in (0.3.7), the modified \mathbf{x}_{n+1} will not lie precisely on the stable manifold of \mathbf{x}^* . Thus the parameter p is perturbed according to (0.3.8) at each time step n in order to achieve control, i.e. attraction to the fixed point. Note that $\delta p_n \rightarrow 0$ as $\delta \mathbf{x}_n \rightarrow \mathbf{0}$ and so the size of the applied perturbations decreases as \mathbf{x}_n approaches the fixed point \mathbf{x}^* .

The derivation of the method discussed here is not the same as the original one given in [53], but rather that according to Dressler and Nitsche [17, 18]. However, it is easily shown that the two are equivalent. In practice, equation (0.3.8) is used when the magnitude of the right hand side does not exceed δp_{\max} . If $|\delta p_n| > \delta p_{\max}$ then we set $\delta p_n = 0$. Since δp_n is linearly dependent on $\delta \mathbf{x}_n$, the parameter perturbations can only be activated when \mathbf{x}_n falls within some small region about the fixed point \mathbf{x}^* .

The OGY method can be applied to period- k orbits by letting \mathbf{x}^* be a fixed point of the k times iterated map \mathbf{F}^k . One then waits until an iterate \mathbf{x}_n falls sufficiently close to \mathbf{x}^* before initiating control. Subsequent control is then not applied at every iteration of the map, but rather at every k th iteration of the map. There is thus no loss in generality when talking only of control of fixed points of the map. There are problems associated with the control of ‘high’ period orbits, but we shall defer any discussion of these problems, and ways to get around them, until the latter part of this Introduction.

It was stated previously that δp_n is chosen so that $\mathbf{x}_{n+1}(p^* + \delta p_n)$ is placed on the linearised stable manifold of \mathbf{x}^* . From (0.3.7) we see that $\delta \mathbf{x}_{n+1}(p^* +$

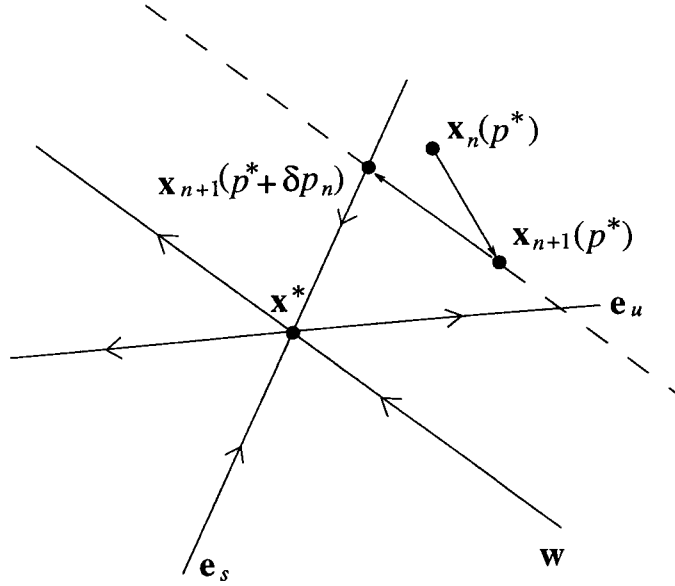


Figure 0.1: Effect of the OGY control algorithm when parameter perturbations are activated at the n th step. The dashed line indicates the direction parallel to \mathbf{w} .

$\delta p_n) \simeq \delta \mathbf{x}_{n+1}(p^*) + \mathbf{w} \delta p_n$ so that, at least in a linear sense, \mathbf{x}_{n+1} moves in the direction of \mathbf{w} from $\mathbf{x}_{n+1}(p^*)$ to $\mathbf{x}_{n+1}(p^* + \delta p_n)$ under the application of parameter perturbations. Thus the effect of the OGY control algorithm at the $(n + 1)$ th step may be geometrically interpreted in the linearised sense as in Fig. 0.1.

0.3.3 Calculation of \mathbf{x}^* , M and \mathbf{w}

If \mathbf{F} is known, \mathbf{x}^* , \mathbf{w} and M are easily found. One simply solves the fixed point equation for \mathbf{x}^* , namely $\mathbf{x}^* = \mathbf{F}(\mathbf{x}^*, p^*)$ and evaluates \mathbf{F}_x and \mathbf{F}_p at (\mathbf{x}^*, p^*) to obtain M and \mathbf{w} respectively. However, it was indicated previously that it is possible to implement the OGY method without prior knowledge of the underlying dynamical equations. Indeed, this is the case and since the dynamical equations describing a system are often unavailable (unless the system can be adequately modelled), we need to estimate the quantities required for implementation of the OGY method. We shall assume that the state of the system is completely observable [46], that is, both components of \mathbf{x}_n are observable for all n . Let us first

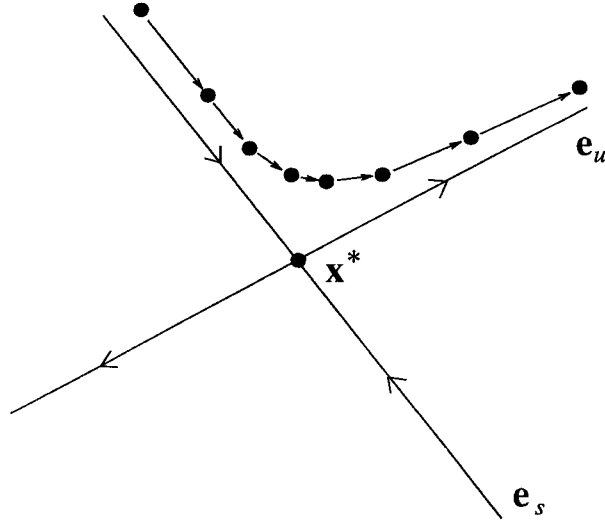


Figure 0.2: Iterates approach the fixed point approximately along the stable manifold and then get pushed away again roughly in the direction of the unstable manifold.

investigate how to find a fixed point of a map from an observed time series. Consider what happens when an iterate of an orbit falls near to the stable manifold of a fixed point \mathbf{x}^* . The orbit approaches the fixed point roughly in the direction of the stable manifold, remaining near to the fixed point for a short time before being pushed away approximately in the direction of the unstable manifold of \mathbf{x}^* (see Fig. 0.2). The detail to note here is that the orbit remains close to the fixed point for a while, and changes very little in position whilst it is there. Hence we look when, for some m , the condition

$$\|\mathbf{x}_m - \mathbf{x}_{m+1}\| < \epsilon \quad (0.3.9)$$

holds for some suitable $\epsilon > 0$. The smaller we take ϵ , the more accurate the estimate of the fixed point we should obtain. Then \mathbf{x}^* may be estimated by

$$\mathbf{x}_{\text{approx}}^* = \frac{1}{2}(\mathbf{x}_m + \mathbf{x}_{m+1}).$$

Assuming a fixed point of the mapping exists (and lies within an attractor of the system), the ergodicity of the orbit guarantees that equation (0.3.9) will be satisfied for some m , but generally speaking, the smaller ϵ , the larger m .

To estimate M we choose a $\delta_M > 0$ and collect all pairs of iterates simultaneously satisfying

$$\|\mathbf{x}_n - \mathbf{x}_{\text{approx}}^*\| < \delta_M$$

and

$$\|\mathbf{x}_{n+1} - \mathbf{x}_{\text{approx}}^*\| < \delta_M$$

i.e. all pairs of iterates $(\mathbf{x}_n, \mathbf{x}_{n+1})$ lying within a δ_M neighbourhood of $\mathbf{x}_{\text{approx}}^*$. Let there be K such pairs of iterates, $(\mathbf{x}_n^{(k)}, \mathbf{x}_{n+1}^{(k)})$, $k = 1, 2, \dots, K$. We note that about the fixed point, in the absence of parameter perturbations, $\delta\mathbf{x}_{n+1} = M\delta\mathbf{x}_n$ so that

$$\mathbf{x}_{n+1} - \mathbf{x}^* = M(\mathbf{x}_n - \mathbf{x}^*)$$

i.e.

$$\begin{aligned}\mathbf{x}_{n+1} &= M\mathbf{x}_n + (I - M)\mathbf{x}^* \\ &= M\mathbf{x}_n + \mathbf{z}\end{aligned}$$

where $\mathbf{z} = (I - M)\mathbf{x}^*$. This is a linear equation in M and \mathbf{z} for given values of \mathbf{x}_n and \mathbf{x}_{n+1} . Writing $\mathbf{x}_n = \begin{pmatrix} x_n \\ y_n \end{pmatrix}$, $\mathbf{z} = \begin{pmatrix} z_1 \\ z_2 \end{pmatrix}$ and $M = \begin{pmatrix} m_{11} & m_{12} \\ m_{21} & m_{22} \end{pmatrix}$ we have

$$\begin{pmatrix} x_{n+1}^{(k)} \\ y_{n+1}^{(k)} \end{pmatrix} = \begin{pmatrix} m_{11} & m_{12} \\ m_{21} & m_{22} \end{pmatrix} \begin{pmatrix} x_n^{(k)} \\ y_n^{(k)} \end{pmatrix} + \begin{pmatrix} z_1 \\ z_2 \end{pmatrix}$$

so that

$$x_{n+1}^{(k)} = m_{11}x_n^{(k)} + m_{12}y_n^{(k)} + z_1 \quad (0.3.10)$$

and

$$y_{n+1}^{(k)} = m_{21}x_n^{(k)} + m_{22}y_n^{(k)} + z_2 \quad (0.3.11)$$

for $k = 1, 2, \dots, K$. The K equations defined by (0.3.10) may be written in the form

$$A\mathbf{h} = \mathbf{b} \quad (0.3.12)$$

where

$$A = \begin{pmatrix} x_n^{(1)} & y_n^{(1)} & 1 \\ x_n^{(2)} & y_n^{(2)} & 1 \\ \vdots & \vdots & \vdots \\ x_n^{(K)} & y_n^{(K)} & 1 \end{pmatrix}, \quad \mathbf{h} = \begin{pmatrix} m_{11} \\ m_{12} \\ z_1 \end{pmatrix} \quad \text{and} \quad \mathbf{b} = \begin{pmatrix} x_{n+1}^{(1)} \\ x_{n+1}^{(2)} \\ \vdots \\ x_{n+1}^{(K)} \end{pmatrix}.$$

Then (0.3.12) defines an overdetermined system of linear equations for \mathbf{h} . We use the method of least squares to obtain a solution to these equations. This constitutes pre-multiplying (0.3.12) by A^T to give

$$A^T A \mathbf{h} = A^T \mathbf{b}$$

where

$$A^T A = \begin{pmatrix} \sum_k (x_n^{(k)})^2 & \sum_k x_n^{(k)} y_n^{(k)} & \sum_k x_n^{(k)} \\ \sum_k x_n^{(k)} y_n^{(k)} & \sum_k (y_n^{(k)})^2 & \sum_k y_n^{(k)} \\ \sum_k x_n^{(k)} & \sum_k y_n^{(k)} & K \end{pmatrix}$$

and

$$A^T \mathbf{b} = \begin{pmatrix} \sum_k x_n^{(k)} x_{n+1}^{(k)} \\ \sum_k y_n^{(k)} x_{n+1}^{(k)} \\ \sum_k x_{n+1}^{(k)} \end{pmatrix}$$

so that \mathbf{h} satisfies a 3×3 system of normal equations. The solution to the normal equations gives the least squares regression estimate to \mathbf{h} and hence m_{11} , m_{12} and z_1 . The quantities m_{21} , m_{22} and z_2 can be estimated in a similar manner using the equations (0.3.11). The regression estimate for the fixed point is then $\mathbf{x}^* = (I - M)^{-1} \mathbf{z}$. Note that application of this process not only gives M , but also refines the approximation to the fixed point.

To calculate \mathbf{w} , firstly let $\mathbf{x}_F(p)$ be a fixed point of \mathbf{F} . Then $\mathbf{x}_F(p)$ satisfies

$$\mathbf{x}_F(p) = \mathbf{F}(\mathbf{x}_F(p), p).$$

Differentiating with respect to p we have,

$$\frac{d\mathbf{x}_F}{dp}(p) = \mathbf{F}_x(\mathbf{x}_F(p), p) \frac{d\mathbf{x}_F}{dp}(p) + \mathbf{F}_p(\mathbf{x}_F(p), p) \quad (0.3.13)$$

so that at the fixed point $\mathbf{x}^* \equiv \mathbf{x}_F(p^*)$,

$$\frac{d\mathbf{x}^*}{dp} = \mathbf{F}_x(\mathbf{x}^*, p^*) \frac{d\mathbf{x}^*}{dp} + \mathbf{F}_p(\mathbf{x}^*, p^*).$$

Defining $\mathbf{g} := \frac{d\mathbf{x}^*}{dp}$ we have

$$\mathbf{g} = M\mathbf{g} + \mathbf{w}$$

i.e.

$$\mathbf{w} = (I - M)\mathbf{g}. \quad (0.3.14)$$

An estimate for the derivative \mathbf{g} , with error of order δp , is

$$\mathbf{g} \simeq \frac{\mathbf{x}_F(p^* + \delta p) - \mathbf{x}^*}{\delta p}$$

for small δp . Alternatively the central difference approximation (which has error of order δp^2) is

$$\mathbf{g} \simeq \frac{\mathbf{x}_F(p^* + \delta p) - \mathbf{x}_F(p^* - \delta p)}{2\delta p}.$$

Then \mathbf{w} follows from (0.3.14). The choice of δp is somewhat arbitrary, but selected such that $|\delta p| \leq \delta p_{\max}$.

In practice, we first iterate the map and find an approximation to the fixed point. A regression is then carried out to refine the estimate of the fixed point and to estimate M . The system parameter is perturbed to $p^* + \delta p$ and the process carried out again to find $\mathbf{x}_F(p^* + \delta p)$ and hence \mathbf{w} . If a central difference approximation to \mathbf{w} is required, p also has to be perturbed to $p^* - \delta p$ and $\mathbf{x}_F(p^* - \delta p)$ found. Once the procedures described above have been carried out, the OGY control algorithm can be implemented.

0.3.4 Continuous Systems and Time Delays

The OGY procedure is only applicable to two-dimensional maps of the form (0.3.6). The control algorithm can also be applied to three-dimensional differential equations of the form

$$\frac{dy}{dt} = \Phi(\mathbf{y}, t)$$

where $\Phi : \mathbb{R}^3 \times \mathbb{R} \mapsto \mathbb{R}^3$, by considering a Poincaré section of the orbits of that differential equation, as described earlier. The OGY method is then applied to the two-dimensional Poincaré map.

Let us suppose now that the dynamical equations describing the system \mathbf{F} are not known and also suppose that it is difficult, even impossible, to measure all (if any) of the elements of the state vector \mathbf{x} and that only a scalar time series $z(t)$ is available. Clearly this scalar time series is somehow representative of the state of the system. Then it is possible to reconstruct the dynamics of the system by the method of time delays [57, 77]. We shall take time to review the reconstruction procedure (in N dimensions) here since systems in which not all elements of the state vector are realisable are often encountered in practice. Let $\mathbf{Y}(t)$ be the state of the system at time t . We have that $z(t) \equiv \mathbf{Z}(\mathbf{Y}(t))$ for some function $\mathbf{Z} : \mathbb{R}^N \mapsto \mathbb{R}$. From this time series we may form an N -dimensional delay coordinate vector

$$\mathbf{X}(t) = (z(t), z(t - \tau), \dots, z(t - (N - 1)\tau))$$

where τ is ~~is~~ known as the delay, a multiple of the time between observations, and N the embedding dimension, the dimension of the system we are attempting to reconstruct from the data. The return map is obtained by requiring that one component of $\mathbf{X}(t)$ is a constant, say $[\mathbf{X}(t_n)]_1 = c$, so that $\mathbf{x}_{n+1} = \mathbf{F}(\mathbf{x}_n)$, where $\mathbf{x}_n \in \mathbb{R}^{N-1}$. The stroboscopic surface of section arises naturally due to the fact that τ is a constant.

To stabilise a fixed point, we apply a control method at time t_n , at which point we change the perturbation parameter from δp_{n-1} to δp_n using one of the formulas derived earlier. We hope to control the dynamics of the original system since for appropriately chosen N and τ there exists a bijective relation $\Phi : \mathbb{R}^N \mapsto \mathbb{R}^N$ such that $\mathbf{X}(t) = \Phi(\mathbf{Y}(t))$. Φ is closely related to the dynamical equations of the system

and therefore on the control parameter p_n also. To reflect this we write $\Phi \equiv \Phi_{p_n}$.

Let us assume that $t_{n+1} - t_n > (N - 1)\tau$. Then the point $\mathbf{X}(t_n)$ is related to the state of the system by $\mathbf{Y}(t_n) = \Phi_{p_{n-1}}^{-1}(c, z(t_n - \tau), \dots, z(t_n - (N - 1)\tau))$. When control is activated, the time development of the original system, from the solution $\mathbf{Y}(t_n)$ until $t = t_{n+1}$, is given by the flow of the system, $\varphi_{p_n}^{t_{n+1}-t_n}$ in the interval (t_n, t_{n+1}) . Thus the state of the system at time t_{n+1} is $\mathbf{Y}(t_{n+1}) = \varphi_{p_n}^{t_{n+1}-t_n}(\mathbf{Y}(t_n))$ and the state in the embedding space is $\mathbf{X}(t_{n+1}) = \Phi_{p_n}(\mathbf{Y}(t_{n+1}))$ and so

$$\begin{aligned}\mathbf{X}(t_{n+1}) &= \Phi_{p_n}(\varphi_{p_n}^{t_{n+1}-t_n}(\mathbf{Y}(t_n))) \\ &= \Phi_{p_n}(\varphi_{p_n}^{t_{n+1}-t_n}(\Phi_{p_{n-1}}^{-1}(\mathbf{X}(t_n)))).\end{aligned}$$

So in the presence of parameter perturbations, Dressler and Nitsche [17] propose that the Poincaré map depends not only on p_n , but also on p_{n-1} , i.e.

$$\mathbf{x}_{n+1} \equiv \mathbf{F}(\mathbf{x}_n, p_n, p_{n-1}).$$

The modified OGY method may be derived by considering the linearisation

$$\delta \mathbf{x}_{n+1} = M \delta \mathbf{x}_n + \mathbf{u} \delta p_n + \mathbf{v} \delta p_{n-1} \quad (0.3.15)$$

where $\mathbf{u} = \frac{d\mathbf{F}}{dp_n}(\mathbf{x}^*, p^*, p^*)$ and $\mathbf{v} = \frac{d\mathbf{F}}{dp_{n-1}}(\mathbf{x}^*, p^*, p^*)$. Then the condition $\mathbf{f}_u^T \delta \mathbf{x}_{n+1} = 0$ gives

$$\delta p_n = -\frac{\lambda_u \mathbf{f}_u^T \delta \mathbf{x}_n}{\mathbf{f}_u^T \mathbf{u}} - \frac{\mathbf{f}_u^T \mathbf{v}}{\mathbf{f}_u^T \mathbf{u}} \delta p_{n-1}$$

provided $\mathbf{f}_u^T \mathbf{u} \neq 0$. Further, if $\left| \frac{\mathbf{f}_u^T \mathbf{v}}{\mathbf{f}_u^T \mathbf{u}} \right| \geq 1$ then it is possible that δp_n could grow until $|\delta p_n| > \delta p_{\max}$, even when $\delta \mathbf{x}_n \rightarrow \mathbf{0}$, so that the range of control is left at some point. This problem may be overcome by devising a control method whereby the system is stabilised on the next but one time step so that the new control criterion is that $\mathbf{f}_u^T \delta \mathbf{x}_{n+2} = 0$ and $\delta p_{n+1} = 0$. Then from (0.3.15),

$$\begin{aligned}\delta \mathbf{x}_{n+2} &= M \delta \mathbf{x}_{n+1} + \mathbf{u} \delta p_{n+1} + \mathbf{v} \delta p_n \\ &= M (M \delta \mathbf{x}_n + \mathbf{u} \delta p_n + \mathbf{v} \delta p_{n-1}) + \mathbf{u} \delta p_{n+1} + \mathbf{v} \delta p_n.\end{aligned}$$

Then using the control criteria we have

$$\mathbf{f}_u^T M^2 \delta \mathbf{x}_n + \mathbf{f}_u^T M \mathbf{u} \delta p_n + \mathbf{f}_u^T M \mathbf{v} \delta p_{n-1} + \mathbf{f}_u^T \mathbf{v} \delta p_n = 0$$

so that

$$\delta p_n = -\frac{\lambda_u^2 \mathbf{f}_u^T \delta \mathbf{x}_n + \lambda_u \mathbf{f}_u^T \mathbf{v} \delta p_{n-1}}{\lambda_u \mathbf{f}_u^T \mathbf{u} + \mathbf{f}_u^T \mathbf{v}}.$$

Since we have stipulated that $\delta p_{n+1} = 0$, the problem of growing parameter perturbations should be resolved.

0.3.5 Higher Period Orbits

We mentioned earlier that the OGY method could be used to stabilise higher period orbits, not only fixed points. One simply applies the parameter perturbations at every k th step, when \mathbf{x}_n lies close to \mathbf{x}^* , where \mathbf{x}^* is now a point in the period- k orbit, rather than at every step. This is the same as stabilising a fixed point of the k times iterated map \mathbf{F}^k . Since the system we are attempting to control is chaotic, points that are initially close together diverge exponentially at a rate depending on the leading Lyapunov exponent of the system. Thus, even if $\|\mathbf{x}_n - \mathbf{x}^*\| \leq \delta p_{\max}$ at the n th step, we may have $\|\mathbf{x}_{n+k} - \mathbf{x}^*\| > \delta p_{\max}$ after a further k time steps, for \mathbf{x}_n initially lying close to \mathbf{x}^* . Then $\delta \mathbf{x}_{n+k}$ will be ‘large’ so that the parameter perturbations will have to be set to zero, and control will not be achieved. We may deduce from this that period- k orbits may only be controlled provided that k is not too large.

Alternatively, we could attempt to estimate the dynamics of the system near to each point on the orbit and apply a perturbation, defined by the local Jacobian at each point (see Paskota *et al.* [58, 59] for a thorough discussion of this technique). For very high period orbits this may become impractical because of the amount of computation involved in estimating numerous Jacobians.

Some attempts at controlling higher period orbits have been successful recently. One of the more notable results is detailed in [35] where a period 23 orbit was stabilised using an adaptation of the OGY control algorithm. An important note here is that one should always take care when attempting to locate higher period orbits of non-prime periodicity. For example, a period- $2k$ point is easily confused with a period- k point twice iterated.

0.3.6 Higher Dimensional Systems

Of course, control methods such as the OGY method would be of little practical value if they could not be generalised for use on higher dimensional systems. Some methods have appeared in the literature that address the problem of the control of such systems. Indeed, Auerbach *et al.* [5] have recently formulated an algorithm, similar to the OGY method, to control an arbitrarily high dimensional dynamical system. The algorithm, again, does not require any knowledge of the underlying dynamical equations of the system. They reduce the problem to only a few dimensions and formulate their algorithm to operate only on those directions. Another markedly different method is the Recursive Projection Method of Shroff and Keller [74]. When applied to stabilise fixed points, their method consists of separating the stable and unstable subspaces and using a Newton iteration on the unstable subspace in order to effect control. The stable subspace is left to iterate on its own. Note that this is in contrast to the OGY method where the problem is split into linear and nonlinear parts, using the linear part as the basis for the iterative procedure. There are also a few contraction mapping approaches such as that of Ushio [80] already discussed and another discussed by Xu and Bishop [86], both applicable to higher dimensional systems.

By far the easiest methods to understand and visualise are those for use on two-

dimensional systems. Indeed, the methods presented in Chapter 1 will all be for use on two-dimensional maps. They can often be generalised for higher dimensional problems, provided that the number of state variables is not too large. In the next chapter, we shall investigate whether better methods than the OGY procedure can be procured, i.e. methods that converge to the fixed point at a faster rate.

Chapter 1

Controlling Chaos – Rates of Convergence

In this chapter we shall investigate the convergence properties of the OGY method in some detail. Several other more efficient methods (in the sense that they converge to the fixed point at a faster rate) are then naturally developed from this analysis.

1.1 Convergence Analysis of the OGY Method

From equation (0.3.8) we note that when control is activated, i.e. parameter perturbations are switched on, p_n depends directly upon \mathbf{x}_n so that $p_n \equiv p_n(\mathbf{x}_n)$. So we may write the iterated map, in the presence of parameter perturbations, as

$$\mathbf{x}_{n+1} = \mathbf{G}(\mathbf{x}_n) \equiv \mathbf{F}(\mathbf{x}_n, p_n(\mathbf{x}_n)). \quad (1.1.1)$$

This is now a modified iteration which does not explicitly involve the perturbation parameter p_n . It is easily seen that this modified iteration has a stable fixed point at \mathbf{x}^* . From (1.1.1),

$$\mathbf{G}(\mathbf{x}^*) = \mathbf{F}(\mathbf{x}^*, p^*) = \mathbf{x}^*$$

so that \mathbf{x}^* is indeed a fixed point of \mathbf{G} . To analyse the stability properties of the fixed point of the new mapping, and hence the convergence properties of the OGY method, we look at the Jacobian of \mathbf{G} , which is

$$\begin{aligned} J(\mathbf{x}_n) &:= D_{\mathbf{x}}\mathbf{F}(\mathbf{x}_n, p_n(\mathbf{x}_n)) \\ &= \mathbf{F}_{\mathbf{x}}(\mathbf{x}_n, p_n(\mathbf{x}_n)) + \mathbf{F}_p(\mathbf{x}_n, p_n(\mathbf{x}_n))D_{\mathbf{x}}p_n(\mathbf{x}_n) \end{aligned}$$

where $D_{\mathbf{x}}$ is the differential operator with respect to \mathbf{x} . Now, δp_n may be written as $\delta p_n = -\frac{\mathbf{f}_u^T M \delta \mathbf{x}_n}{\mathbf{f}_u^T \mathbf{w}}$ so that

$$D_{\mathbf{x}}\delta p_n = -\frac{\mathbf{f}_u^T M}{\mathbf{f}_u^T \mathbf{w}}$$

Also, $p_n(\mathbf{x}_n) = p^* + \delta p_n(\mathbf{x}_n)$ and so $D_{\mathbf{x}}p_n(\mathbf{x}_n) = D_{\mathbf{x}}\delta p_n(\mathbf{x}_n)$. Then evaluating $J(\mathbf{x}_n)$ at the fixed point we have

$$J := J(\mathbf{x}^*) = M - \mathbf{w} \frac{\mathbf{f}_u^T M}{\mathbf{f}_u^T \mathbf{w}} = \left(I - \frac{\mathbf{w} \mathbf{f}_u^T}{\mathbf{f}_u^T \mathbf{w}} \right) M.$$

Writing $P = \left(I - \frac{\mathbf{w} \mathbf{f}_u^T}{\mathbf{f}_u^T \mathbf{w}} \right)$ we see that $P^2 = P$ and so P is a projection operator. Note that the projection only applies to the linear part of \mathbf{G} and not to higher order terms.

Let us now look for the eigenvalues and eigenvectors of J . We have that

$$J\mathbf{e}_s = \left(I - \frac{\mathbf{w} \mathbf{f}_u^T}{\mathbf{f}_u^T \mathbf{w}} \right) \lambda_s \mathbf{e}_s = \lambda_s \mathbf{e}_s.$$

Also,

$$\mathbf{f}_u^T J = (\mathbf{f}_u^T - \mathbf{f}_u^T) M = 0$$

so that \mathbf{e}_s is a right eigenvector of J with eigenvalue λ_s and \mathbf{f}_u^T is a left eigenvector of J corresponding to a zero eigenvalue. Suppose that $\mathbf{e} = c\mathbf{e}_s + d\mathbf{e}_u$ is the right eigenvector of J corresponding to the zero eigenvalue for some non-zero constants c and d . Then

$$\begin{aligned} J(c\mathbf{e}_s + d\mathbf{e}_u) &= \left(I - \frac{\mathbf{w} \mathbf{f}_u^T}{\mathbf{f}_u^T \mathbf{w}} \right) (c\lambda_s \mathbf{e}_s + d\lambda_u \mathbf{e}_u) \\ &= c\lambda_s \mathbf{e}_s + d\lambda_u \mathbf{e}_u - \frac{d\lambda_u}{\mathbf{f}_u^T \mathbf{w}} \mathbf{w}. \end{aligned}$$

Now write $\mathbf{w} = \eta \mathbf{e}_s + \xi \mathbf{e}_u$ where $\eta = \mathbf{f}_s^T \mathbf{w}$ and $\xi = \mathbf{f}_u^T \mathbf{w}$. Then we have that

$$\begin{aligned} J(c\mathbf{e}_s + d\mathbf{e}_u) &= c\lambda_s \mathbf{e}_s + d\lambda_u \mathbf{e}_u - \frac{d\lambda_u \mathbf{f}_s^T \mathbf{w}}{\mathbf{f}_u^T \mathbf{w}} \mathbf{e}_s - d\lambda_u \mathbf{e}_u \\ &= \left(c\lambda_s - \frac{d\lambda_u \mathbf{f}_s^T \mathbf{w}}{\mathbf{f}_u^T \mathbf{w}} \right) \mathbf{e}_s + (d\lambda_u - d\lambda_u) \mathbf{e}_u \end{aligned}$$

so that if $c\mathbf{e}_s + d\mathbf{e}_u$ corresponds to the zero eigenvalue we require that

$$c = \frac{\lambda_u \mathbf{f}_s^T \mathbf{w}}{\lambda_s \mathbf{f}_u^T \mathbf{w}} d.$$

Setting $d = 1$ we have that $\chi \mathbf{e}_s + \mathbf{e}_u$ is the eigenvector we seek, where $\chi = \frac{\lambda_u \mathbf{f}_s^T \mathbf{w}}{\lambda_s \mathbf{f}_u^T \mathbf{w}}$.

It is then easily shown that $\mathbf{f}_u^T = \mathbf{f}_s^T - \chi \mathbf{f}_u^T$ is the left eigenvector corresponding to the non-zero eigenvalue λ_s . Since the eigenvalues of J are 0 and λ_s , with $|\lambda_s| < 1$, this proves convergence in the presence of parameter perturbations, given that \mathbf{x}_n is sufficiently close to \mathbf{x}^* [9].

1.2 Related methods

In this section we derive methods similar in nature to the OGY method but with better convergence properties. We begin with a review and an investigation of another method whose convergence properties are dependent upon the directions of the eigenvectors of the Jacobian at the fixed point. It does not rely on the existence of a saddle fixed point, but cannot be used to stabilise all fixed points.

1.2.1 The Shortest Distance Method

The criterion for choosing δp_n in the OGY method was $\mathbf{f}_u^T \delta \mathbf{x}_{n+1} = 0$, which placed \mathbf{x}_{n+1} on the stable manifold of \mathbf{x}^* . Suppose we use a different criterion in that δp_n is chosen such that \mathbf{x}_{n+1} is placed as near as possible to the fixed point [23]. Now, under a perturbation of the parameter p , \mathbf{x}_{n+1} moves along the line through \mathbf{x}_{n+1} , parallel to \mathbf{w} , so diagrammatically we have a scenario as depicted in Fig. 1.1.

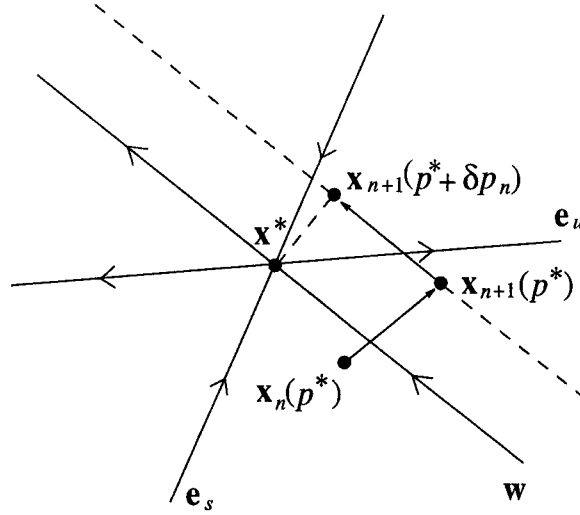


Figure 1.1: $\mathbf{x}_{n+1}(p_n)$ is placed as close to \mathbf{x}^* as possible in a linear sense.

The criterion for choosing δp_n is simply $\mathbf{w}^T \delta \mathbf{x}_{n+1} = 0$ since \mathbf{x}_{n+1} is closest to \mathbf{x}^* at the point on the line through \mathbf{x}_{n+1} parallel to \mathbf{w} where $\delta \mathbf{x}_{n+1}$ is orthogonal to this line. In that case, using the linearisation (0.3.7),

$$\delta p_n = -\frac{\mathbf{w}^T M \delta \mathbf{x}_n}{\mathbf{w}^T \mathbf{w}}.$$

This time,

$$D_{\mathbf{x}} \delta p_n = -\frac{\mathbf{w}^T M}{\mathbf{w}^T \mathbf{w}}$$

so that in the presence of parameter perturbations,

$$J = \left(I - \frac{\mathbf{w} \mathbf{w}^T}{\mathbf{w}^T \mathbf{w}} \right) M = (I - \mathbf{v} \mathbf{v}^T) M$$

where $\mathbf{v} = \frac{\mathbf{w}}{\|\mathbf{w}\|}$. Note that $\mathbf{v}^T \mathbf{v} = 1$. Writing $P = (I - \mathbf{v} \mathbf{v}^T)$ we see that P is an orthogonal projection, since $P^2 = P$ and $P^T = P$. In this case, \mathbf{x} may be decomposed as $\mathbf{x} = \alpha \mathbf{u} + \beta \mathbf{v}$ where $\mathbf{u}^T \mathbf{v} = 0$ and $\mathbf{u}^T \mathbf{u} = 1$. Define a transformation of coordinates such that

$$\begin{pmatrix} x \\ y \end{pmatrix} = T \begin{pmatrix} \alpha \\ \beta \end{pmatrix}.$$

The transformation matrix is then $T = \begin{pmatrix} \mathbf{u} & \mathbf{v} \end{pmatrix}$ and the inverse transformation is $T^{-1} = \begin{pmatrix} \mathbf{u}^T \\ \mathbf{v}^T \end{pmatrix}$. Thus,

$$T^{-1} J T = \begin{pmatrix} \mathbf{u}^T \\ \mathbf{v}^T \end{pmatrix} (I - \mathbf{v} \mathbf{v}^T) M \begin{pmatrix} \mathbf{u} & \mathbf{v} \end{pmatrix}$$

$$= \begin{pmatrix} \mathbf{u}^T M \mathbf{u} & \mathbf{u}^T M \mathbf{v} \\ 0 & 0 \end{pmatrix}$$

and so the eigenvalues of the Jacobian J are 0 and $\mathbf{u}^T M \mathbf{u}$.

The method does not rely on the existence of a stable manifold as with the OGY method. Thus, provided that $|\mathbf{u}^T M \mathbf{u}| < 1$, it may be possible to stabilise an unstable fixed point in particular cases, where both the eigenvalues of M are greater than unity in absolute value. However, the method will fail to converge if $|\mathbf{u}^T M \mathbf{u}| \geq 1$. If it turned out that $\mathbf{u} = \mathbf{e}_u$ for example, then

$$|\mathbf{u}^T M \mathbf{u}| = |\mathbf{e}_u^T M \mathbf{e}_u| = |\lambda_u| > 1$$

so that convergence will not occur. This renders the method inoperable in certain circumstances and so the shortest distance (SD) method cannot be used as a ‘black box’ control algorithm. In the example given here, \mathbf{e}_u and \mathbf{w} are orthogonal and the method has the effect of placing \mathbf{x}_{n+1} on the unstable manifold of \mathbf{x}^* (in the linearised sense) and so it is clear that the method will fail.

1.2.2 Reducing the Spectral Radius of J

In the OGY method, the rate of convergence to the fixed point is governed by the spectral radius of J , $\rho(J) = |\lambda_s|$ [9]. By a suitable choice of δp_n , it may be possible to reduce $\rho(J)$ and thus increase the rate of convergence. Suppose we choose a vector \mathbf{k}^T such that our control criterion is $\mathbf{k}^T \delta \mathbf{x}_{n+1} = 0$, giving $\delta p_n = -\frac{\mathbf{k}^T M \delta \mathbf{x}_n}{\mathbf{k}^T \mathbf{w}}$. Then the Jacobian for this method in the presence of parameter perturbations is

$$J = \left(I - \frac{\mathbf{w} \mathbf{k}^T}{\mathbf{k}^T \mathbf{w}} \right) M.$$

We shall now explore several possibilities for the choice of \mathbf{k}^T , all of which will give an improved rate of convergence to the fixed point.

The Linear Perturbation Method

Define \mathbf{m} and \mathbf{l} such that $\mathbf{m}^T \mathbf{w} = 0$ and $\mathbf{k}^T \mathbf{l} = 0$, i.e. \mathbf{m} is orthogonal to \mathbf{w} and \mathbf{l} is orthogonal to \mathbf{k} . Write

$$\mathbf{x} = \alpha \mathbf{l} + \beta \mathbf{w}.$$

The transformation matrix is then $T = \begin{pmatrix} \mathbf{l} & \mathbf{w} \end{pmatrix}$ with inverse transformation $T^{-1} = \begin{pmatrix} \frac{\mathbf{m}^T}{\mathbf{k}^T \mathbf{l}} \\ \frac{\mathbf{m}^T \mathbf{l}}{\mathbf{k}^T \mathbf{w}} \end{pmatrix}$. We have

$$\begin{aligned} T^{-1} J T &= \begin{pmatrix} \frac{\mathbf{m}^T}{\mathbf{k}^T \mathbf{l}} \\ \frac{\mathbf{m}^T \mathbf{l}}{\mathbf{k}^T \mathbf{w}} \end{pmatrix} \left(I - \frac{\mathbf{w} \mathbf{k}^T}{\mathbf{k}^T \mathbf{w}} \right) M \begin{pmatrix} \mathbf{l} & \mathbf{w} \end{pmatrix} \\ &= \begin{pmatrix} \frac{\mathbf{m}^T M \mathbf{l}}{\mathbf{m}^T \mathbf{l}} & \frac{\mathbf{m}^T M \mathbf{w}}{\mathbf{m}^T \mathbf{l}} \\ 0 & 0 \end{pmatrix}. \end{aligned}$$

Thus to reduce $\rho(J)$ we need to reduce $|\lambda_\rho| := \left| \frac{\mathbf{m}^T M \mathbf{l}}{\mathbf{m}^T \mathbf{l}} \right|$. We know that when $\mathbf{k} = \mathbf{f}_u$, $\lambda_\rho = \lambda_s$ and so we choose \mathbf{k} as a perturbation of \mathbf{f}_u .

We may write $\mathbf{f}_u^T = \begin{pmatrix} \cos \theta & \sin \theta \end{pmatrix}$ for suitable θ , as it is the direction of \mathbf{f}_u^T that is important and this is characterised by θ . Since $\mathbf{f}_u^T \mathbf{e}_s = 0$, we may also write $\mathbf{e}_s = \begin{pmatrix} -\sin \theta \\ \cos \theta \end{pmatrix}$. Now, \mathbf{k} is a perturbation of \mathbf{f}_u so that we may write \mathbf{k} as

$$\mathbf{k} = \begin{pmatrix} \cos(\theta + \epsilon) \\ \sin(\theta + \epsilon) \end{pmatrix} \simeq \begin{pmatrix} \cos \theta \\ \sin \theta \end{pmatrix} + \epsilon \begin{pmatrix} -\sin \theta \\ \cos \theta \end{pmatrix} = \mathbf{f}_u + \epsilon \mathbf{e}_s$$

to a first order approximation. Also, \mathbf{l} can be chosen as

$$\mathbf{l} = \begin{pmatrix} -\sin(\theta + \epsilon) \\ \cos(\theta + \epsilon) \end{pmatrix} \simeq \begin{pmatrix} -\sin \theta \\ \cos \theta \end{pmatrix} + \epsilon \begin{pmatrix} -\cos \theta \\ -\sin \theta \end{pmatrix} = \mathbf{e}_s - \epsilon \mathbf{f}_u.$$

Note that the first order approximations to \mathbf{k} and \mathbf{l} are also orthogonal for suitably chosen eigenvectors \mathbf{f}_u^T and \mathbf{e}_s . We now impose a constraint on \mathbf{m} such that $\mathbf{m}^T \mathbf{e}_s = 1$. Using the decomposition $M = \lambda_u \mathbf{e}_u \mathbf{f}_u^T + \lambda_s \mathbf{e}_s \mathbf{f}_s^T$ [53], we have that

$$\begin{aligned} \lambda_\rho &= \frac{\mathbf{m}^T M (\mathbf{e}_s - \epsilon \mathbf{f}_u)}{\mathbf{m}^T (\mathbf{e}_s - \epsilon \mathbf{f}_u)} \\ &= (\lambda_s - \epsilon (\lambda_s \mathbf{f}_s^T \mathbf{f}_u + \lambda_u \mathbf{m}^T \mathbf{f}_u)) (1 - \epsilon \mathbf{m}^T \mathbf{f}_u)^{-1} \\ &= (\lambda_s - \epsilon (\lambda_s \mathbf{f}_s^T \mathbf{f}_u + \lambda_u \mathbf{m}^T \mathbf{f}_u)) (1 + \epsilon \mathbf{m}^T \mathbf{f}_u + O(\epsilon^2)) \end{aligned}$$

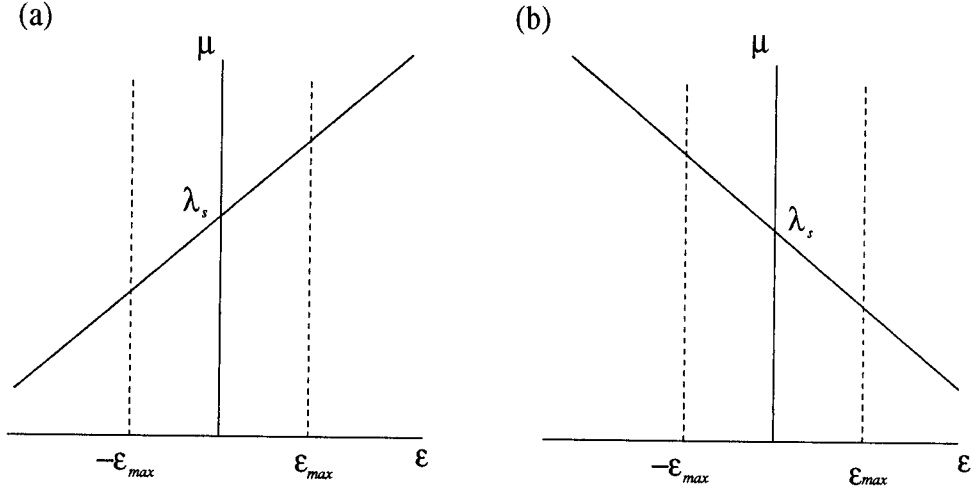


Figure 1.2: The linear approximation for λ_ρ plotted against ϵ for (a) $d_l < 0$ and (b) $d_l > 0$.

$$\begin{aligned}
 &= \lambda_s - \epsilon(\lambda_s \mathbf{f}_s^T \mathbf{f}_u + \lambda_u \mathbf{m}^T \mathbf{f}_u - \lambda_s \mathbf{m}^T \mathbf{f}_u) + O(\epsilon^2) \\
 &= \lambda_s - d_l \epsilon
 \end{aligned}$$

to first order in ϵ , where $d_l = \lambda_s \mathbf{f}_s^T \mathbf{f}_u + \lambda_u \mathbf{m}^T \mathbf{f}_u - \lambda_s \mathbf{m}^T \mathbf{f}_u$. Generically, d_l is non-zero so plotting λ_ρ against ϵ we have either Fig. 1.2(a) or (b). Clearly, for non-zero d_l , changing \mathbf{f}_u to \mathbf{k} via a small perturbation ϵ in θ of appropriate sign should result in a control method whose convergence is faster than that of the OGY method.

The value of δp_n is found by considering the expansion of $-\mathbf{k}^T M \delta \mathbf{x}_n (\mathbf{k}^T \mathbf{w})^{-1}$ to first order in ϵ . It is easily shown that

$$\delta p_n \simeq -\frac{1}{\mathbf{f}_u^T \mathbf{w}} \left(\mathbf{f}_u^T + \epsilon \left(\mathbf{e}_s^T - \frac{\mathbf{e}_s^T \mathbf{w}}{\mathbf{f}_u^T \mathbf{w}} \mathbf{f}_u^T \right) \right) M \delta \mathbf{x}_n. \quad (1.2.2)$$

We now need to choose a particular value for ϵ in order to evaluate λ_ρ and δp_n . Clearly, the approximations above are only valid for small ϵ so we require $|\epsilon| < \epsilon_{\max}$ for some suitable $\epsilon_{\max} > 0$. Also, $|\delta p_n|$ must not be too large since it is restricted by δp_{\max} . But (1.2.2) gives a linear relationship between δp_n and ϵ so that, from (1.2.2),

$$|\delta p_n| \leq \frac{1}{|\mathbf{f}_u^T \mathbf{w}|} \left(\left| \mathbf{f}_u^T M \delta \mathbf{x}_n \right| + |\epsilon| \left| \left(\mathbf{e}_s^T - \frac{\mathbf{e}_s^T \mathbf{w}}{\mathbf{f}_u^T \mathbf{w}} \mathbf{f}_u^T \right) M \delta \mathbf{x}_n \right| \right) \leq \delta p_{\max}$$

which gives

$$|\epsilon| \leq \frac{\delta p_{\max} |\mathbf{f}_u^T \mathbf{w}| - |\mathbf{f}_u^T M \delta \mathbf{x}_n|}{\left| \left(\mathbf{e}_s^T - \frac{\mathbf{e}_s^T \mathbf{w}}{\mathbf{f}_u^T \mathbf{w}} \mathbf{f}_u^T \right) M \delta \mathbf{x}_n \right|} \equiv \epsilon_0.$$

Ideally we would like λ_ρ to be zero. This occurs when $|\epsilon| = \hat{\epsilon} = \left| \frac{\lambda_s}{d_l} \right|$, at least to a linear approximation. So we choose $\epsilon = \text{sgn} \left(\frac{\lambda_s}{d_l} \right) \min(\epsilon_{\max}, \epsilon_0, \hat{\epsilon})$.

The Quadratic Perturbation Method

We have only included terms linear in ϵ in the above method. For greater accuracy, terms quadratic in ϵ can also be included. We have, to second order in ϵ ,

$$\mathbf{k} = \mathbf{f}_u + \epsilon \mathbf{e}_s - \frac{\epsilon^2}{2} \mathbf{f}_u, \quad \mathbf{l} = \mathbf{e}_s - \epsilon \mathbf{f}_u - \frac{\epsilon^2}{2} \mathbf{e}_s.$$

Then by substituting the second order expansion of \mathbf{l} into the equation for λ_ρ we obtain, after a little algebra,

$$\lambda_\rho = \lambda_s - d_l \epsilon - d_q \epsilon^2 + O(\epsilon^3)$$

where $d_q = \lambda_s \mathbf{f}_s^T \mathbf{f}_u \mathbf{m}^T \mathbf{f}_u + \lambda_u (\mathbf{m}^T \mathbf{f}_u)^2 - \frac{\lambda_s}{2} (\mathbf{m}^T \mathbf{f}_u)^2$. The value of the perturbation parameter is then found, to second order, as

$$\delta p_n = -\frac{1}{\mathbf{f}_u^T \mathbf{w}} \left(\mathbf{f}_u^T + \epsilon \left(\mathbf{e}_s^T - \frac{\mathbf{e}_s^T \mathbf{w}}{\mathbf{f}_u^T \mathbf{w}} \mathbf{f}_u^T \right) + \epsilon^2 \left(\frac{\mathbf{e}_s^T \mathbf{w}}{\mathbf{f}_u^T \mathbf{w}} (\mathbf{f}_u^T - \mathbf{e}_s^T) \right) \right) M \delta \mathbf{x}_n. \quad (1.2.3)$$

This time, we have a quadratic equation for δp_n . We solve (1.2.3) with $\delta p_n = \delta p_{\max}$ for ϵ and set ϵ_0 to the ‘sensible’ value. We also choose $\hat{\epsilon}$ such that λ_ρ is either zero or as close to zero as possible, with $|\hat{\epsilon}| < \epsilon_{\max}$. The same criterion for choosing ϵ as above is then valid.

The Zero Spectral Radius (ZSR) Method

Suppose now that $\mathbf{k} = \alpha \begin{pmatrix} \cos \beta \\ \sin \beta \end{pmatrix}$ for suitable β and scalar α chosen such that $\mathbf{k}^T \mathbf{w} = 1$. Then $\mathbf{l} = \alpha \begin{pmatrix} -\sin \beta \\ \cos \beta \end{pmatrix}$. We then have that

$$\lambda(\beta) = \frac{\mathbf{m}^T M \begin{pmatrix} -\sin \beta \\ \cos \beta \end{pmatrix}}{\mathbf{m}^T \begin{pmatrix} -\sin \beta \\ \cos \beta \end{pmatrix}}.$$

We aim to minimise the spectral radius of J . Clearly, $\rho(J) = 0$ if $\lambda_\rho(\beta) = 0$. This happens when

$$\mathbf{m}^T M \begin{pmatrix} -\sin \beta \\ \cos \beta \end{pmatrix} = 0 \quad (1.2.4)$$

assuming $\mathbf{m}^T \mathbf{l} \neq 0$. Let $\mathbf{m}^T M = \begin{pmatrix} a & b \end{pmatrix}$ for scalars a and b . Then from (1.2.4), $\lambda_\rho(\beta) = 0$ if

$$-a \sin \beta + b \cos \beta = 0$$

i.e.

$$\tan \beta = \frac{b}{a}$$

which implies

$$\beta = \tan^{-1} \frac{b}{a}.$$

Since $\delta p_n = \frac{\mathbf{k}^T M \delta \mathbf{x}_n}{\mathbf{k}^T \mathbf{w}}$, the value of α does not in fact need to be found, so once we have β , the value of δp_n is defined and hence the new control algorithm is defined.

Alternatively, we may write \mathbf{k}^T in terms of the eigenvalues and eigenvectors of M . Since the method was derived by requiring that $\mathbf{m}^T M \mathbf{l} = 0$, \mathbf{k}^T must be some multiple of $\mathbf{m}^T M$. Thus we let $\mathbf{k}^T = \alpha \mathbf{m}^T M$. Writing $\mathbf{w} = \eta \mathbf{e}_s + \xi \mathbf{e}_u$, we can deduce that since $\mathbf{m}^T \mathbf{w} = 0$ and $\mathbf{m}^T \mathbf{e}_s = 1$, $\mathbf{m}^T = \mathbf{f}_s^T - \frac{\eta}{\xi} \mathbf{f}_u^T$ and so

$$\begin{aligned} \mathbf{k}^T &= \alpha \mathbf{m}^T M \\ &= \alpha \left(\mathbf{f}_s^T - \frac{\eta}{\xi} \mathbf{f}_u^T \right) M \\ &= \alpha \lambda_s \left(\mathbf{f}_s^T - \chi \mathbf{f}_u^T \right) \end{aligned}$$

for some scalar α . Note that \mathbf{k}^T lies in the direction of the left eigenvector corresponding to the eigenvalue λ_s of the Jacobian of the modified mapping of the OGY method. As far as the formula for δp_n is concerned, the value of α is unimportant. Also, we have that, up to a scalar multiple,

$$\mathbf{l} = \frac{\eta}{\xi} \lambda_u \mathbf{e}_s + \lambda_s \mathbf{e}_u = \frac{1}{\lambda_s} (\chi \mathbf{e}_s + \mathbf{e}_u).$$

The method starts to break down if $\mathbf{m}^T \mathbf{l}$ approaches zero. Now, $\mathbf{m}^T \mathbf{l} = \frac{\eta}{\xi} \lambda_u - \frac{\eta}{\xi} \lambda_s = \frac{\eta}{\xi} (\lambda_u - \lambda_s)$ and so $\mathbf{m}^T \mathbf{l} = 0$ if and only if $\eta = \mathbf{f}_s^T \mathbf{w} = 0$. Similarly, δp_n is undefined if $\xi = \mathbf{f}_u^T \mathbf{w} = 0$. Thus the ZSR method breaks down if \mathbf{w} is an eigenvector of M .

To analyse convergence of the new method, we observe that

$$\tilde{J} = T^{-1} J T = \begin{pmatrix} 0 & j \\ 0 & 0 \end{pmatrix}$$

where $j = \frac{\mathbf{m}^T M \mathbf{w}}{\mathbf{m}^T \mathbf{l} \mathbf{k}^T \mathbf{w}}$. We have that

$$\mathbf{x}_{n+1} - \mathbf{x}^* = \tilde{J}(\mathbf{x}_n - \mathbf{x}^*) + K(\mathbf{x}_n - \mathbf{x}^*)^T(\mathbf{x}_n - \mathbf{x}^*) + \dots$$

where K is a constant matrix, so that

$$\begin{aligned} \|\mathbf{x}_{n+2} - \mathbf{x}^*\| &= \|\tilde{J}(\mathbf{x}_{n+1} - \mathbf{x}^*) + K(\mathbf{x}_{n+1} - \mathbf{x}^*)^T(\mathbf{x}_{n+1} - \mathbf{x}^*) + \dots\| \\ &= \|\tilde{J}^2(\mathbf{x}_n - \mathbf{x}^*) + K'(\mathbf{x}_n - \mathbf{x}^*)^T(\mathbf{x}_n - \mathbf{x}^*) + \dots\| \\ &\leq C \|\mathbf{x}_n - \mathbf{x}^*\|^2 \end{aligned}$$

for some constant C and constant matrix K' , since $\tilde{J}^2 = 0$ and so the convergence of the method is two-step quadratic [81].

The geometrical interpretation of this new method is simple. We derived the control formula upon the assumption that $\mathbf{m}^T M \mathbf{l} = 0$. This implies that $M \mathbf{l} = \alpha \mathbf{w}$, for some scalar α , so that all points on the line $\alpha \mathbf{l}$ are mapped onto the line $\alpha \mathbf{w}$ in the linearised sense in the absence of parameter perturbations. Thus if we manage to place an iterate on $\alpha \mathbf{l}$ it will be mapped onto the line $\alpha \mathbf{w}$ (which passes through

the fixed point). Then a perturbation of the parameter p will push the iterate back onto $\alpha\mathbf{l}$, which to a linear approximation intersects $\alpha\mathbf{w}$ at the fixed point and so in two iterations the iterate has been placed on the fixed point (in a linear sense). The inclusion of nonlinear effects distorts this picture slightly. Under a parameter perturbation, an iterate will not be placed precisely on the line $\alpha\mathbf{l}$. Hence it will not be mapped exactly onto $\alpha\mathbf{w}$ and similarly to the fixed point \mathbf{x}^* . Clearly then, the algorithm must be applied repeatedly in order to effect control.

The Two-Step Method

The preceding methods, with the exception of the shortest distance method, were all derived upon the same principle, namely that a value for δp_n was determined in order that \mathbf{x}_{n+1} is placed on some line in phase space. The specific choice of line was entirely dependent on the choice of control criterion. Now suppose that our control criterion is that \mathbf{x}_{n+2} lies on the fixed point itself, that is, $\delta\mathbf{x}_{n+2} = \mathbf{0}$. Using the linearised map (0.3.7) twice, we have

$$\delta\mathbf{x}_{n+2} = M^2\delta\mathbf{x}_n + M\mathbf{w}\delta p_n + \mathbf{w}\delta p_{n+1}.$$

and using our control criterion we have that

$$M\mathbf{w}\delta p_n + \mathbf{w}\delta p_{n+1} = -M^2\delta\mathbf{x}_n$$

which can be written in matrix form as

$$\begin{pmatrix} M\mathbf{w} & \mathbf{w} \end{pmatrix} \begin{pmatrix} \delta p_n \\ \delta p_{n+1} \end{pmatrix} = -M^2\delta\mathbf{x}_n.$$

It is then easily verified that

$$\begin{pmatrix} \delta p_n \\ \delta p_{n+1} \end{pmatrix} = - \begin{pmatrix} \frac{\mathbf{m}^T}{\mathbf{m}^T M \mathbf{w}} \\ \frac{\mathbf{m}^T M^{-1}}{\mathbf{m}^T M^{-1} \mathbf{w}} \end{pmatrix} M^2 \delta\mathbf{x}_n. \quad (1.2.5)$$

Note that two perturbations are evaluated in one go. Thus the perturbations are calculated at every other step of the map. Geometrically, the two-step method

is identical to the ZSR method only in the linearised sense. The first step of the method involves making a perturbation defined by $\delta p_n = -\frac{\mathbf{m}^T M^2 \delta \mathbf{x}_n}{\mathbf{m}^T M \mathbf{w}}$ and noting that in the ZSR method, $\mathbf{k}^T = \mathbf{m}^T M$, so that the first step perturbations are identical. However, calculation of δp_{n+1} according to the ZSR method results in a different value to that defined in equation (1.2.5). This is simply because the ZSR method uses the observed value of \mathbf{x}_{n+1} in the calculation of the parameter perturbation, whilst the two-step method uses a linear approximation to \mathbf{x}_{n+1} . It is easily seen that the new control methods rate of convergence is two-step quadratic. The two-step modified mapping is

$$\delta \mathbf{x}_{n+2} = \left(I - \frac{M \mathbf{w} \mathbf{m}^T}{\mathbf{m}^T M \mathbf{w}} - \frac{\mathbf{w} \mathbf{m}^T M^{-1}}{\mathbf{m}^T M^{-1} \mathbf{w}} \right) M^2 \delta \mathbf{x}_n.$$

Now,

$$\begin{pmatrix} M \mathbf{w} & \mathbf{w} \end{pmatrix} \begin{pmatrix} \frac{\mathbf{m}^T}{\mathbf{m}^T M \mathbf{w}} \\ \frac{\mathbf{m}^T M^{-1}}{\mathbf{m}^T M^{-1} \mathbf{w}} \end{pmatrix} = \frac{M \mathbf{w} \mathbf{m}^T}{\mathbf{m}^T M \mathbf{w}} + \frac{\mathbf{w} \mathbf{m}^T M^{-1}}{\mathbf{m}^T M^{-1} \mathbf{w}} = I.$$

Thus the Jacobian of the modified two-step mapping is the zero matrix giving two-step quadratic convergence [81].

1.2.3 Quadratic Methods

Another way to possibly increase the rate of convergence of a control method is to make it more accurate. Instead of using a linear approximation in order to evaluate δp_n , we could use a quadratic approximation to the map. Let us return to equation (0.3.6) now. Expanding about (\mathbf{x}^*, p^*) and including terms up to second order we have

$$\mathbf{x}_{n+1} = M \mathbf{x}_n + \mathbf{w} \delta p_n + \frac{1}{2} \left(\mathbf{F}_{\mathbf{x}\mathbf{x}}^* \delta \mathbf{x}_n \delta \mathbf{x}_n + 2 \mathbf{F}_{\mathbf{x}p}^* \delta \mathbf{x}_n \delta p_n + \mathbf{F}_{pp}^* \delta p_n^2 \right) + \dots \quad (1.2.6)$$

where the superscript asterisk denotes evaluation at (\mathbf{x}^*, p^*) . Calculation of second order derivatives may not always prove possible if the map is not known. But it is often possible to estimate the map in low dimensional systems and hence calculate

these second order derivatives. See for example Shinbrot *et. al.* [72] where the Poincaré section of Lorenz's equation is seen to be well approximated by a one-dimensional map.

Using (0.3.13) and differentiating again we have

$$\frac{d^2 \mathbf{x}}{dp^2} = \left(\mathbf{F}_{\mathbf{x}\mathbf{x}} \frac{d\mathbf{x}}{dp} + \mathbf{F}_{\mathbf{x}p} \right) \frac{d\mathbf{x}}{dp} + \mathbf{F}_{\mathbf{x}} \frac{d^2 \mathbf{x}}{dp^2} + \mathbf{F}_{\mathbf{x}p} \frac{d\mathbf{x}}{dp} + \mathbf{F}_{pp}$$

so that at the fixed point \mathbf{x}^* ,

$$(I - M) \frac{d^2 \mathbf{x}^*}{dp^2} = \left(\mathbf{F}_{\mathbf{x}\mathbf{x}}^* \frac{d\mathbf{x}^*}{dp} + \mathbf{F}_{\mathbf{x}p}^* \right) \frac{d\mathbf{x}^*}{dp} + \mathbf{F}_{\mathbf{x}p}^* \frac{d\mathbf{x}^*}{dp} + \mathbf{F}_{pp}^*. \quad (1.2.7)$$

Now, $M(p) = \mathbf{F}_{\mathbf{x}}(\mathbf{x}(p), p)$. Thus

$$\begin{aligned} \tilde{M} &:= \frac{dM(p)}{dp} = \mathbf{F}_{\mathbf{x}\mathbf{x}} \frac{d\mathbf{x}}{dp} + \mathbf{F}_{\mathbf{x}p} \\ &= \mathbf{F}_{\mathbf{x}\mathbf{x}}^* \frac{d\mathbf{x}^*}{dp} + \mathbf{F}_{\mathbf{x}p}^* \end{aligned}$$

when evaluated at the fixed point. Thus, substituting into (1.2.7),

$$(I - M) \frac{d^2 \mathbf{x}^*}{dp^2} = \tilde{M} \frac{d\mathbf{x}^*}{dp} + \mathbf{F}_{\mathbf{x}p}^* \frac{d\mathbf{x}^*}{dp} + \mathbf{F}_{pp}^*$$

and substituting for \mathbf{F}_{pp}^* in the second order expansion (1.2.6) gives

$$\begin{aligned} \delta \mathbf{x}_{n+1} &\simeq M \delta \mathbf{x}_n + \mathbf{w} \delta p_n + \frac{1}{2} \left(\mathbf{F}_{\mathbf{x}\mathbf{x}}^* \delta \mathbf{x}_n \delta \mathbf{x}_n + 2 \mathbf{F}_{\mathbf{x}p}^* \delta \mathbf{x}_n \delta p_n - \mathbf{F}_{\mathbf{x}p}^* \frac{d\mathbf{x}}{dp} \delta p_n^2 \right. \\ &\quad \left. + \left((I - M) \frac{d^2 \mathbf{x}^*}{dp^2} - \tilde{M} \frac{d\mathbf{x}^*}{dp} \right) \delta p_n^2 \right). \end{aligned}$$

In the case where the map \mathbf{F} is unknown, we do not know $\mathbf{F}_{\mathbf{x}\mathbf{x}}^*$ and $\mathbf{F}_{\mathbf{x}p}^*$ and so discarding terms involving these derivatives, we have the semi-second order expansion

$$\delta \mathbf{x}_{n+1} \simeq M \delta \mathbf{x}_n + \mathbf{w} \delta p_n + \frac{1}{2} \left((I - M) \frac{d^2 \mathbf{x}^*}{dp^2} - \tilde{M} \frac{d\mathbf{x}^*}{dp} \right) \delta p_n^2. \quad (1.2.8)$$

Using $\mathbf{f}_u^T \delta \mathbf{x}_{n+1} = 0$ we obtain a semi-quadratic equation for δp_n , whose solution will in general give two values for the perturbation parameter. We then work

out the value of δp_n according to the OGY method and take the nearest solution obtained from the semi-quadratic expansion as our perturbation parameter (since the same criterion is used in evaluating each). A quadratic ZSR method can also be derived by using the criterion $\mathbf{k}^T \delta \mathbf{x}_{n+1} = 0$ in order to evaluate δp_n . Note that (1.2.8) gives rise to three methods. We may include, as the coefficient of δp_n^2 , only $(I - M) \frac{d^2 \mathbf{x}^*}{dp^2}$, or $\tilde{M} \frac{d\mathbf{x}^*}{dp}$ or both. Discarding some of the second order terms is a little ad hoc, but they are only discarded if they cannot be calculated. The inclusion of only some of the second order terms can improve the rate of convergence in certain cases, but this cannot be guaranteed.

If we use the central difference approximation to estimate \mathbf{w} , the calculation of $\frac{d^2 \mathbf{x}^*}{dp^2}$ is straightforward. The well-known approximation to order δp^2 is

$$\frac{d^2 \mathbf{x}^*}{dp^2} \simeq \frac{\mathbf{x}_F(p + \delta p) - 2\mathbf{x}_F(p) + \mathbf{x}_F(p - \delta p)}{\delta p^2}$$

and that for \tilde{M} is

$$\tilde{M} \simeq \frac{M(p) - M(-p)}{2p}.$$

Clearly, if we are using the central difference approximation to $\frac{d\mathbf{x}^*}{dp}$, the calculation of $\frac{d^2 \mathbf{x}^*}{dp^2}$ and \tilde{M} requires little extra computation.

1.3 Higher Dimensional Systems

We have seen that a control algorithm may be formed in many ways, each formulation having different convergence properties. But the methods discussed previously are limited in that they are applicable only to two-dimensional maps. It would clearly be useful to be generalise these methods for application to the N -dimensional problem

We shall assume an N -dimensional map of the usual form

$$\mathbf{x}_{n+1} = \mathbf{F}(\mathbf{x}_n, p_n) \tag{1.3.9}$$

where $\mathbf{F} : \mathbb{R}^N \times \mathbb{R} \mapsto \mathbb{R}^N$. We may form an N -step quadratic method in one of two ways. The first is the higher dimensional analogy of the ZSR method. One simply uses the results obtained in Section 1.2.2 where this time, the matrices and vectors are replaced with their $N \times N$ and N -dimensional counterparts respectively. It can be shown that the method will converge provided that \mathbf{w} is not an eigenvector of M [46].

An alternative approach is an extension of the two-step method of Section 1.2.2. We begin by defining a subspace π_1 which contains both \mathbf{w} and the vector \mathbf{l} which is orthogonal to \mathbf{k}^T and intersects \mathbf{w} at the origin. This plane is unique provided that \mathbf{w} is not an eigenvector of M . We determine a vector orthogonal to π_1 and call it \mathbf{h}_1 . Combining this with π_1 we may form a three-dimensional subspace π_2 containing \mathbf{l} , \mathbf{w} and \mathbf{h}_1 . Then form a vector orthogonal the subspace π_2 and call it \mathbf{h}_2 . Repeat the process until one obtains π_{N-1} , which is of dimension N . The vectors $\mathbf{h}_1, \mathbf{h}_2, \dots, \mathbf{h}_{N-2}$ are easily determined via the well-known Gram-Schmidt orthogonalisation process. Then we make the following elementary observation. In the two-dimensional problems considered earlier, we attempted to place an iterate on a line, or more precisely a one-dimensional subspace of the plane. The required value of δp_n was determined by premultiplying the linearisation of the map with a vector orthogonal to the subspace within which we were attempting to place the iterate. Analogously, by the application of $N - 2$ parameter perturbations we may ‘step down’ through $N - 2$ dimensions and place an iterate in the subspace π_1 . The perturbations are given by

$$\delta p_{n+i} = -\frac{\mathbf{h}_{N-i-1}^T M \delta \mathbf{x}_n}{\mathbf{h}_{N-i-1}^T \mathbf{w}} \quad (1.3.10)$$

for $i = 1, 2, \dots, N - 2$. Once in the subspace π_1 , we could apply the either the two-dimensional ZSR method or the two-step method. Since nonlinearities have been ignored in this analysis, we repeat the process, starting from the beginning, at every N th step.

Remarks

It has been demonstrated that a wide range of dynamical systems can be controlled via the application of only small parameter perturbations. We have developed several methods in the vein of the OGY approach but which have improved convergence properties. It should be noted that the methods derived here should be adapted if they are to be used on time-delay reconstructed systems. We will not discuss that here, but a similar approach to that of Dressler and Nitché [17, 18] as discussed in the Introduction should be employed.

It has been stated [17] that a problem associated with the OGY algorithm is the effect of noise. When attempting to stabilise a fixed point, noise can knock an iterate out of the region suitable for control (to be discussed in Chapter 3) so that control is not realised. There is little that can be done about the effect of noise, apart from trying to reduce the noise level itself (see [39]). In the numerical example below, it is demonstrated that one method might be more tolerant to noise than another. We will investigate why this may be so in Chapter 3.

Before control can be achieved, an orbit will wander chaotically about the attractor until it falls sufficiently close to the fixed point so that control can be activated. The length of time that the orbit wanders is known as the transient time and is closely related to the measure of the attractor in a particular region about the fixed point. It also depends upon the maximum allowed perturbation, δp_{\max} . Obviously, long transient times are undesirable and we shall investigate this and methods for their reduction in Chapters 3 and 4. The effects of noise and the possibility of long transient times are reported as being the two main problems associated with the control of chaotic dynamics [17]. The OGY and related methods are surprisingly tolerant to inaccuracies in the estimates for \mathbf{x}^* ,

w and M and we shall pursue this fact in Chapter 2.

1.4 Numerical Example

Having derived several new control algorithms in this chapter, we shall apply them, and the OGY method, to the paradigmatic map in the study of dynamical systems, the Hénon map. The Hénon map can be written as

$$\begin{aligned} x_{n+1} &= 1 - Ax_n^2 + y_n \\ y_{n+1} &= Bx_n. \end{aligned} \tag{1.4.11}$$

We shall take $A = 1.4$ and $B = 0.3$ as the nominal parameter values at which (1.4.11) possesses a chaotic attractor as shown in Fig. 1.3.

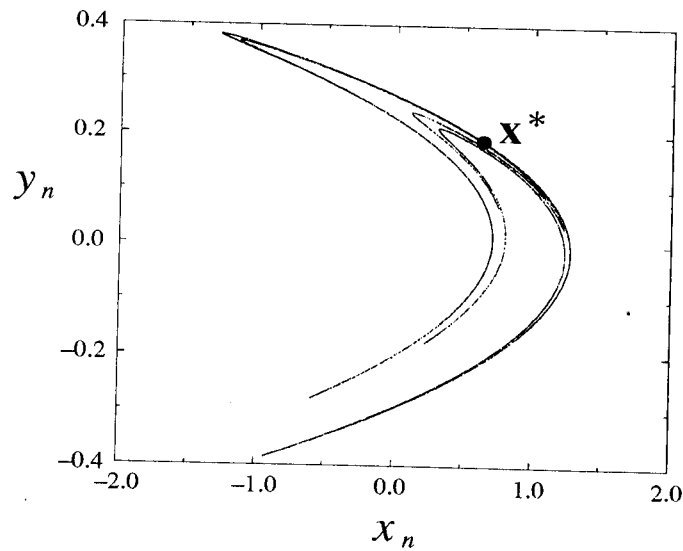


Figure 1.3: The Hénon attractor at the parameter values $A = 1.4$ and $B = 0.3$. A saddle fixed point of the mapping lies at $\mathbf{x}^{*T} = (0.631354, 0.189406)$.

Perturbations will be applied to the parameter A in order to achieve control of a fixed point of the map lying at $\mathbf{x}^{*T} = (0.631354, 0.189406)$. The Jacobian of the mapping at that point is

$$J(\mathbf{x}^*) = \begin{pmatrix} -1.767793 & 1 \\ 0.3 & 0 \end{pmatrix}$$

which has eigenvalues $\lambda_u = -1.923739$ and $\lambda_s = 0.155946$ and so \mathbf{x}^{*T} is a saddle fixed point of the mapping (1.4.11). The other relevant vector quantities are

$$\begin{aligned}\mathbf{e}_s^T &= (0.486654, 0.936195), & \mathbf{e}_u^T &= (0.988058, -0.154084), \\ \mathbf{f}_s^T &= (0.154084, 0.988058), & \mathbf{f}_u^T &= (0.936195, -0.486654)\end{aligned}$$

and

$$\mathbf{w}^T = (-0.398608, 0).$$

In order to draw a comparison between the performance of the methods, we shall take an ensemble of 136 initial conditions centered about the fixed point (Fig. 1.4) and apply each of the control algorithms in order to stabilise the fixed point \mathbf{x}^* . A method shall be deemed to have converged to the fixed point when it manages to place an iterate in an δ -neighbourhood of \mathbf{x}^* , where $\delta = 10^{-9}$. The number of iterations required to obtain convergence is averaged over all the initial conditions. The results are summarised in Table 1.1. See Fig. 1.7 for the number of iterations required until convergence for each of the initial conditions and each of the methods. Note that accurate values (up to fifteen decimal places) for the fixed point and the Jacobian matrix are used in order to obtain a fair comparison between the methods, but only six decimal places are quoted here. Approximations could introduce bias since one method might be more tolerant to inaccuracies than another.

The situation investigated here is a somewhat idealised one since most systems will contain at least some element of noise. To reflect this, let us investigate the noisy Hénon map

$$\begin{aligned}x_{n+1} &= 1 - 1.4x_n^2 + y_n + v_{1n} \\ y_{n+1} &= 0.3x_n + v_{2n}\end{aligned}\tag{1.4.12}$$

where the v_{in} are independently distributed random noise variables, $i = 1, 2$. With the noise distributed as $\text{Normal}(0, 1.8 \times 10^{-7})$ any small scale structure in the map is fuzzed out (Fig. 1.5) but the methods are still effective. They remain so provided

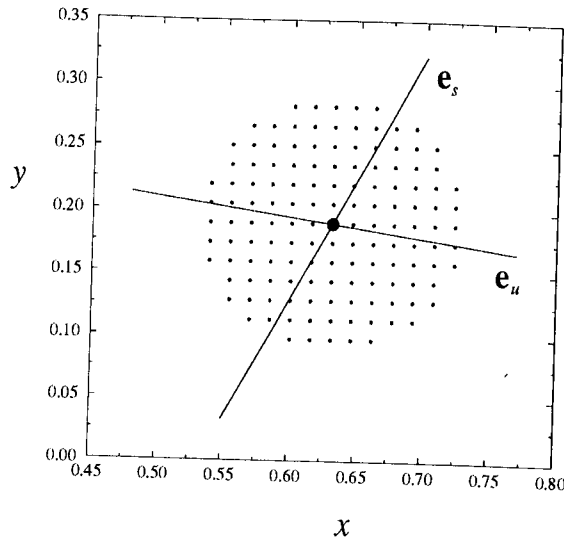


Figure 1.4: The fixed point is at the centre of an ensemble of 136 evenly spaced initial conditions within a distance of 0.1 of \mathbf{x}^* . Also shown here are the linearised stable and unstable manifolds of \mathbf{x}^* . The vector \mathbf{w} lies parallel to the x -axis.

that the noise signal is not too large. With this level of noise and a maximum perturbation of $\delta p_{\max} = 0.06$, the map cannot be completely controlled using the OGY method and bursts of chaotic motion are frequently observed, as can be seen in Fig. 1.6. These bursts occur when an iterate is pushed outside the region suitable for control. The iterates then wander chaotically around the uncontrolled attractor until they land sufficiently close to the fixed point for control to be attempted again. In the presence of noise, one must use estimates to the fixed point and the Jacobian. The estimates in this case are $\mathbf{x}^{*T} = (0.627213, 0.177937)$ and

$$J(\mathbf{x}^*) \simeq \begin{pmatrix} 1.757488 & 0.997021 \\ 0.294546 & -0.009457 \end{pmatrix}$$

whose eigenvalues are $\lambda_u = -1.911856$ and $\lambda_s = 0.144911$, comparing favourably with the true values. The eigenvectors of the Jacobian are also close to the true values. The worst estimate here seems to be $\mathbf{w}^T = (-0.396521, -0.142562)$ whose second entry has been pushed well away from zero. These estimates are obtained using $N = 40$ pairs of iterates in the regression procedure, collected within a

Control Method	Iterations Before Convergence
OGY	12.34
Linear Perturbation ($\epsilon = 0.15$)	11.29
Quadratic Perturbation ($\epsilon = 0.15$)	10.67
Quadratic Perturbation ($\epsilon = 0.20$)	10.04
Shortest Distance	6.73
ZSR	6.73
Two-Step	10.75
Quadratic	9.45
Semi-Quadratic	10.01

Table 1.1: The average number of iterations required to observe convergence to the fixed point $\mathbf{x}^* = (0.631354 \dots, 0.189406 \dots)$ for various control algorithms.

distance of 2.5×10^{-2} from the (estimated) fixed point.

With the same level of noise present, the ZSR method manages to completely control the mapping. In fact, a maximum perturbation of $\delta p_{\max} = 0.05$ suffices to completely effect control, and control is easily maintained for over 10,000 iterations of the mapping (1.4.12). To obtain the same results with the OGY method, a maximum perturbation of $\delta p_{\max} = 0.062$ must be used. This is a good indication that the ZSR method copes better in the presence of noise than the OGY method. A possible explanation for this is that the ZSR method seeks to place an iterate on the fixed point as quickly as possible, in fact, in two iterations of the map. The fixed point lies at the centre of the region where control may be effected, as we shall see in Chapter 3. On the other hand, the OGY method places iterates on the linearised stable manifold of the fixed point where they are more vulnerable to being thrown from the region suitable for control activation. This explanation will be clarified in Chapter 3.

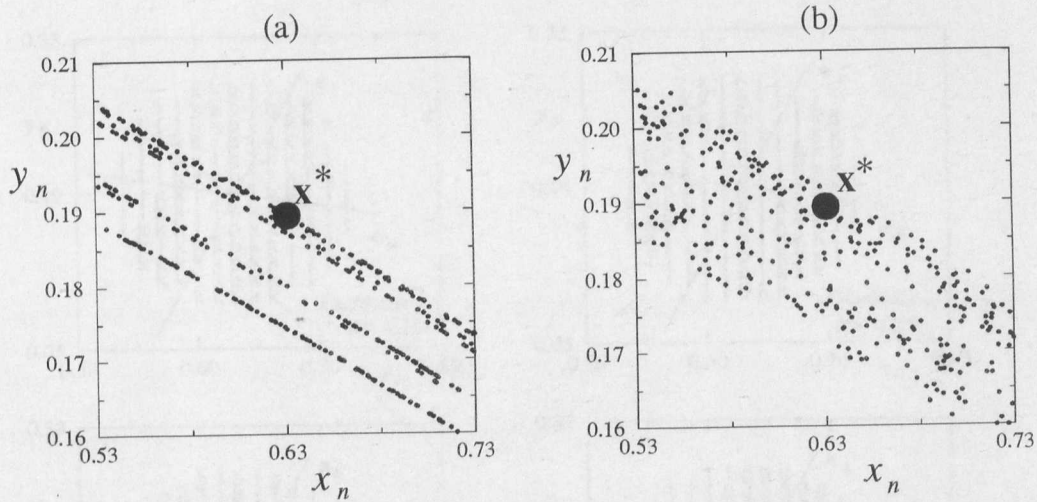


Figure 1.5: Small scale structure of the Hénon map (a) in the absence of noise, and (b) with noise distributed as $\text{Normal}(0, 1.8 \times 10^{-7})$.

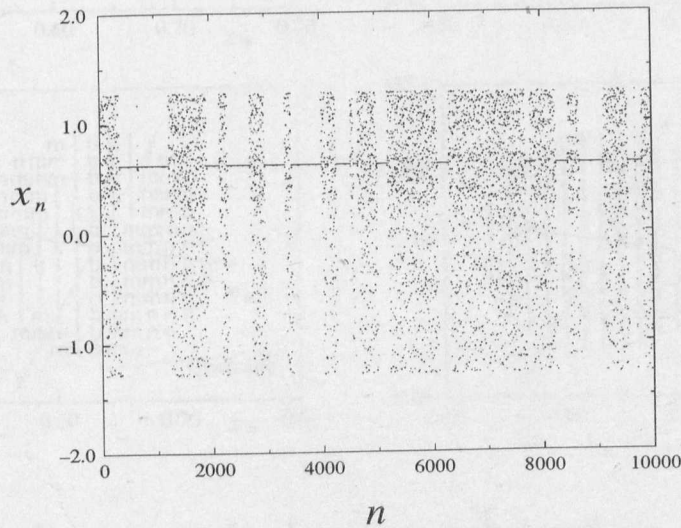


Figure 1.6: The Hénon map proves impossible to fully control in the presence of small amplitude noise with the OGY method. Only ‘windows’ of controlled behaviour are observed.

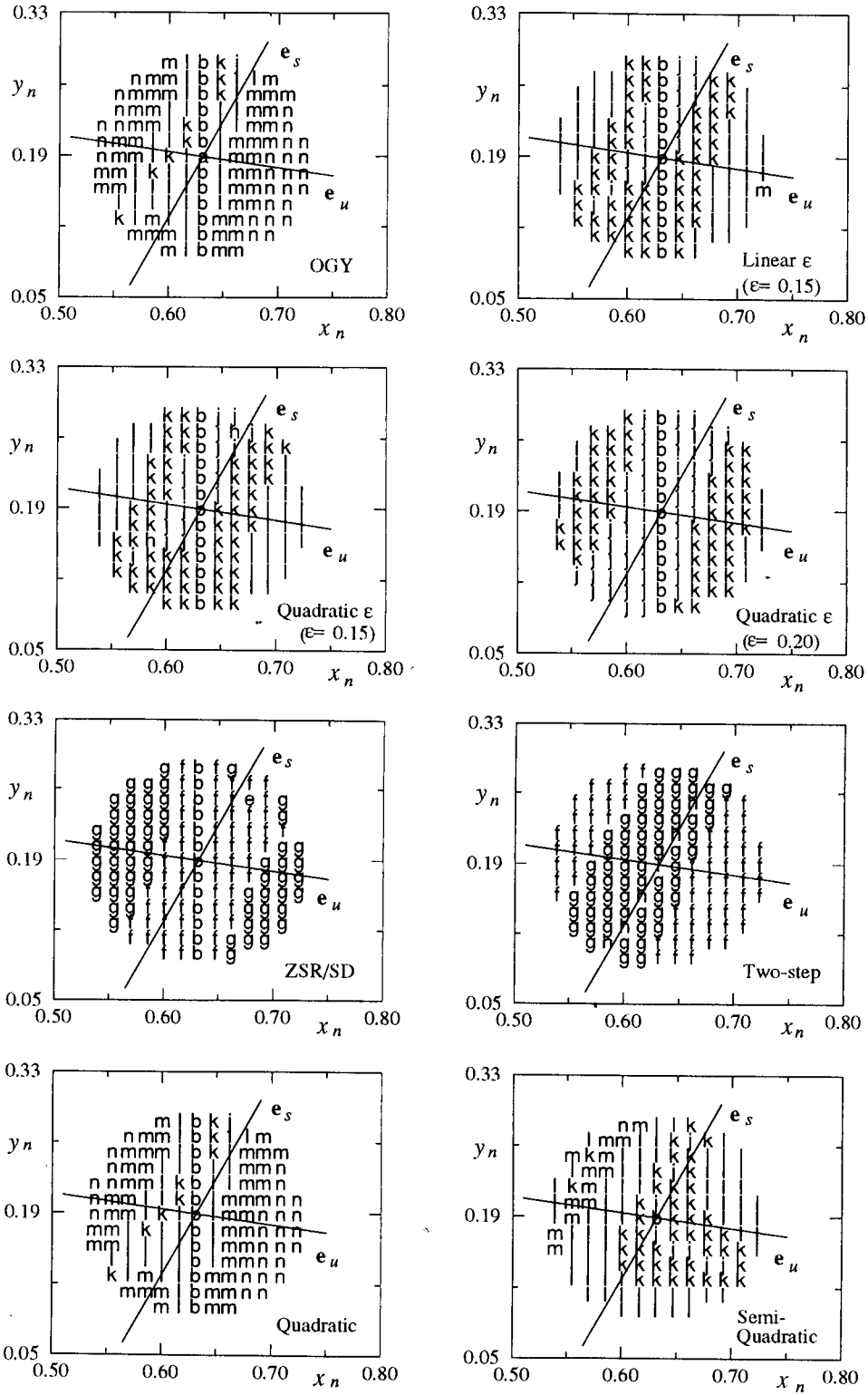


Figure 1.7: Rates of convergence for the various control methods. The n th letter of the alphabet represents n iterations until convergence for the 136 evenly spaced initial conditions.

Chapter 2

Robust Methods and Tolerance

In Chapter 1 we derived several new methods for the control of chaos and analysed their convergence properties. The Hénon map was used as a numerical example for these methods in which we find an approximate fixed or periodic point and estimate the local linearised map about that point. We now concern ourselves with the fact that we often only have *approximations* to the fixed point \mathbf{x}^* and indeed to \mathbf{w} and M and it is precisely these approximations that we have to implement the methods with. But are these approximations always acceptable? Indeed, how accurate do these approximations have to be in order that the control of chaos may still be achieved? We look at the effects of these inherent inaccuracies in the estimation of the quantities we need in order to implement both the OGY method and the strongest of our new methods, the ZSR method. Firstly though, we shall investigate whether it is possible to derive robust methods, that is, methods that are robust in the presence of inaccuracies in our estimations for \mathbf{x}^* , \mathbf{w} and M . We shall look separately at the cases when only one quantity, either \mathbf{x}^* , \mathbf{w} or M is perturbed whilst the other quantities used in the implementation of the methods are taken to be exact. In practice this will rarely be the case but it is justifiable for the proceeding analysis. For suppose we have a function of several variables $H(x, y, z)$, the number of variables being three in this case. Then if x , y and z are

perturbed to $x + \delta x$, $y + \delta y$ and $z + \delta z$ respectively, the function H changes to $H(x + \delta x, y + \delta y, z + \delta z)$. This change in H may be investigated by carrying out a Taylor expansion about (x, y, z) giving

$$\begin{aligned}\delta H &= H(x + \delta x, y + \delta y, z + \delta z) - H(x, y, z) \\ &= \frac{\partial H}{\partial x}(x, y, z)\delta x + \frac{\partial H}{\partial y}(x, y, z)\delta y + \frac{\partial H}{\partial z}(x, y, z)\delta z\end{aligned}$$

to a first order approximation. δH represents the change in H due to a change in the variables x , y and z . $\frac{\partial H}{\partial x}$, $\frac{\partial H}{\partial y}$ and $\frac{\partial H}{\partial z}$ are measures of the magnitude of the effects of perturbations in x , y and z respectively. We can investigate the change in H due to the change in each individual variable, the overall change in H being the sum of the changes due to each of the variables. The proceeding analyses are analogous to looking at each of the first order partial derivatives in turn.

2.1 Robust Methods

In this section we shall be interested in methods that, in the presence of inaccuracies, converge well (in the sense of the rate at which they converge) and simultaneously, converge to the true fixed point \mathbf{x}^* . The need for the latter is not immediately apparent. However, one could envisage encountering problems if the point we were attempting to stabilise actually lay on the unstable manifold of some nearby true fixed point of the map. This could indeed occur if we were to procure a ‘bad’ estimate to the fixed point in our approximations. In such a scenario, iterates of the map could quite easily be rapidly pushed from the control region and render the control ineffective.

In Chapter 1 we mainly sought control formulas of the form

$$\delta p_n = -\frac{\mathbf{h}^T M \delta \mathbf{x}_n}{\mathbf{h}^T \mathbf{w}} \quad (2.1.1)$$

where \mathbf{h}^T assumed a different value for each of the different control criteria. In the proceeding sections we shall seek forms for \mathbf{h}^T whereby convergence to the true fixed point \mathbf{x}^* occurs at some pre-determined acceptable rate. We shall consider inaccuracies in \mathbf{x}^* , \mathbf{w} and M separately.

2.1.1 Inaccuracies in \mathbf{x}^*

For some given ‘bad’ approximation to the fixed point, call it \mathbf{x}_R^* , the operational control formula is simply

$$\begin{aligned}\delta\hat{p}_n &:= -\frac{\mathbf{h}^T M}{\mathbf{h}^T \mathbf{w}}(\mathbf{x}_n - \mathbf{x}_R^*) \\ &= -\frac{\mathbf{h}^T M \delta \mathbf{x}_n}{\mathbf{h}^T \mathbf{w}} - \frac{\mathbf{h}^T M}{\mathbf{h}^T \mathbf{w}}(\mathbf{x}^* - \mathbf{x}_R^*) \\ &= \delta p_n + q\end{aligned}\tag{2.1.2}$$

where δp_n is defined as in (2.1.1) and $q := -\frac{\mathbf{h}^T M}{\mathbf{h}^T \mathbf{w}}(\mathbf{x}^* - \mathbf{x}_R^*)$ is a small constant, since \mathbf{x}_R^* is assumed to lie close to the true fixed point \mathbf{x}^* . The mapping in the presence of parameter perturbations is then

$$\mathbf{x}_{n+1} = \mathbf{F}(\mathbf{x}_n, \delta p_n(\mathbf{x}_n) + q).\tag{2.1.3}$$

Suppose we converge to some fixed point using the control formula defined by (2.1.2). Denote this fixed point by \mathbf{x}^+ . Note that it is almost certainly not a fixed point of the dynamical system when $p = p^*$ but a newly created one near to the true fixed point \mathbf{x}^* . However, it must be a fixed point of the modified mapping (2.1.3). Now write

$$\mathbf{x}_n = \mathbf{x}^* + q\bar{\mathbf{x}} + O(q^2)\tag{2.1.4}$$

for some suitable $\bar{\mathbf{x}}$. Then

$$\begin{aligned}\delta p_n(\mathbf{x}_n) &= \delta p_n(\mathbf{x}^* + q\bar{\mathbf{x}} + O(q^2)) \\ &= \delta p_n(\mathbf{x}^*) + qD_{\mathbf{x}}\delta p_n(\mathbf{x}^*)\bar{\mathbf{x}} + O(q^2).\end{aligned}$$

Substituting into (2.1.3) and evaluating at the fixed point (where $\mathbf{x}_{n+1} = \mathbf{x}_n$), we have

$$\begin{aligned} \mathbf{x}^* + q\bar{\mathbf{x}} + O(q^2) &= \mathbf{F}(\mathbf{x}^* + q\bar{\mathbf{x}} + O(q^2), \delta p_n(\mathbf{x}^*) + qD_{\mathbf{x}}\delta p_n(\mathbf{x}^*)\bar{\mathbf{x}} + q + O(q^2)) \\ &= \mathbf{F}(\mathbf{x}^*, \delta p_n(\mathbf{x}^*)) + \mathbf{F}_{\mathbf{x}}(\mathbf{x}^*, \delta p_n(\mathbf{x}^*)) (q\bar{\mathbf{x}} + O(q^2)) \\ &\quad + \mathbf{F}_p(\mathbf{x}^*, \delta p_n(\mathbf{x}^*)) (qD_{\mathbf{x}}\delta p_n(\mathbf{x}^*)\bar{\mathbf{x}} + q + O(q^2)) \end{aligned}$$

Thus

$$q\bar{\mathbf{x}} = M(q\bar{\mathbf{x}} + O(q^2)) + \mathbf{w} \left(-q \frac{\mathbf{h}^T M}{\mathbf{h}^T \mathbf{w}} \bar{\mathbf{x}} + q + O(q^2) \right).$$

Equating coefficients in $O(q)$, we have that

$$\bar{\mathbf{x}} = \left(I - \frac{\mathbf{w}\mathbf{h}^T}{\mathbf{h}^T \mathbf{w}} \right) M\bar{\mathbf{x}} + \mathbf{w}$$

and so

$$(I - PM)\bar{\mathbf{x}} = \mathbf{w} \tag{2.1.5}$$

where $P = \left(I - \frac{\mathbf{w}\mathbf{h}^T}{\mathbf{h}^T \mathbf{w}} \right)$. From (2.1.4),

$$\bar{\mathbf{x}} \simeq \frac{\mathbf{x}_n - \mathbf{x}^*}{q}$$

so that when $\mathbf{x}_n = \mathbf{x}^+$,

$$\bar{\mathbf{x}} \simeq \frac{\mathbf{x}^+ - \mathbf{x}^*}{q}.$$

Thus

$$(I - PM)(\mathbf{x}^+ - \mathbf{x}^*) \simeq q\mathbf{w}.$$

Now,

$$q\mathbf{w} = -\frac{\mathbf{w}\mathbf{h}^T M}{\mathbf{h}^T \mathbf{w}}(\mathbf{x}^* - \mathbf{x}_R^*) = (P - I)M(\mathbf{x}^* - \mathbf{x}_R^*)$$

and so

$$(I - PM)(\mathbf{x}^+ - \mathbf{x}^*) \simeq (P - I)M(\mathbf{x}^* - \mathbf{x}_R^*)$$

which gives that

$$(I - PM)\mathbf{x}^+ \simeq (I - P)M\mathbf{x}_R^*.$$

Hence

$$\mathbf{x}^+ = (I - PM)^{-1}(I - P)M\mathbf{x}_R^* \quad (2.1.6)$$

to a first order approximation. Thus by a suitable choice of P , one can actually choose the location of the fixed point that the control method converges to. This endows us with a degree of flexibility which we would not normally have if \mathbf{x}_R^* were indeed the true fixed point of the dynamical system. We could of course choose P so that convergence occurs at some ‘optimum’ rate, if so desired.

As a specific example of choosing the fixed point we converge to, Fig. 2.1 shows an estimated fixed point of the Hénon map as used in Chapter 1. By choosing different projections P , we obtain a one parameter family of fixed points \mathbf{x}^+ of the modified mapping shown by the line approximately emanating from the fixed point \mathbf{x}_R^* . It is possible to obtain system behaviour that would not normally be observed, since we are able to find methods that converge to a fixed point that is not even on the attractor itself. This fixed point is of course spurious in that it is not a fixed point of the dynamical system in the absence of parameter perturbations, but only a fixed point of the modified mapping (2.1.3). Note that, by setting $\mathbf{x}^+ = \mathbf{x}_R^*$ in equation (2.1.6), we will converge to the fixed point \mathbf{x}_R^* only if $(I - M)\mathbf{x}_R^* = \mathbf{0}$. Clearly then, convergence to \mathbf{x}_R^* will never occur, since M would have to be the identity matrix. Similarly, for convergence to the true fixed point to occur we would require that $\mathbf{x}^* = (I - PM)^{-1}(I - P)\mathbf{x}_R^*$. But as P is a one parameter family of projections (since only the angle of \mathbf{h}^T is important), this will generically never occur.

Upon convergence to the fixed point \mathbf{x}^+ , parameter perturbations will settle down to some non-zero value, say δp^+ , since $\mathbf{x}^+ \neq \mathbf{x}_R^*$. It is then the Jacobian of the modified iteration $\mathbf{x}_{n+1} = \mathbf{F}(\mathbf{x}_n, p^* + \delta \hat{p}_n(\mathbf{x}_n))$, evaluated at \mathbf{x}^+ , which governs the rate of convergence to the fixed point \mathbf{x}^+ . This Jacobian is simply

$D_{\mathbf{x}}\mathbf{F}(\mathbf{x}^+, p^* + \delta p(\mathbf{x}^+))$. Let us expand this as a Taylor series about (\mathbf{x}^*, p^*) by writing

$$\begin{aligned} D_{\mathbf{x}}\mathbf{F}(\mathbf{x}^+, p^* + \delta p(\mathbf{x}^+)) &= D_{\mathbf{x}}\mathbf{F}(\mathbf{x}^* + (\mathbf{x}^+ - \mathbf{x}^*), p^* + \delta p(\mathbf{x}^* + (\mathbf{x}^+ - \mathbf{x}^*))) \\ &= D_{\mathbf{x}}\mathbf{F}(\mathbf{x}^* + \delta\mathbf{x}^+, p^* + \delta p(\mathbf{x}^* + \delta\mathbf{x}^+)) \end{aligned}$$

where $\delta\mathbf{x}^+ = \mathbf{x}^+ - \mathbf{x}^*$. We have that

$$\delta p(\mathbf{x}^* + \delta\mathbf{x}^+) = \delta p(\mathbf{x}^*) + D_{\mathbf{x}}\delta p(\mathbf{x}^*)\delta\mathbf{x}^+ + \dots = D_{\mathbf{x}}\delta p(\mathbf{x}^*)\delta\mathbf{x}^+ + \dots$$

by a Taylor expansion, since $\delta p(\mathbf{x}^*) = 0$. Also,

$$\begin{aligned} \mathbf{F}_{\mathbf{x}}(\mathbf{x}^+, p^* + \delta p^+) &= \mathbf{F}_{\mathbf{x}}^* + \mathbf{F}_{\mathbf{xx}}^*\delta\mathbf{x}^+ - \mathbf{F}_{\mathbf{x}p}^* \frac{\mathbf{h}^T M}{\mathbf{h}^T \mathbf{w}} \delta\mathbf{x}^+ + \dots, \\ \mathbf{F}_p(\mathbf{x}^+, p^* + \delta p^+) &= \mathbf{F}_p^* + \mathbf{F}_{xp}^*\delta\mathbf{x}^+ - \mathbf{F}_{pp}^* \frac{\mathbf{h}^T M}{\mathbf{h}^T \mathbf{w}} \delta\mathbf{x}^+ + \dots \end{aligned}$$

where $\mathbf{F}_{\mathbf{x}}^* = \mathbf{F}(\mathbf{x}^*, p^*)$ etc. Then to a first order approximation

$$\begin{aligned} \mathbf{F}_{\mathbf{x}}^+ := D_{\mathbf{x}}\mathbf{F}(\mathbf{x}^+, p^* + \delta p^+) &= \mathbf{F}_{\mathbf{x}}^* + \mathbf{F}_{\mathbf{xx}}^*\delta\mathbf{x}^+ - \mathbf{F}_{\mathbf{x}p}^* \frac{\mathbf{h}^T M}{\mathbf{h}^T \mathbf{w}} \delta\mathbf{x}^+ \\ &\quad - \left(\mathbf{F}_p^* + \mathbf{F}_{xp}^*\delta\mathbf{x}^+ - \mathbf{F}_{pp}^* \frac{\mathbf{h}^T M}{\mathbf{h}^T \mathbf{w}} \delta\mathbf{x}^+ \right) \frac{\mathbf{h}^T M}{\mathbf{h}^T \mathbf{w}} \\ &= \left(I - \frac{\mathbf{w}\mathbf{h}^T}{\mathbf{h}^T \mathbf{w}} \right) M + \mathbf{F}_{\mathbf{xx}}^*\delta\mathbf{x}^+ - \mathbf{F}_{\mathbf{x}p}^* \frac{\mathbf{h}^T M}{\mathbf{h}^T \mathbf{w}} \delta\mathbf{x}^+ \\ &\quad - \left(\mathbf{F}_{xp}^*\delta\mathbf{x}^+ - \mathbf{F}_{pp}^* \frac{\mathbf{h}^T M}{\mathbf{h}^T \mathbf{w}} \delta\mathbf{x}^+ \right) \frac{\mathbf{h}^T M}{\mathbf{h}^T \mathbf{w}} \\ &= \left(I - \frac{\mathbf{w}\mathbf{h}^T}{\mathbf{h}^T \mathbf{w}} \right) M + \tilde{J} \end{aligned} \tag{2.1.7}$$

where $\tilde{J} = \mathbf{F}_{\mathbf{xx}}^*\delta\mathbf{x}^+ - \mathbf{F}_{xp}^* \frac{\mathbf{h}^T M}{\mathbf{h}^T \mathbf{w}} \delta\mathbf{x}^+ - \left(\mathbf{F}_{xp}^*\delta\mathbf{x}^+ - \mathbf{F}_{pp}^* \frac{\mathbf{h}^T M}{\mathbf{h}^T \mathbf{w}} \delta\mathbf{x}^+ \right) \frac{\mathbf{h}^T M}{\mathbf{h}^T \mathbf{w}}$. Thus the Jacobian of the iteration is perturbed by the use of \mathbf{x}_R^* in the control formula. We can conclude that any method using an inaccurate value of \mathbf{x}^* its implementation is not robust in the sense it will not converge to the true fixed point, nor will it converge at its ‘true’ rate but rather at some different rate.

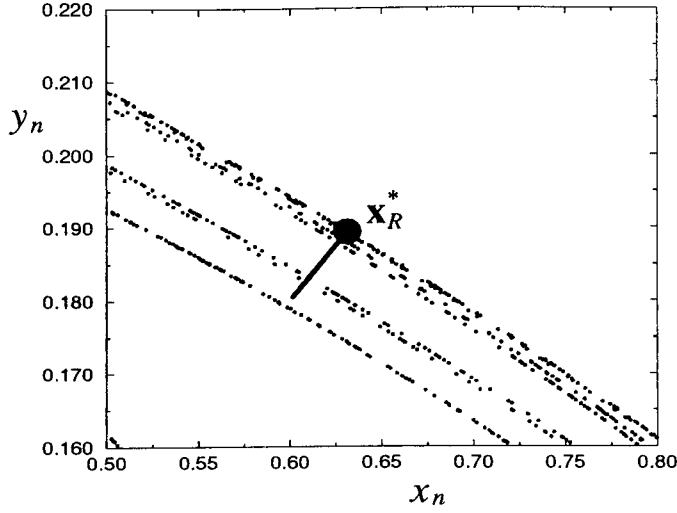


Figure 2.1: A family of fixed points of the Hénon map created using different forms for the projection P .

2.1.2 Inaccuracies in \mathbf{w}

Now suppose the estimate of \mathbf{w} is inaccurate. Denote this estimate by $\hat{\mathbf{w}}$. Let us write $\hat{\mathbf{w}} = \alpha\mathbf{w} + \beta\mathbf{h}^\perp$ where \mathbf{h}^\perp is orthogonal to \mathbf{h} . Note that $\mathbf{h}^T\mathbf{w} \neq 0$ which implies $\mathbf{h}^\perp \neq \mathbf{w}$ and so this is a valid representation of $\hat{\mathbf{w}}$. The control formula is then given by

$$\delta\hat{p}_n := -\frac{\mathbf{h}^T M \delta\mathbf{x}_n}{\mathbf{h}^T \hat{\mathbf{w}}} = -\frac{\mathbf{h}^T M \delta\mathbf{x}_n}{\alpha \mathbf{h}^T \mathbf{w}}$$

and so the linearised modified mapping in the presence of parameter perturbations is

$$\delta\mathbf{x}_{n+1} = M\delta\mathbf{x}_n - \frac{\mathbf{w}\mathbf{h}^T M \delta\mathbf{x}_n}{\alpha \mathbf{h}^T \mathbf{w}}$$

whose Jacobian is clearly

$$\hat{J} := \left(I - \frac{\mathbf{w}\mathbf{h}^T}{\alpha \mathbf{h}^T \mathbf{w}} \right) M. \quad (2.1.8)$$

The rate at which convergence occurs will be affected by the size and sign of α , if indeed, convergence occurs at all. We will show later that convergence does occur for a range of values of α . Note that \mathbf{x}^* is still a fixed point of the nonlinear map,

and so for particular values of α , convergence to the true fixed point will occur. Thus in attempting to construct a robust method, our problem is to choose \mathbf{h} such that the eigenvalues of (2.1.8) can be kept inside the unit circle for a wide range of values of α .

Let us write $\mathbf{w} = \eta \mathbf{e}_s + \xi \mathbf{e}_u$ and $\mathbf{h}^T = \theta_1 \mathbf{f}_s^T + \theta_2 \mathbf{f}_u^T$. A normalisation condition is set on \mathbf{h}^T such that $\mathbf{h}^T \mathbf{e}_u = 1$ in order to simplify the algebra below. We may then write $\mathbf{h}^T = \theta \mathbf{f}_s^T + \mathbf{f}_u^T$ where $\theta = \frac{\theta_1}{\theta_2}$. In that case,

$$\hat{J} = M - \frac{(\eta \mathbf{e}_s + \xi \mathbf{e}_u)(\theta \lambda_s \mathbf{f}_s^T + \lambda_u \mathbf{f}_u^T)}{\alpha(\theta \eta + \xi)}.$$

We now look for an eigenvector of the form $c \mathbf{e}_s + d \mathbf{e}_u$ with corresponding eigenvalue $\lambda_\alpha(\theta)$. Then

$$\hat{J}(c \mathbf{e}_s + d \mathbf{e}_u) = \left(c \lambda_s - \frac{\eta(c \theta \lambda_s + d \lambda_u)}{\alpha(\theta \eta + \xi)} \right) \mathbf{e}_s + \left(d \lambda_u - \frac{\xi(c \theta \lambda_s + d \lambda_u)}{\alpha(\theta \eta + \xi)} \right) \mathbf{e}_u$$

and so the eigenvalue problem is to simultaneously solve

$$\begin{aligned} c \lambda_\alpha(\theta) &= c \lambda_s - \frac{\eta(c \theta \lambda_s + d \lambda_u)}{\alpha(\theta \eta + \xi)} \\ d \lambda_\alpha(\theta) &= d \lambda_u - \frac{\xi(c \theta \lambda_s + d \lambda_u)}{\alpha(\theta \eta + \xi)} \end{aligned} \quad (2.1.9)$$

for λ_α and say c in terms of d . One can certainly solve (2.1.9), but the solutions (of which there are two) thus produced are extremely complicated. Then we may set d arbitrarily to obtain the eigenvalues and eigenvectors of \hat{J} in terms of α and θ . Now write $\lambda_\alpha(\theta)$ as

$$\lambda_\alpha(\theta) = \lambda_1(\theta) + (\alpha - 1) \frac{d\lambda_1}{d\alpha}(\theta) + \dots \quad (2.1.10)$$

where $\lambda_1(\theta) \equiv \lambda_\alpha(\theta)$ evaluated at $\alpha = 1$. The solutions to (2.1.9) prove to be useful, since they allow the calculation of the derivative in (2.1.10). One can then determine a value of θ which minimises the absolute value of the derivative $\frac{d\lambda_1}{d\alpha}$. If the derivative term can be set to zero then $\lambda_\alpha(\theta)$ will be perturbed by $O((\alpha - 1)^2)$ terms, which can be assumed to be small for α close to unity. It turns out that the derivative is zero only when $\mathbf{h}^T = \mathbf{f}_u^T$, i.e. the perturbations are precisely those

defined by the OGY control algorithm. Thus the most robust method in the presence of inaccuracies in \mathbf{w} is the OGY method.

2.1.3 Inaccuracies in M

Let us suppose that our estimate for M is inaccurate. Denote the estimate by \hat{M} . Then the operational value of the perturbation parameter is

$$\delta \hat{p}_n = -\frac{\mathbf{h}^T \hat{M} \delta \mathbf{x}_n}{\mathbf{h}^T \mathbf{w}}. \quad (2.1.11)$$

In this case, if convergence occurs it will be to the true fixed point since \mathbf{x}^* is again a fixed point of the nonlinear map $\mathbf{x}_{n+1} = \mathbf{F}(\mathbf{x}_n, p^* + \delta \hat{p}_n(\mathbf{x}_n))$. Let us write $\hat{M} = M + \tilde{M}$ for some small matrix \tilde{M} , i.e. $\|\tilde{M}\| < \epsilon$ for some $\epsilon > 0$. Then the Jacobian of the modified mapping may be written as

$$\begin{aligned} J(\tilde{M}) &= \left(I - \frac{\mathbf{w} \mathbf{h}^T}{\mathbf{h}^T \mathbf{w}} \right) M - \frac{\mathbf{w} \mathbf{h}^T \tilde{M}}{\mathbf{h}^T \mathbf{w}} \\ &= J - \frac{\mathbf{w} \mathbf{h}^T \tilde{M}}{\mathbf{h}^T \mathbf{w}}. \end{aligned} \quad (2.1.12)$$

We may view (2.1.12) as a perturbation in J , the Jacobian of the modified mapping in the absence of any inaccuracies, provided that \tilde{M} is sufficiently small.

Wilkinson [83] gives a useful result for determining the perturbation of eigenvalues corresponding to a perturbation in a matrices elements. We give here a brief summary of Wilkinsons result in the two dimensional case. Let A and B be two square matrices of order two. Let λ_1 be a simple eigenvalue of A . We may examine the corresponding eigenvalue of $A + \epsilon B$ as follows. Assume there exists a complete set of left and right eigenvectors of A ψ_1^T, ψ_2^T and ϕ_1, ϕ_2 respectively. Then to first order λ_1 is perturbed to

$$\frac{\psi_1^T (A + \epsilon B) \phi_1}{\psi_1^T \phi_1} = \lambda_1 + \epsilon \frac{\psi_1^T B \phi_1}{\psi_1^T \phi_1}.$$

We note here that $A + \epsilon B$ defines a one-parameter family of matrices from A to $A + \epsilon B$. A and B are fixed matrices and thus we are only considering a perturbation in one parameter, namely ϵ . Examining a perturbed matrix $A + B'$ where B' is the perturbation is a much more complicated problem since this represents a four parameter problem, the four parameters being each of the entries of B' .

One can conclude from this that, up to first order, simple eigenvalues are perturbed smoothly away from their nominal values (i.e. those in the absence of any inaccuracies). Thus the obvious choice for \mathbf{h}^T in (2.1.11) is $\mathbf{k}^T = \mathbf{m}^T M$, so that the eigenvalues are perturbed away from zero in the presence of inaccuracies. Using the ZSR method and placing the unperturbed eigenvalues at zero means that they are as far as possible from their critical value on the unit circle where convergence of the control procedure will break down. Note that in its present form, Wilkinsons result is not applicable to the ZSR approach since the unperturbed Jacobian does not possess simple eigenvalues. However, the result can be generalised as follows. Let A be a matrix with an eigenvalue λ of algebraic multiplicity two. If the geometric multiplicity of λ is 1 then A only possesses a one-dimensional eigenspace. In that case we may form the generalised eigenvectors from the eigenvector corresponding to the eigenvalue λ . Let the ψ_1 and ϕ_1 be the left and right eigenvectors of A . Then the generalised eigenvectors of A can be formed by solving $\psi_2^T(A - \lambda I) = \psi_1^T$ and $(A - \lambda I)\phi_2 = \phi_1$ for ψ_2 and ϕ_2 . Let T be the matrix whose columns are the right generalised eigenvectors of A . Then T^{-1} has rows which are the left eigenvectors of A . T and T^{-1} must be chosen such that $T^{-1}T = I$ through suitable normalisation and arrangement of the eigenvectors. Then it is well known that

$$T^{-1}AT = \begin{pmatrix} \lambda & 1 \\ 0 & \lambda \end{pmatrix}$$

Suppose that $T = \begin{pmatrix} \phi_1 & \phi_2 \end{pmatrix}$ and $T^{-1} = \begin{pmatrix} \psi_2^T \\ \psi_1^T \end{pmatrix}$. Let A be perturbed to $A + \epsilon B$.

Then

$$\begin{aligned} T^{-1}(A + \epsilon B)T &= \begin{pmatrix} \lambda & 1 \\ 0 & \lambda \end{pmatrix} + \epsilon \begin{pmatrix} b_{11} & b_{12} \\ b_{21} & b_{22} \end{pmatrix} \\ &= \begin{pmatrix} \lambda + \epsilon b_{11} & 1 + \epsilon b_{12} \\ \epsilon b_{21} & \lambda + \epsilon b_{22} \end{pmatrix} \end{aligned} \quad (2.1.13)$$

where $b_{ij} = \psi_{3-i} B \phi_j$. The characteristic polynomial of (2.1.13) is

$$\mu^2 - (2\lambda + \epsilon(b_{11} + b_{22}))\mu + \lambda^2 - \epsilon(b_{21} - \lambda(b_{11} + b_{22})) + \epsilon^2(b_{11}b_{22} - b_{12}b_{21}) = 0$$

and so

$$\mu_{\pm} = \lambda + \frac{1}{2}\epsilon(b_{11} + b_{22}) \pm \frac{1}{2}\epsilon^{\frac{1}{2}}\sqrt{4b_{21} + \epsilon(b_{11}^2 - 2b_{11}b_{22} + b_{22}^2 + 4b_{12}b_{21})}.$$

By carrying out an expansion in powers of $\epsilon^{\frac{1}{2}}$, the eigenvalues of (2.1.13) are

$$\mu_{\pm} = \lambda \pm b_{21}^{\frac{1}{2}}\epsilon^{\frac{1}{2}} + \frac{1}{2}(b_{11} + b_{22})\epsilon + O(\epsilon^{\frac{3}{2}}). \quad (2.1.14)$$

Using this result we can thus tell, to an order ϵ approximation, what happens to the eigenvalues of J under a small perturbation. We shall be using this result in a subsequent section. Again though, (2.1.14) tells us that a method whose modified mapping possesses two zero eigenvalues will have those eigenvalues perturbed smoothly away from zero in the presence of inaccuracies in M . Hence the most suitable method to use in this case is the ZSR method.

2.2 Tolerance

We shall now closely analyse the effect of inaccuracies in estimates of \mathbf{x}^* , \mathbf{w} and M for both the OGY method and the ZSR method and attempt to ascertain how inaccurate quantities have to be before the methods begin to break down. The analysis for perturbations in \mathbf{x}^* leads to a neat and effective method for the dynamic refinement of the estimate to the fixed point.

2.2.1 The OGY Method

Perturbations in \mathbf{x}^*

Using the results of Section 2.1.1, application of the OGY control formula with an estimate \mathbf{x}_R^* to the fixed point, convergence to some fixed point \mathbf{x}^+ occurs at a geometrical rate governed by the eigenvalues of

$$\hat{J} = \left(I - \frac{\mathbf{w}\mathbf{f}_u^T}{\mathbf{f}_u^T\mathbf{w}} \right) M + \tilde{J} \quad (2.2.15)$$

where

$$\tilde{J} = \mathbf{F}_{\mathbf{xx}}^* \delta \mathbf{x}^+ - \mathbf{F}_{\mathbf{x}p}^* \frac{\mathbf{f}_u^T M}{\mathbf{f}_u^T \mathbf{w}} \delta \mathbf{x}^+ - \left(\mathbf{F}_{\mathbf{x}p}^* \delta \mathbf{x}^+ - \mathbf{F}_{pp}^* \frac{\mathbf{f}_u^T M}{\mathbf{f}_u^T \mathbf{w}} \delta \mathbf{x}^+ \right) \frac{\mathbf{f}_u^T M}{\mathbf{f}_u^T \mathbf{w}}.$$

If one of the eigenvalues of (2.2.15) lies outside the unit circle, convergence will not occur.

We can tell when convergence will occur by using Wilkinsons result for perturbations in matrices with distinct eigenvalues on (2.2.15). In Chapter 1 we found that the left and right eigenvectors of $J = \left(I - \frac{\mathbf{w}\mathbf{f}_u^T}{\mathbf{f}_u^T \mathbf{w}} \right) M$ were $\psi_1^T = \mathbf{f}_s^T - \chi \mathbf{f}_u^T$, $\phi_1 = \mathbf{e}_s$ corresponding to the non-zero eigenvalue and $\psi_2^T = \mathbf{f}_u^T$, $\phi_2 = \chi \mathbf{e}_s + \mathbf{e}_u$ for the zero eigenvalue, where $\chi = \frac{\lambda_u \mathbf{f}_s^T \mathbf{w}}{\lambda_s \mathbf{f}_u^T \mathbf{w}}$. Clearly, $\psi_1^T \phi_1 = 1$ and $\psi_2^T \phi_2 = 1$. Thus the non-zero eigenvalue λ_s is perturbed to

$$\left(\mathbf{f}_s^T - \chi \mathbf{f}_u^T \right) \mathbf{F}_{\mathbf{x}}^+ \mathbf{e}_s = \lambda_s + \left(\mathbf{f}_s^T - \chi \mathbf{f}_u^T \right) \tilde{J} \mathbf{e}_s$$

and the zero eigenvalue is perturbed to

$$\mathbf{f}_u^T \mathbf{F}_{\mathbf{x}}^+ (\chi \mathbf{e}_s + \mathbf{e}_u) = 0 + \mathbf{f}_u^T \tilde{J} (\chi \mathbf{e}_s + \mathbf{e}_u).$$

So in the case where \mathbf{F} is known, or can be globally well estimated, we can evaluate \tilde{J} since the second derivatives are then known.

If the OGY method does converge to the fixed point \mathbf{x}^+ , then it is possible to refine the estimate of the fixed point. In doing so, one can produce a more robust control method. From (2.1.5) we have that

$$(I - PM)\bar{\mathbf{x}} = \mathbf{w} \quad (2.2.16)$$

where $P = \left(I - \frac{\mathbf{w}\mathbf{f}_u^T}{\mathbf{f}_u^T\mathbf{w}}\right)$ is the usual projection operator for the OGY method. Note that $(I - PM)$ has eigenvalues 1 and $1 - \lambda_s$, since PM has eigenvalues 0 and λ_s , so it is non-singular and hence invertible.

The value of $\bar{\mathbf{x}}$ can be found from (2.2.16) as $\bar{\mathbf{x}} = (I - PM)^{-1}\mathbf{w}$. However, it is possible to find a simpler formula for $\bar{\mathbf{x}}$ in terms of the eigenvectors and eigenvalues of M as follows. Pre-multiplying (2.2.16) by \mathbf{f}_u^T we have

$$\mathbf{f}_u^T(I - PM)\bar{\mathbf{x}} = \mathbf{f}_u^T\mathbf{w}$$

so that

$$\mathbf{f}_u^T\bar{\mathbf{x}} = \mathbf{f}_u^T\mathbf{w}.$$

Using the familiar representation $\mathbf{w} = \eta\mathbf{e}_s + \xi\mathbf{e}_u$ and writing $\bar{\mathbf{x}} = a\mathbf{e}_s + b\mathbf{e}_u$ for suitable a and b , we then have

$$\begin{aligned} PM\bar{\mathbf{x}} &= \left(I - \frac{\mathbf{w}\mathbf{f}_u^T}{\mathbf{f}_u^T\mathbf{w}}\right)M(a\mathbf{e}_s + b\mathbf{e}_u) \\ &= \lambda_s a\mathbf{e}_s - \lambda_u \eta\mathbf{e}_s. \end{aligned}$$

From (2.2.16),

$$\bar{\mathbf{x}} - PM\bar{\mathbf{x}} - \mathbf{w} = 0$$

i.e.

$$a\mathbf{e}_s + b\mathbf{e}_u - \lambda_s a\mathbf{e}_s + \lambda_u \eta\mathbf{e}_s - \eta\mathbf{e}_s - \xi\mathbf{e}_u = 0.$$

Then equating coefficients of \mathbf{e}_s and \mathbf{e}_u gives

$$a = \left(\frac{1 - \lambda_u}{1 - \lambda_s}\right)\eta$$

and

$$b = \xi.$$

Thus

$$\begin{aligned}\bar{\mathbf{x}} &= \left(\frac{1 - \lambda_u}{1 - \lambda_s} \right) \eta \mathbf{e}_s - \xi \mathbf{e}_u \\ &= \frac{1}{1 - \lambda_s} ((1 - \lambda_u) \eta \mathbf{e}_s + (1 - \lambda_s) \xi \mathbf{e}_u).\end{aligned}$$

Clearly, if λ_s is close to unity or $|\lambda_u| \gg 1$ then $\bar{\mathbf{x}}$ is likely to be large. Similarly, if \mathbf{w} is large then $\bar{\mathbf{x}}$ could be large so that \mathbf{x}^+ is likely to be relatively far away from \mathbf{x}^* and we will converge to a fixed point that is not necessarily close to the true fixed point, nor the regression estimate to that fixed point.

When the OGY control algorithm has been used and \mathbf{x}^+ found, the relation $\mathbf{x}^* = \mathbf{x}^+ - q_{OGY} \bar{\mathbf{x}}$ may be used to find a better approximation to \mathbf{x}^* . This improved estimate may then be used when calculating δp_n . If a value of δp_n with this new estimate of \mathbf{x}^* is used and the control procedure allowed to settle to the new fixed point \mathbf{x}^+ , then \mathbf{x}^+ should procure a better approximation to \mathbf{x}^* than before. The process can then be repeated to further refine the estimate to the fixed point. See Xu and Bishop [87] for an alternative approach to refining the estimate of a fixed point. Note that in practice q_{OGY} is found from the (non-zero) value of the perturbation parameter once convergence has occurred. We have that, to a linear approximation,

$$\begin{aligned}\delta p(\mathbf{x}^+) &= -\frac{\mathbf{f}_u^T M}{\mathbf{f}_u^T \mathbf{w}} (\mathbf{x}^* + q_{OGY} \bar{\mathbf{x}} - \mathbf{x}_R^*) \\ &= q_{OGY} - q_{OGY} \frac{\mathbf{f}_u^T M}{\mathbf{f}_u^T \mathbf{w}} \bar{\mathbf{x}}\end{aligned}$$

and so

$$q_{OGY} = \frac{\delta p(\mathbf{x}^+)}{1 - \frac{\mathbf{f}_u^T M}{\mathbf{f}_u^T \mathbf{w}} \bar{\mathbf{x}}}.$$

Perturbations in \mathbf{w}

Suppose again that the approximation to \mathbf{w} is $\hat{\mathbf{w}}$ which can be expressed as $\hat{\mathbf{w}} = \alpha\mathbf{w} + \beta\mathbf{e}_s$. Recall that, from Section 2.1.2, the Jacobian of the modified iteration is

$$\hat{J}(x^*) = \left(I - \frac{\mathbf{w}\mathbf{f}_u^T}{\alpha\mathbf{f}_u^T\mathbf{w}} \right) M \quad (2.2.17)$$

It is easily shown that

$$\hat{J}\mathbf{e}_s = \lambda_s\mathbf{e}_s$$

so that λ_s is an eigenvalue of \hat{J} with (right) eigenvector \mathbf{e}_s . Also,

$$\mathbf{f}_u^T \hat{J} = \lambda_u \left(1 - \frac{1}{\alpha} \right) \mathbf{f}_u^T$$

so that $\lambda_\alpha := \lambda_u \left(1 - \frac{1}{\alpha} \right)$ is the other eigenvalue of \hat{J} with (left) eigenvector \mathbf{f}_u^T . This is not a first order result but applies to ‘large’ perturbations in \mathbf{w} , but of course still assuming that M and \mathbf{x}^* are unperturbed. Note that \mathbf{x}^* remains a fixed point of the iteration $\mathbf{x}_{n+1} = \mathbf{F}(\mathbf{x}_n, p^* + \delta\hat{p}_n(\mathbf{x}_n))$, however its stability under parametric perturbations now depends upon α .

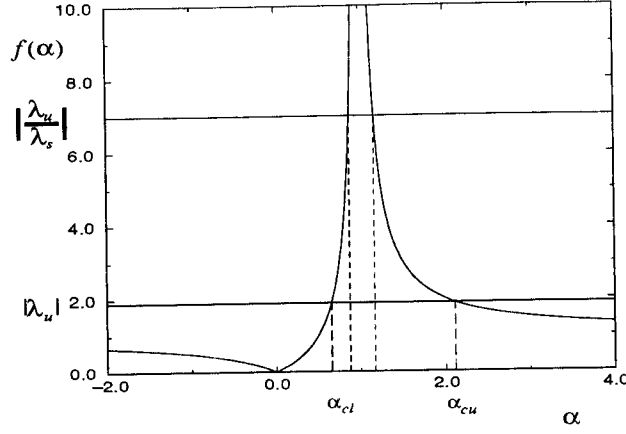
From (2.2.17) we note that it is the perturbation of \mathbf{w} to $\hat{\mathbf{w}}$ in the \mathbf{w} direction itself which is of significance and a perturbation in the \mathbf{e}_s direction, no matter how large, has no effect upon the performance of the method, at least in a linear sense. Clearly, if $\alpha = 1$, then $\lambda_\alpha = 0$ so that $\rho(\hat{J}) = |\lambda_s|$ as is expected. On the contrary, if $\alpha \neq 1$ then $\lambda_\alpha \neq 0$ and if the absolute value of λ_α were to pass through unity we might not expect the OGY method to converge to \mathbf{x}^* . Now, $|\lambda_\alpha| < 1$ when

$$\left| \lambda_u \left(1 - \frac{1}{\alpha} \right) \right| < 1$$

i.e.

$$\left| \frac{\alpha}{\alpha - 1} \right| < |\lambda_u|.$$

Thus we have a condition for the OGY method to converge to the fixed point \mathbf{x}^* .


 Figure 2.2: Plot of $f(\alpha) = \left| \frac{\alpha}{\alpha-1} \right|$.

Plotting $f(\alpha) = \left| \frac{\alpha}{\alpha-1} \right|$ against α we see that there are a range of values of α for which convergence to \mathbf{x}^* occurs, defined by the two points at which $f(\alpha) = |\lambda_u|$ (Fig. 2.2). We may determine this range of values of α explicitly by solving

$$\left| \lambda_u \left(1 - \frac{1}{\alpha} \right) \right| = 1$$

thus giving the upper and lower critical values of α at which convergence to the fixed point breaks down. Call these upper and lower critical values α_{cu} and α_{cl} respectively. Suppose that λ_u is positive. Then the lower limit satisfies

$$\lambda_u \left(1 - \frac{1}{\alpha} \right) = -1$$

i.e.

$$\alpha_{cl} = \frac{\lambda_u}{\lambda_u + 1}.$$

The upper limit satisfies

$$\lambda_u \left(1 - \frac{1}{\alpha} \right) = 1$$

and so

$$\alpha_{cu} = \frac{\lambda_u}{\lambda_u - 1}.$$

If λ_u is negative, these limits are reversed so that $\alpha_{cl} = \frac{\lambda_u}{\lambda_u - 1}$ and $\alpha_{cu} = \frac{\lambda_u}{\lambda_u + 1}$. Note that the limits are uniquely determined by the single quantity λ_u . It is the

absolute size of λ_u that determines the range of values of α for which the method converges to \mathbf{x}^* . If $|\lambda_u|$ is close to unity then this range is relatively large, but for increased values of $|\lambda_u|$, the range diminishes (see Fig. 2.2).

It was stated earlier that the rate of convergence of the OGY method is governed by the spectral radius of J , $\rho(J) = |\lambda_s|$. When \mathbf{w} is perturbed however, we must look at $\rho(\hat{J})$ for the rate of convergence. Clearly, the rate of convergence will be unaltered provided that $\rho(\hat{J}) = |\lambda_s|$. This will certainly be the case if

$$\left| \lambda_u \left(1 - \frac{1}{\alpha} \right) \right| \leq |\lambda_s|$$

the equality holding if $\alpha = \frac{\lambda_u}{\lambda_u \pm \lambda_s}$. So if $\lambda_u \lambda_s < 0$ and $\alpha \in \left[\frac{\lambda_u}{\lambda_u - \lambda_s}, \frac{\lambda_u}{\lambda_u + \lambda_s} \right]$, the rate of convergence of the method is unaffected. For $\lambda_u \lambda_s > 0$, the rate of convergence is unaffected for $\alpha \in \left[\frac{\lambda_u}{\lambda_u + \lambda_s}, \frac{\lambda_u}{\lambda_u - \lambda_s} \right]$, the limits of the interval simply reversing. This interval is small if λ_u is large compared with λ_s .

We now look at what effect a value of α outside this range has on the performance of the OGY method. Numerical simulations, using the Hénon map as a specific example, show that when values of α slightly above α_{cu} or below α_{cl} are encountered the method still often manages to converge. The OGY method does not immediately break down as one might expect, but actually converges to a slightly different fixed point or even settles on a period-2 orbit. This suggests that there is some sort of bifurcation occurring at the critical values of α .

Let us investigate this phenomena further. Define the fixed point equation for the map \mathbf{F} by

$$\mathbf{G}(\mathbf{x}, \alpha) := \mathbf{F}(\mathbf{x}, \alpha) - \mathbf{x} = 0 \quad (2.2.18)$$

where $\mathbf{G} : \mathbb{R}^2 \times \mathbb{R} \mapsto \mathbb{R}^2$. A bifurcation of \mathbf{G} occurs when an eigenvalue of $\mathbf{F}_{\mathbf{x}}$ passes through ± 1 . These bifurcations may be classified by the sign of the eigenvalue. A transcritical bifurcation of fixed points occurs when the eigenvalue

passes through $+1$ and a period doubling pitchfork bifurcation occurs when the eigenvalue passes through -1 . A useful tool for the local analysis of these bifurcations is the Lyapunov-Schmidt reduction process. Equation (2.2.18) can be reduced to a single equation $g(x, \alpha) = 0$, $g : \mathbb{R} \times \mathbb{R} \mapsto \mathbb{R}$ via application of this process. Generally, g is defined implicitly and so cannot be solved directly for x . In that case, the low order derivatives suffice to describe the species of bifurcation and the stability properties of the solutions of the original equation \mathbf{G} . We shall use the Lyapunov-Schmidt reduction process here where \mathbf{F} is the Hénon map. A semi-rigorous approach to the problem will be employed, but see Golubitsky and Schaeffer [27] for a more thorough treatment of the process.

Let (\mathbf{x}_0, α_0) be a bifurcation point of $\mathbf{G}(\mathbf{x}, \alpha)$ and suppose that $\mathbf{F}_{\mathbf{x}}^0 = \mathbf{F}_{\mathbf{x}}(\mathbf{x}_0, \alpha_0)$ has an eigenvalue of $+1$, the other eigenvalue lying within the unit circle. At that point, $\mathbf{G}_{\mathbf{x}}^0 = \mathbf{G}(\mathbf{x}_0, \alpha_0)$ is singular, has a simple eigenvalue and thus possesses a one-dimensional null space. Let ψ and ϕ denote the left and right eigenvectors of $\mathbf{G}_{\mathbf{x}}^0$ corresponding to the zero eigenvalue. We may decompose the domain (call it X) and the co-domain (Y) of \mathbf{G} as

$$\begin{aligned} X &= \ker(\mathbf{G}_{\mathbf{x}}^0) \oplus U \\ Y &= V \oplus \text{range}(\mathbf{G}_{\mathbf{x}}^0) \end{aligned}$$

where U and V are vector space complements to $\ker(\mathbf{G}_{\mathbf{x}}^0)$ and $\text{range}(\mathbf{G}_{\mathbf{x}}^0)$ respectively. Note that $\dim \ker(\mathbf{G}_{\mathbf{x}}^0) = \dim U = \dim V = \dim \text{range}(\mathbf{G}_{\mathbf{x}}^0) = 1$ in this case. Write $\mathbf{y} \in Y$ as

$$\mathbf{y} = \beta \mathbf{v} + \mathbf{r}$$

where $\mathbf{v} \in V$ and $\mathbf{r} \in \text{range}(\mathbf{G}_{\mathbf{x}}^0)$. Noting that $\mathbf{G}_{\mathbf{x}}^0 \phi_0 = \mathbf{0}$, $\psi_0^T \mathbf{G}_{\mathbf{x}}^0 = \mathbf{0}^T$ and $\text{range}(\mathbf{G}_{\mathbf{x}}^0) = \{\mathbf{x} \in X : \psi_0^T \mathbf{x} = 0\}$, we have that

$$\psi_0^T \mathbf{y} = \beta \psi_0^T \mathbf{v} + \psi_0^T \mathbf{r} = \beta \psi_0^T \mathbf{v}$$

and so

$$\beta = \frac{\psi_0^T \mathbf{y}}{\psi_0^T \mathbf{v}}.$$

Then

$$\mathbf{r} = \mathbf{y} - \beta \mathbf{v} = \mathbf{y} - \frac{\mathbf{v} \psi_0^T \mathbf{y}}{\psi_0^T \mathbf{v}} = P \mathbf{y}$$

where $P = \left(I - \frac{\mathbf{v} \psi_0^T}{\psi_0^T \mathbf{v}} \right)$ is the projection operator on Y such that $P : Y \mapsto \text{range}(\mathbf{G}_{\mathbf{x}}^0)$. Now, $\mathbf{G}(\mathbf{x}, \alpha) = 0$ iff

$$P \mathbf{G}(\mathbf{x}, \alpha) = 0 \tag{2.2.19}$$

and

$$(I - P) \mathbf{G}(\mathbf{x}, \alpha) = 0. \tag{2.2.20}$$

Then (2.2.19) can be solved for one of the components of \mathbf{x} , which can then be substituted into (2.2.20) for the remaining component. It can then be shown that the solutions of (2.2.18) can be put into one-to-one correspondence with the solutions of the scalar equation

$$g(x, \alpha) = \frac{1}{2} x^2 \psi_0^T \mathbf{G}_{\mathbf{xx}}^0 \phi_0 \phi_0 + x \delta \alpha \psi_0^T \mathbf{G}_{\mathbf{x}\alpha}^0 \phi_0$$

to lowest order. This is sufficient to describe the behaviour of solutions near to the bifurcation point (\mathbf{x}_0, α_0) . To analyse the period doubling pitchfork bifurcation we look at the system of equations defined by

$$\begin{pmatrix} \mathbf{x} \\ \mathbf{y} \end{pmatrix} = \tilde{\mathbf{G}}(\mathbf{x}, \mathbf{y}, \alpha) = \begin{pmatrix} \mathbf{G}(\mathbf{y}, \alpha) \\ \mathbf{G}(\mathbf{x}, \alpha) \end{pmatrix}.$$

Note that this system possesses the symmetry defined by $S \begin{pmatrix} \mathbf{x} \\ \mathbf{y} \end{pmatrix} = \begin{pmatrix} \mathbf{y} \\ \mathbf{x} \end{pmatrix}$. In particular we shall be interested in the fixed point equation

$$\begin{pmatrix} \mathbf{G}(\mathbf{y}, \alpha) - \mathbf{x} \\ \mathbf{G}(\mathbf{x}, \alpha) - \mathbf{y} \end{pmatrix} = \mathbf{0} \tag{2.2.21}$$

which is satisfied by period two solutions of the mapping \mathbf{G} . The Jacobian when evaluated at this solution to (2.2.21) is

$$\tilde{\mathbf{G}}_{\mathbf{X}}^0 = \begin{pmatrix} -I_2 & \mathbf{G}_{\mathbf{x}}^0 \\ \mathbf{G}_{\mathbf{x}}^0 & -I_2 \end{pmatrix}$$

where I_2 is the 2×2 identity matrix and $\mathbf{X} = \begin{pmatrix} \mathbf{x} \\ \mathbf{y} \end{pmatrix}$. Now,

$$\tilde{\mathbf{G}}_{\mathbf{X}}^0 \begin{pmatrix} \phi_0 \\ -\phi_0 \end{pmatrix} = \begin{pmatrix} -I_2 & \mathbf{G}_{\mathbf{x}}^0 \\ \mathbf{G}_{\mathbf{x}}^0 & -I_2 \end{pmatrix} \begin{pmatrix} \phi_0 \\ -\phi_0 \end{pmatrix} = - \begin{pmatrix} (I_2 + \mathbf{G}_{\mathbf{x}}^0)\phi_0 \\ -(I_2 + \mathbf{G}_{\mathbf{x}}^0)\phi_0 \end{pmatrix}$$

so that if $\mathbf{G}_{\mathbf{x}}^0$ has an eigenvalue of -1 , $\tilde{\mathbf{G}}_{\mathbf{X}}^0$ has a zero eigenvalue and thus a one-dimensional null space given by $\text{span}\{\phi_1\}$ where $\phi_1 := \begin{pmatrix} \phi_0 \\ -\phi_0 \end{pmatrix}$. It is easily verified that $\psi_1^T := \begin{pmatrix} \phi_0 & -\phi_0 \end{pmatrix}$ is the left eigenvector of $\tilde{\mathbf{G}}_{\mathbf{X}}^0$ corresponding to the zero eigenvalue. Thus the period doubling pitchfork bifurcation can be analysed with the theory discussed previously. In this case though, it can be shown that the reduced equation (see for example [11]) has the form

$$g(x, \alpha) = \frac{1}{6} x^3 \psi_1^T (\tilde{\mathbf{G}}_{\mathbf{X}\mathbf{X}\mathbf{X}}^0 \phi_1 \phi_1 \phi_1 + 3 \tilde{\mathbf{G}}_{\mathbf{X}\mathbf{X}}^0 \phi_1 \mathbf{r}_1) + x \delta \alpha \psi_1^T \tilde{\mathbf{G}}_{\mathbf{X}\alpha}^0 \phi_1$$

with \mathbf{r}_1 satisfying

$$\tilde{\mathbf{G}}_{\mathbf{X}}^0 \mathbf{r}_1 = -\tilde{\mathbf{G}}_{\mathbf{X}\mathbf{X}}^0 \phi_1 \phi_1.$$

For the Hénon map we find that

$$\mathbf{G}_{\mathbf{x}}^0 = \begin{pmatrix} 1.955147 & -0.519821 \\ 0.3 & 0 \end{pmatrix}$$

which has eigenvalues 0 and -0.844054 . The left and right eigenvectors corresponding to the zero eigenvalue are $\psi^T = (0.936195, -0.486654)$ and $\phi^T = (0.398609, 0.119583)$ respectively. Then $\psi_0^T \mathbf{G}_{\mathbf{x}\alpha}^0 \phi_0 = -1.399631$ and $\psi_0^T \mathbf{G}_{\mathbf{x}\mathbf{x}}^0 \phi_0 \phi_0 = 3.818406$ thus giving the reduced equation

$$-1.399631 x \delta \alpha + 1.909203 x^2$$

which has solutions $x = 0$ and $x = 0.733097 \delta \alpha$. For the period doubling bifurcation the reduced equation is

$$2.121464 x (x^2 - 0.620982 \delta \alpha)$$

which has solutions $x = 0$ and $x^2 = 0.620982 \delta \alpha$. Thus we would expect a trans-critical bifurcation with positive slope at $\alpha = \alpha_c$ and a period doubling bifurcation

at $\alpha = \alpha_{cu}$ whose solutions are stable for $\alpha > \alpha_{cu}$, indicating that the fixed point becomes unstable at the upper bifurcation point.

At the transcritical bifurcation, there is always a stable bifurcating branch beyond the bifurcation point, but for the period doubling bifurcation, the direction of branching determines whether or not there are stable branches (see Fig. 2.3) past the bifurcation point. If α is such that we are beyond one of the bifurcation points then it is 'safer' that we are beyond the transcritical bifurcation point rather than the period doubling point since in this case convergence to a fixed point will at least occur. Otherwise we may settle on a period-2 orbit, if indeed the control method settles down at all. Since only one eigenvalue of the modified Jacobian changes under a perturbation of \mathbf{w} , only period doubling and pitchfork bifurcations may be seen in higher dimensions. A Hopf bifurcation could not occur as this would require a pair of complex conjugate eigenvalues to pass through the unit circle.

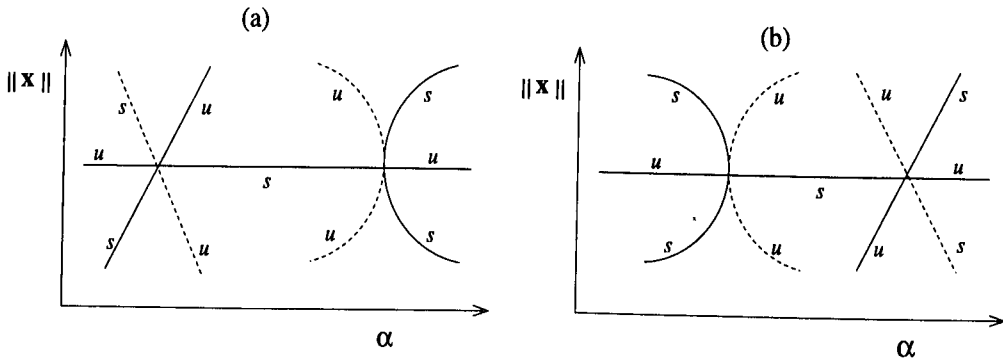


Figure 2.3: Possible bifurcations and stabilities for (a) $\lambda_u < 0$ and (b) $\lambda_u > 0$.

On a global scale, in the case where \mathbf{F} is known, we can use a numerical path following package such as AUTO [16] to produce bifurcation diagrams for \mathbf{x}^* . AUTO simply varies the parameter α and solves the resulting fixed point equation for the mapping. In the case of the Hénon map, the fixed point equation is

$$\mathbf{G}(x, y) = \begin{pmatrix} 1 - (1.4 + \delta p)x^2 + y - x \\ 0.3x - y \end{pmatrix} = \mathbf{0}.$$

where

$$\delta p = -\frac{\mathbf{f}_u^T M}{\alpha \mathbf{f}_u^T \mathbf{w}} \begin{pmatrix} x \\ y \end{pmatrix}.$$

Fig. 2.4 shows a transcritical bifurcation in $\|\mathbf{x}\|$ at α_{cl} and a period-doubling pitchfork bifurcation at the upper critical value α_{cu} . We would also expect the values δp_n to undergo some sort of bifurcation at the critical values of α , and this is indeed the case, as can be seen in Fig. 2.5.

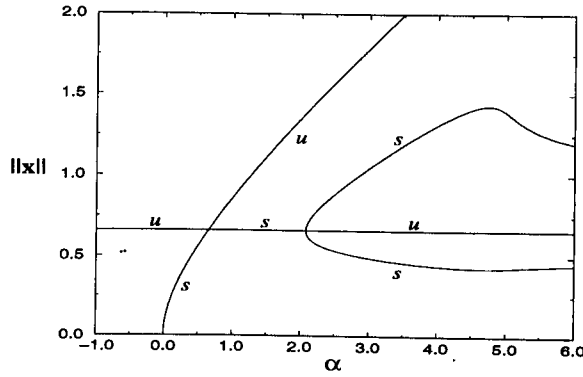


Figure 2.4: Bifurcation diagram for $\|\mathbf{x}\|$.

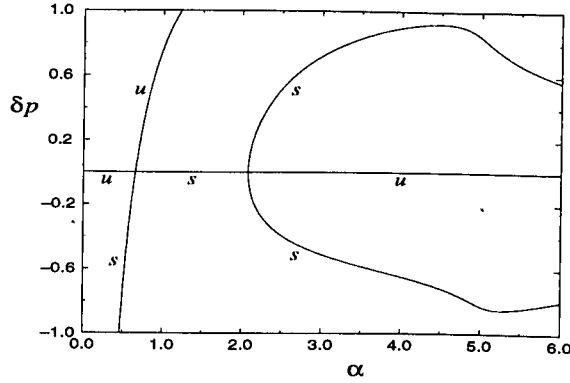


Figure 2.5: Bifurcation diagram for δp .

It may just happen in practice that \mathbf{w} is estimated badly, for example when $|\lambda_u|$ is large there is little margin for error since the range of values of α for which convergence to \mathbf{x}^* occurs is relatively small. In this instance it may be possible to apply a correction to the estimated value of \mathbf{w} to aid convergence to the true fixed point. This correction may be achieved as follows. Suppose that $\lambda_u < 0$.

- (i) The method settles on a period-2 orbit, in which case we know that $\alpha > 1$.

Then scale the estimated value of \mathbf{w} by a factor $\frac{1}{\alpha_{cu}}$;

- (ii) The method converges to a fixed point and the perturbation parameter settles down to a non-zero value. In this instance $\alpha < 1$, so scale the estimated value of \mathbf{w} by a factor $\frac{1}{\alpha_{cl}}$.

If $\lambda_u > 0$ then the scaling factors should be swapped around. The control method should then be applied again, with hopefully better results. If the problem still persists then the above process should be reapplied until a satisfactory result is obtained. Note that in case (ii), the estimate of the fixed point should first be corrected via the method discussed in Section 2.2.1, for if it is not, a bad estimate of \mathbf{x}^* can cause the control algorithm to settle down onto a fixed point with a non-zero value of the perturbation parameter. It is also advisable to take ‘non-zero’ here as meaning greater than some tolerance ϵ to compensate for any numerical errors or noise in the system. By such a scaling there is no chance of ‘overcorrecting’ \mathbf{w} since it is based on the premise that α is at, or just outside, its critical value and as such will be scaled back near to 1.

The estimated value of \mathbf{w} could be rescaled deliberately by some factor k in order to attempt to locate the bifurcation points. Once a bifurcation point is located, a more accurate estimate to the true length of \mathbf{w} could be obtained. Recall that when the representation $\hat{\mathbf{w}} = \alpha\mathbf{w} + \beta\mathbf{e}_s$ was used in the OGY control formula, only the factor α was significant and the \mathbf{e}_s term could be neglected. Suppose that $\hat{\mathbf{w}}$ is scaled by the factor $k > 1$ and the upper bifurcation point at $\alpha = \alpha_{cu}$ is located. Then we have that

$$k\mathbf{f}_u^T \hat{\mathbf{w}} = k\alpha\mathbf{f}_u^T \mathbf{w} = \alpha_{cu}\mathbf{f}_u^T \mathbf{w}$$

and so

$$\alpha = \frac{\alpha_{cu}}{k}.$$

Rescaling $\hat{\mathbf{w}}$ by the factor $\frac{k}{\alpha_{cu}}$ will result in setting α equal to unity. It may be useful to carry out this procedure if the control algorithm is converging at a rate slower than that indicated by the spectral radius of J .

Perturbations in M

Suppose now that M has not been estimated accurately. Let the estimate of M be \hat{M} . For the proceeding analysis we assume that \hat{M} is not too dissimilar to M , thus \hat{M} may be considered as a perturbation of M . Let $\hat{\lambda}_u$ be the unstable eigenvalue of \hat{M} with corresponding left eigenvector $\hat{\mathbf{f}}_u^T$. Then $\hat{\lambda}_u$ and $\hat{\mathbf{f}}_u^T$ can be considered as perturbations of λ_u and \mathbf{f}_u^T respectively. To this effect, write $\hat{\lambda}_u = \lambda_u + \tilde{\lambda}_u$ for a suitable small scalar $\tilde{\lambda}_u$ and write $\hat{\mathbf{f}}_u^T = \mathbf{f}_u^T + \tilde{\mathbf{f}}_u^T$ for a small vector $\tilde{\mathbf{f}}_u^T$. By ‘small’ we mean $\|\tilde{\mathbf{f}}_u^T\| < \epsilon$ for scalar ϵ .

The Jacobian of the system evaluated at the fixed point \mathbf{x}^* in the presence of parameter perturbations is

$$\begin{aligned} \hat{J} &= M - \frac{\mathbf{w}\hat{\mathbf{f}}_u^T\hat{M}}{\hat{\mathbf{f}}_u^T\mathbf{w}} \\ &= M - \frac{\mathbf{w}\hat{\lambda}_u\hat{\mathbf{f}}_u^T}{\hat{\mathbf{f}}_u^T\mathbf{w}} \\ &= M - \frac{\mathbf{w}(\lambda_u + \tilde{\lambda}_u)(\mathbf{f}_u^T + \tilde{\mathbf{f}}_u^T)}{(\mathbf{f}_u^T + \tilde{\mathbf{f}}_u^T)\mathbf{w}} \end{aligned} \quad (2.2.22)$$

Note that this is only a three-dimensional perturbation as opposed to a four dimensional perturbation which one may expect since M has four entries. The three perturbations come from the two entries of $\hat{\mathbf{f}}_u^T$ and $\tilde{\lambda}_u$. Now write $\tilde{\mathbf{f}}_u^T = \alpha\mathbf{f}_u^T + \beta\mathbf{m}^T$ for small scalars α and β where, we recall, $\mathbf{m}^T\mathbf{w} = 0$ and $\mathbf{m}^T\mathbf{e}_s = 1$. We can then write (2.2.22) as

$$\hat{J} = M - \frac{\mathbf{w}(\lambda_u + \tilde{\lambda}_u)(\mathbf{f}_u^T + \tilde{\mathbf{f}}_u^T)}{(1 + \alpha)\mathbf{f}_u^T\mathbf{w}}$$

$$\begin{aligned}
 &= M - \frac{\mathbf{w}}{\mathbf{f}_u^T \mathbf{w}} (\lambda_u + \tilde{\lambda}_u) (\mathbf{f}_u^T + \tilde{\mathbf{f}}_u^T) (1 + \alpha)^{-1} \\
 &= M - \frac{\mathbf{w}}{\mathbf{f}_u^T \mathbf{w}} (\lambda_u + \tilde{\lambda}_u) (\mathbf{f}_u^T + \alpha \mathbf{f}_u^T + \beta \mathbf{m}^T) (1 - \alpha) \quad (2.2.23)
 \end{aligned}$$

by expanding $(1 + \alpha)^{-1}$ to first order in α . We now have a relatively simple approximation to \hat{J} in terms of the parameters α and β and $\tilde{\lambda}_u$.

Let us look at the first order change in the eigenvalues, using Wilkinsons result.

We have that

$$\begin{aligned}
 \left(\mathbf{f}_s^T - \frac{\mathbf{f}_s^T \mathbf{w} \lambda_u}{\mathbf{f}_u^T \mathbf{w} \lambda_s} \mathbf{f}_u^T \right) \hat{J} \mathbf{e}_s &= \lambda_s + \frac{\mathbf{f}_s^T \mathbf{w} \lambda_u}{\mathbf{f}_u^T \mathbf{w} \lambda_s} (\lambda_u + \tilde{\lambda}_u) \beta (1 - \alpha) \\
 &\quad - \frac{\mathbf{f}_s^T \mathbf{w}}{\mathbf{f}_u^T \mathbf{w}} (\lambda_u + \tilde{\lambda}_u) \beta (1 - \alpha) \\
 &= \lambda_s + \beta \frac{\mathbf{f}_s^T \mathbf{w} \lambda_u^2}{\mathbf{f}_u^T \mathbf{w} \lambda_s} - \beta \frac{\mathbf{f}_s^T \mathbf{w}}{\mathbf{f}_u^T \mathbf{w}} \lambda_u
 \end{aligned}$$

to a first order approximation. Thus the non-zero eigenvalue is perturbed to

$$\lambda_s + \beta \frac{\mathbf{f}_s^T \mathbf{w}}{\mathbf{f}_u^T \mathbf{w}} \lambda_u \left(\frac{\lambda_u}{\lambda_s} - 1 \right) = \lambda_s + \beta \frac{\mathbf{f}_s^T \mathbf{w} \lambda_u}{\mathbf{f}_u^T \mathbf{w} \lambda_s} (\lambda_u - \lambda_s).$$

So the non-zero eigenvalue is particularly sensitive to perturbations in M if:

- (i) λ_u and λ_s are of opposite sign;
- (ii) λ_u and λ_s are considerably different in magnitude, or,
- (iii) the ratio $\frac{\mathbf{f}_s^T \mathbf{w}}{\mathbf{f}_u^T \mathbf{w}}$ is large, which implies that the \mathbf{w} direction is close to that of \mathbf{e}_s , the linearised stable manifold.

We now look at what happens to the zero eigenvalue under perturbations in M . It is easily shown that under the assumption that \mathbf{m} is normalised such that $\mathbf{m}^T \mathbf{e}_s = 1$, $\mathbf{e}_u + \chi \mathbf{e}_s$ has the alternative form $\lambda_s \mathbf{w} - (\mathbf{m}^T M \mathbf{w}) \mathbf{e}_s$. We shall use this alternative form for the right eigenvector of the modified mapping in order to

simplify calculations below. Then using (2.2.23),

$$\begin{aligned}
 & \frac{\mathbf{f}_u^T}{\mathbf{f}_u^T \mathbf{w}} \hat{J} (\lambda_s \mathbf{w} - \mathbf{m}^T M \mathbf{w} \mathbf{e}_s) \\
 &= \frac{\mathbf{f}_u^T}{\mathbf{f}_u^T \mathbf{w}} \left(M - \frac{\mathbf{w}}{\mathbf{f}_u^T \mathbf{w}} (\lambda_u + \tilde{\lambda}_u) (\mathbf{f}_u^T + \alpha \mathbf{f}_u^T + \beta \mathbf{m}^T) \right) (\lambda_s \mathbf{w} - \mathbf{m}^T M \mathbf{w} \mathbf{e}_s) (1 - \alpha) \\
 &= \frac{1}{\mathbf{f}_u^T \mathbf{w}} (\lambda_u \mathbf{f}_u^T - (\lambda_u + \tilde{\lambda}_u) (\mathbf{f}_u^T + \alpha \mathbf{f}_u^T + \beta \mathbf{m}^T)) (\lambda_s \mathbf{w} - \mathbf{m}^T M \mathbf{w} \mathbf{e}_s) (1 - \alpha) \\
 &= \frac{1}{\mathbf{f}_u^T \mathbf{w}} (\lambda_u \lambda_s \mathbf{f}_u^T \mathbf{w} - \lambda_s (\lambda_u + \tilde{\lambda}_u) (1 + \alpha) \mathbf{f}_u^T \mathbf{w} + (\lambda_u + \tilde{\lambda}_u) \beta \mathbf{m}^T M \mathbf{w}) (1 - \alpha) \\
 &= \frac{1}{\mathbf{f}_u^T \mathbf{w}} \left(-\lambda_s \lambda_u \alpha \mathbf{f}_u^T \mathbf{w} - \lambda_s \tilde{\lambda}_u \mathbf{f}_u^T \mathbf{w} - \lambda_s \tilde{\lambda}_u \alpha \mathbf{f}_u^T \mathbf{w} \right. \\
 &\quad \left. + \lambda_u \beta \mathbf{m}^T M \mathbf{w} + \tilde{\lambda}_u \beta \mathbf{m}^T M \mathbf{w} \right) (1 - \alpha) \\
 &= -\lambda_s \lambda_u \alpha - \lambda_s \tilde{\lambda}_u + \frac{\lambda_u \mathbf{m}^T M \mathbf{w}}{\mathbf{f}_u^T \mathbf{w}} \beta \tag{2.2.24}
 \end{aligned}$$

to a first order approximation. Thus the zero eigenvalue is sensitive to perturbations in M if:

- (i) $\lambda_s \lambda_u$ is large,
- (ii) $|\lambda_s|$ is close to unity, or
- (iii) $\frac{\lambda_u \mathbf{m}^T M \mathbf{w}}{\mathbf{f}_u^T \mathbf{w}}$ is large.

In conclusion, the theory above shows that there are many factors that determine the sensitivity of the OGY control algorithm to errors. Perhaps the most important factors are the eigenvalues of the Jacobian matrix M . They characterise the strengths of attraction and repulsion to and from the fixed point, respectively, and are of course entirely dependent upon the fixed point one wishes to control. Interestingly, it has been observed that the method still works well even in the presence of large errors in the estimated quantities. Control can often still be achieved with errors in the Jacobian matrix as large as fifty percent. However, not every system could tolerate such large errors.

2.2.2 The Zero Spectral Radius Method

The analysis in this section is similar in some respects to that for the OGY method. The relevant theory for the perturbation in eigenvalues for a matrix possessing eigenvalues of algebraic multiplicity two has been discussed previously. We shall use that theory here, and we begin by showing that $\psi_1^T = \frac{1}{\mathbf{k}^T \mathbf{w}} \mathbf{k}^T$, $\psi_2^T = \frac{1}{\mathbf{k}^T \mathbf{w} \lambda_s} \mathbf{m}^T$, $\phi_1 = \frac{\mathbf{k}^T \mathbf{w} \lambda_s}{\mathbf{m}^T \mathbf{l}} \mathbf{l}$ and $\phi_2 = \mathbf{w}$ are the left and right generalised eigenvectors of J we require to form the matrices T and T^{-1} . We have that

$$\begin{aligned} T^{-1} J T &= \begin{pmatrix} \frac{1}{\mathbf{k}^T \mathbf{w} \lambda_s} \mathbf{m}^T \\ \frac{1}{\mathbf{k}^T \mathbf{w}} \mathbf{k}^T \end{pmatrix} \left(I - \frac{\mathbf{w} \mathbf{k}^T}{\mathbf{k}^T \mathbf{w}} \right) M \begin{pmatrix} \frac{\mathbf{k}^T \mathbf{w} \lambda_s}{\mathbf{m}^T \mathbf{l}} \mathbf{l} & \mathbf{w} \end{pmatrix} \\ &= \begin{pmatrix} \frac{\mathbf{m}^T M \mathbf{l}}{\mathbf{m}^T \mathbf{l}} & \frac{\mathbf{m}^T M \mathbf{w}}{\mathbf{k}^T \mathbf{w} \lambda_s} \\ 0 & 0 \end{pmatrix}. \end{aligned}$$

By definition, $\frac{\mathbf{m}^T M \mathbf{l}}{\mathbf{m}^T \mathbf{l}} = 0$ assuming $\mathbf{l} \neq \mathbf{e}_s$. For simplicity, we introduce a normalisation on \mathbf{k} such that $\mathbf{k}^T \mathbf{e}_s = 1$. Let $\mathbf{w} = \gamma \mathbf{l} + \zeta \mathbf{e}_s$ where $\gamma = \frac{\mathbf{f}_u^T \mathbf{w}}{\mathbf{f}_u^T \mathbf{l}}$ and $\zeta = \mathbf{k}^T \mathbf{w}$. Then

$$\begin{aligned} \mathbf{m}^T M \mathbf{w} &= \mathbf{m}^T M (\gamma \mathbf{l} + \zeta \mathbf{e}_s) \\ &= \mathbf{k}^T \mathbf{w} \lambda_s \end{aligned}$$

and so

$$\frac{\mathbf{m}^T M \mathbf{w}}{\mathbf{k}^T \mathbf{w} \lambda_s} = 1.$$

Clearly $T^{-1} T = I$ and so ψ_1^T , ψ_2^T , ϕ_1 and ϕ_2 are indeed the generalised eigenvectors we seek.

Perturbations in \mathbf{x}^*

In this case, application of the control algorithm with our estimated value of \mathbf{x}^* gives us the formula for the control parameter as

$$\delta p_n = -\frac{\mathbf{k}^T M}{\mathbf{k}^T \mathbf{w}} (\mathbf{x}_n - \mathbf{x}_R^*). \quad (2.2.25)$$

After applying this control algorithm, we converge to the fixed point \mathbf{x}^+ , with a non-zero value of the perturbation parameter, δp^+ . Then by using the same Taylor expansion as in the analysis for the OGY method we find that, to a first order approximation,

$$\begin{aligned} D_{\mathbf{x}}\mathbf{F}(\mathbf{x}^+, p^+) &= \left(I - \frac{\mathbf{w}\mathbf{k}^T}{\mathbf{k}^T\mathbf{w}} \right) M + \mathbf{F}_{\mathbf{xx}}^* \delta \mathbf{x}^+ - \mathbf{F}_{\mathbf{x}p}^* \frac{\mathbf{k}^T M}{\mathbf{k}^T \mathbf{w}} \delta \mathbf{x}^+ \\ &\quad - \left(\mathbf{F}_{\mathbf{x}p}^* \delta \mathbf{x}^+ - \mathbf{F}_{pp}^* \frac{\mathbf{k}^T M}{\mathbf{k}^T \mathbf{w}} \delta \mathbf{x}^+ \right) \frac{\mathbf{k}^T M}{\mathbf{k}^T \mathbf{w}}. \end{aligned} \quad (2.2.26)$$

The eigenvalues of (2.2.26) can then be determined using (2.1.14).

The method for the improvement of the estimate to the fixed point is very similar to that for the OGY method. This time the value for the perturbation parameter for any \mathbf{x} is

$$\delta p(\mathbf{x}) = -\frac{\mathbf{k}^T M}{\mathbf{k}^T \mathbf{w}} (\mathbf{x} - \mathbf{x}_R^*) \quad (2.2.27)$$

so that, at the fixed point \mathbf{x}^* ,

$$\begin{aligned} \delta p(\mathbf{x}^*) &= -\frac{\mathbf{k}^T M}{\mathbf{k}^T \mathbf{w}} (\mathbf{x}^* - \mathbf{x}_R^*) \\ &= q_{ZSR} \end{aligned}$$

where this time, $q_{ZSR} = -\frac{\mathbf{k}^T M}{\mathbf{k}^T \mathbf{w}} (\mathbf{x}^* - \mathbf{x}_R^*)$. Then from (2.2.27), $\delta p(\mathbf{x}^+) = cq_{ZSR}$ where $c := 1 - \frac{\mathbf{k}^T M \bar{\mathbf{x}}}{\mathbf{k}^T \mathbf{w}}$ and $\bar{\mathbf{x}}$ satisfies the first order approximation $\mathbf{x}^+ \simeq \mathbf{x}^* + q_{ZSR} \bar{\mathbf{x}}$. Then at the fixed point \mathbf{x}^+ ,

$$\bar{\mathbf{x}} \simeq M \bar{\mathbf{x}} + \mathbf{w}c$$

i.e.

$$\bar{\mathbf{x}} = \bar{\mathbf{x}} + \mathbf{w} \left(1 - \frac{\mathbf{k}^T M \bar{\mathbf{x}}}{\mathbf{k}^T \mathbf{w}} \right)$$

to a first order approximation so that

$$\left(I - \left(I - \frac{\mathbf{w}\mathbf{k}^T}{\mathbf{k}^T \mathbf{w}} \right) M \right) \bar{\mathbf{x}} = \mathbf{w}. \quad (2.2.28)$$

Pre-multiplying (2.2.28) by \mathbf{k}^T we have

$$\mathbf{k}^T \bar{\mathbf{x}} = \mathbf{k}^T \mathbf{w}. \quad (2.2.29)$$

Write $\mathbf{w} = \zeta \mathbf{e}_s + \gamma \mathbf{l}$ and let $\bar{\mathbf{x}} = a\mathbf{e}_s + b\mathbf{l}$. Then from (2.2.29),

$$\mathbf{k}^T(a\mathbf{e}_s + b\mathbf{l}) = \mathbf{k}^T(\zeta \mathbf{e}_s + \gamma \mathbf{l})$$

so that

$$a = \zeta.$$

Pre-multiplying (2.2.28) by \mathbf{f}_u^T we have

$$\left(\mathbf{f}_u^T - \left(\mathbf{f}_u^T - \frac{\mathbf{f}_u^T \mathbf{w}}{\mathbf{k}^T \mathbf{w}} \mathbf{k}^T \right) M \right) \bar{\mathbf{x}} = \mathbf{f}_u^T \mathbf{w}.$$

Hence

$$\left(\mathbf{f}_u^T - \left(\mathbf{f}_u^T - \frac{\mathbf{f}_u^T \mathbf{w}}{\mathbf{k}^T \mathbf{w}} \mathbf{k}^T \right) M \right) (a\mathbf{e}_s + b\mathbf{l}) = \mathbf{f}_u^T (\zeta \mathbf{e}_s + \gamma \mathbf{l}).$$

This can then be rearranged to obtain

$$b = \frac{(1 - \lambda_s) \mathbf{f}_u^T \mathbf{w}}{\mathbf{f}_u^T \mathbf{l} - \left(\mathbf{f}_u^T - \frac{\mathbf{f}_u^T \mathbf{w}}{\mathbf{k}^T \mathbf{w}} \mathbf{k}^T \right) M \mathbf{l}}$$

and so the value of $\bar{\mathbf{x}}$ has been determined. The new approximation to the fixed point \mathbf{x}^* is then

$$\mathbf{x}^* \simeq \mathbf{x}^+ - q_{ZSR} \left((\mathbf{k}^T \mathbf{w}) \mathbf{e}_s + \frac{(1 - \lambda_s) \mathbf{f}_u^T \mathbf{w}}{\mathbf{f}_u^T \mathbf{l} - \left(\mathbf{f}_u^T - \frac{\mathbf{f}_u^T \mathbf{w}}{\mathbf{k}^T \mathbf{w}} \mathbf{k}^T \right) M \mathbf{l}} \mathbf{l} \right).$$

Perturbations in \mathbf{w}

Perturbing \mathbf{w} in the zero spectral radius method has an effect on the choice of \mathbf{k} .

Suppose that \mathbf{w} is perturbed to $\hat{\mathbf{w}}$. Then \mathbf{m} , \mathbf{l} and \mathbf{k} will be perturbed to $\hat{\mathbf{m}}$, $\hat{\mathbf{l}}$ and $\hat{\mathbf{k}}$ respectively. The value of the perturbation parameter is then

$$\delta p_n = \frac{\hat{\mathbf{k}}^T M \delta \mathbf{x}_n}{\hat{\mathbf{k}}^T \hat{\mathbf{w}}}.$$

The Jacobian in the presence of parameter perturbations is

$$\hat{J} = \left(I - \frac{\mathbf{w} \hat{\mathbf{k}}^T}{\hat{\mathbf{k}}^T \hat{\mathbf{w}}} \right) M. \quad (2.2.30)$$

Let us write $\mathbf{w} = \eta \mathbf{e}_s + \xi \mathbf{e}_u$ where $\eta = \mathbf{f}_s^T \mathbf{w}$ and $\xi = \mathbf{f}_u^T \mathbf{w}$. Then let $\hat{\mathbf{w}} = \hat{\eta} \mathbf{e}_s + \hat{\xi} \mathbf{e}_u$ where $\hat{\eta}$ and $\hat{\xi}$ are perturbations of η and ξ respectively, such that $\hat{\eta} = \eta + \tilde{\eta}$ and $\hat{\xi} = \xi + \tilde{\xi}$ for small $\tilde{\eta}$ and $\tilde{\xi}$. Then it is easy to show that $\hat{\mathbf{m}} = -\frac{1}{\xi} (\hat{\eta} \mathbf{f}_u - \hat{\xi} \mathbf{f}_s)$, $\hat{\mathbf{l}} = \lambda_u \hat{\eta} \mathbf{e}_s + \lambda_s \hat{\xi} \mathbf{e}_u$ and $\hat{\mathbf{k}} = -\frac{1}{\xi \lambda_s} (\lambda_u \hat{\eta} \mathbf{f}_u - \lambda_s \hat{\xi} \mathbf{f}_s)$. Thus substituting the values of $\hat{\mathbf{k}}$ and $\hat{\mathbf{w}}$ into (2.2.30) we have

$$\begin{aligned} \hat{J} &= \left(I - \frac{(\eta \mathbf{e}_s + \xi \mathbf{e}_u)(\lambda_u \hat{\eta} \mathbf{f}_u - \lambda_s \hat{\xi} \mathbf{f}_s)}{(\lambda_u \hat{\eta} \mathbf{f}_u - \lambda_s \hat{\xi} \mathbf{f}_s)(\hat{\eta} \mathbf{e}_s + \hat{\xi} \mathbf{e}_u)} \right) M \\ &= M - \frac{(\eta \mathbf{e}_s + \xi \mathbf{e}_u)(\lambda_u^2 \hat{\eta} \mathbf{f}_u^T - \lambda_s^2 \hat{\xi} \mathbf{f}_s^T)}{\hat{\eta} \hat{\xi} (\lambda_u - \lambda_s)} \\ &= M - \frac{(\eta \hat{\eta} \lambda_u^2 \mathbf{e}_s \mathbf{f}_u^T - \eta \hat{\xi} \lambda_s^2 \mathbf{e}_s \mathbf{f}_s^T + \hat{\eta} \xi \lambda_u^2 \mathbf{e}_u \mathbf{f}_u^T - \xi \hat{\xi} \lambda_s^2 \mathbf{e}_u \mathbf{f}_s^T)}{\hat{\eta} \hat{\xi} (\lambda_u - \lambda_s)}. \end{aligned} \quad (2.2.31)$$

Now $\frac{1}{\hat{\eta}} = \frac{1}{\eta} \left(1 - \frac{\tilde{\eta}}{\eta} \right)$ to a first order approximation. Similarly, $\frac{1}{\hat{\xi}} = \frac{1}{\xi} \left(1 - \frac{\tilde{\xi}}{\xi} \right)$ to first order. Thus the terms only involving $\hat{\eta}$ and $\hat{\xi}$ are

$$\begin{aligned} &\frac{1}{\eta \xi (\lambda_u - \lambda_s)} \left(1 - \frac{\tilde{\eta}}{\eta} \right) \left(1 - \frac{\tilde{\xi}}{\xi} \right) (\eta (\eta + \tilde{\eta}) \lambda_u^2 \mathbf{e}_s \mathbf{f}_u^T - \eta (\xi + \tilde{\xi}) \lambda_s^2 \mathbf{e}_s \mathbf{f}_s^T \\ &\quad - \eta (\xi + \tilde{\xi}) \lambda_s^2 \mathbf{e}_s \mathbf{f}_s^T + (\eta + \tilde{\eta}) \xi \lambda_u^2 \mathbf{e}_u \mathbf{f}_u^T - \xi (\xi + \tilde{\xi}) \lambda_s^2 \mathbf{e}_u \mathbf{f}_s^T). \end{aligned} \quad (2.2.32)$$

Looking at the zero order terms in $\tilde{\eta}$ and $\tilde{\xi}$ we have

$$\frac{\eta^2 \lambda_u^2 \mathbf{e}_s \mathbf{f}_u^T - \eta \xi \lambda_s^2 \mathbf{e}_s \mathbf{f}_s^T + \eta \xi \lambda_u^2 \mathbf{e}_u \mathbf{f}_u^T - \xi^2 \lambda_s^2 \mathbf{e}_u \mathbf{f}_s^T}{\eta \xi (\lambda_u - \lambda_s)}$$

and so the zero order terms in (2.2.31) are simply J in the unperturbed case. This can be seen by setting $\hat{\eta} = \eta$ and $\hat{\xi} = \xi$ in (2.2.31). The first order terms in $\tilde{\eta}$ and $\tilde{\xi}$ of (2.2.32) are, after simplification,

$$\tilde{J} := \frac{\xi \lambda_s^2 \tilde{\eta} (\mathbf{e}_s + \frac{\xi}{\eta} \mathbf{e}_u) \mathbf{f}_s^T - \eta \lambda_u^2 \tilde{\xi} (\mathbf{e}_u + \frac{\eta}{\xi} \mathbf{e}_s) \mathbf{f}_u^T}{\eta \xi (\lambda_u - \lambda_s)}.$$

So to first order, $\hat{J} = J + \tilde{J}$, thus \hat{J} is a perturbation in J . We have that

$$\psi_1^T = \frac{1}{\eta \xi \lambda_s (\lambda_u - \lambda_s)} (\eta \mathbf{f}_u^T - \xi \mathbf{f}_s^T), \quad \psi_2^T = \frac{1}{\eta \xi (\lambda_u - \lambda_s)} (\lambda_u \eta \mathbf{f}_u^T - \lambda_s \xi \mathbf{f}_s^T)$$

and

$$\phi_1 = -(\lambda_u \eta \mathbf{e}_s + \lambda_s \xi \mathbf{e}_u), \quad \phi_2 = \eta \mathbf{e}_s + \xi \mathbf{e}_u.$$

It can be verified, by performing a similarity transformation on J defined by the matrix $T^{-1} = \begin{pmatrix} \psi_2^T \\ \psi_1^T \end{pmatrix}$ that $T^{-1}JT = \begin{pmatrix} 0 & 1 \\ 0 & 0 \end{pmatrix}$. Also,

$$T^{-1}\tilde{J}T = \frac{1}{\eta\xi(\lambda_u - \lambda_s)} \begin{pmatrix} 0 & 0 \\ \lambda_u\lambda_s(\xi\lambda_s\tilde{\eta} - \eta\lambda_u\tilde{\xi}) & \xi\lambda_s^2\tilde{\eta} - \eta\lambda_u\tilde{\xi} \end{pmatrix}$$

and so from (2.1.14), the two zero eigenvalues are perturbed to

$$\pm \sqrt{\frac{\lambda_u\lambda_s(\xi\lambda_s\tilde{\eta} - \eta\lambda_u\tilde{\xi})}{\eta\xi(\lambda_u - \lambda_s)}} + \frac{\xi\lambda_s^2\tilde{\eta} - \eta\lambda_u\tilde{\xi}}{2\eta\xi(\lambda_u - \lambda_s)}$$

to a first order approximation. The sign of the quantity under the square root governs the direction in which the eigenvalues are perturbed. If this quantity is positive then the eigenvalues will move out along the real axis. If the sign is negative however, the eigenvalues will move into the complex plane. Also, if the value of λ_u is close to that of λ_s , then the method is more sensitive to perturbations in \mathbf{w} .

Perturbations in M

Suppose that M is perturbed to \hat{M} . Then \mathbf{k} will also be perturbed and take on the value $\hat{\mathbf{k}}$ say. The the Jacobian in the presence of parameter perturbations is then

$$\hat{J} = M - \frac{\mathbf{w}\hat{\mathbf{k}}^T}{\hat{\mathbf{k}}^T\mathbf{w}}\hat{M}.$$

Let $\hat{\mathbf{k}} = \mathbf{k} + \tilde{\mathbf{k}}$ and $\hat{M} = M + \tilde{M}$ for a small vector $\tilde{\mathbf{k}}$ and a small matrix \tilde{M} . Then it can be shown that $\hat{J} = J + \tilde{J}$ where

$$\tilde{J} = -\frac{\mathbf{w}}{\mathbf{k}^T\mathbf{w}} \left(\mathbf{k}^T\tilde{M} + \tilde{\mathbf{k}}^T M + \tilde{\mathbf{k}}^T\tilde{M} - \frac{\tilde{\mathbf{k}}^T\mathbf{w}}{\mathbf{k}^T\mathbf{w}} (\mathbf{k}^T M + \mathbf{k}^T\tilde{M} + \tilde{\mathbf{k}}^T M + \tilde{\mathbf{k}}^T\tilde{M}) \right) \quad (2.2.33)$$

and so from (2.1.14), the eigenvalues are perturbed to

$$\tilde{\lambda}_{\pm} = \pm \sqrt{\psi_2^T \tilde{J} \phi_1} + \frac{1}{2} (\psi_1^T \tilde{J} \phi_1 + \psi_2^T \tilde{J} \phi_2). \quad (2.2.34)$$

Looking at the first order terms in (2.2.33) and noting that $\tilde{\mathbf{k}}^T \mathbf{w} = \mathbf{m}^T \tilde{M} \mathbf{w}$ we have that

$$\begin{aligned} \tilde{J} &\simeq -\frac{\mathbf{w}}{\mathbf{k}^T \mathbf{w}} \left(\mathbf{k}^T \tilde{M} + \tilde{\mathbf{k}}^T M - \frac{\mathbf{m}^T \tilde{M} \mathbf{w}}{\mathbf{k}^T \mathbf{w}} \mathbf{k}^T M \right) \\ &= -\frac{\mathbf{w}}{\mathbf{k}^T \mathbf{w}} \left(\mathbf{k}^T \tilde{M} + \mathbf{m}^T \tilde{M} \left(I - \frac{\mathbf{w} \mathbf{k}^T}{\mathbf{k}^T \mathbf{w}} \right) M \right) \\ &= -\frac{\mathbf{w}}{\mathbf{k}^T \mathbf{w}} \left(\mathbf{k}^T \tilde{M} + \mathbf{m}^T \tilde{M} J \right). \end{aligned}$$

Thus from (2.2.34),

$$\tilde{\lambda}_{\pm} = \pm \sqrt{-\frac{\psi_2^T \mathbf{w}}{\mathbf{k}^T \mathbf{w}} \mathbf{k}^T \tilde{M} \phi_1 - \frac{1}{2\mathbf{k}^T \mathbf{w}} \left(\phi_1^T \mathbf{w} \mathbf{k}^T \tilde{M} \phi_1 + \psi_2^T \mathbf{w} \mathbf{k}^T \tilde{M} \phi_2 \right)}$$

since $J\phi_1 = J\phi_2 = 0$. Typically then, small inaccuracies in M are likely to have a small effect on the eigenvalues of the modified mapping and hence on the rate of convergence of the ZSR method.

Summary

In conclusion, there is no single method that is robust in the presence of inaccuracies. To attempt to choose a robust control method, one would have to determine which of the quantities \mathbf{x}^* , \mathbf{w} or M , were most likely to be inaccurate. Fortunately, control methods can be very tolerant to errors indeed. Small errors are inevitable when estimating local dynamics, but it would seem that control methods can cope well with such errors.

2.3 Numerical Example

As the numerical example for this chapter, we shall return to the Hénon map with the same parameter values as used in Chapter 1. We shall first study the mapping (1.4.11), i.e. the mapping in the absence of noise. Collecting $N = 10$

pairs of iterates in an ϵ -neighbourhood of the approximately found fixed point, where $\epsilon = 0.1$ and performing a regression on this data yields

$$\mathbf{x}_R^* = \begin{pmatrix} 0.631030 \\ 0.189309 \end{pmatrix}, \quad \mathbf{w} \simeq \begin{pmatrix} -0.377948 \\ 0.0 \end{pmatrix}$$

and

$$J(\mathbf{x}_R^*) \simeq \begin{pmatrix} -1.731851 & 1.000361 \\ 0.3 & 0.0 \end{pmatrix}.$$

Application of the OGY procedure results in the stabilisation of the fixed point $\mathbf{x}^{+T} = (0.631030, 0.189309)$. The value of the perturbation parameter must be maintained at $\delta p^+ = -0.004148$ in order to sustain stabilisation of \mathbf{x}^+ .

Then using the formulae of Section 2.2.1, we obtain

$$\bar{\mathbf{x}} = \begin{pmatrix} -0.449334 \\ -0.134800 \end{pmatrix}, \quad c = 2.872646 \quad \text{and} \quad q = -0.001444$$

and so the correction procedure can be applied to refine the estimate of the fixed point. Here, a fixed point is first stabilised (using the regression estimate \mathbf{x}_R^* in the control formula) and refined, then the refined estimate is used in place of \mathbf{x}_R^* when evaluating the value of the perturbation parameter. This new value for δp_n is then used to stabilise a close by new fixed point and the process repeated again as required. Table 2.1 illustrates the numerical effect of the correction procedure for the OGY method. In only four applications, a fixed point accurate to 10^{-7} can be found and stabilised. This is an excellent approximation to \mathbf{x}^* considering that approximations to M and \mathbf{w} are used in obtaining it.

Application	q_{OGY}	OGY Method
1	-1.44387×10^{-3}	(0.631030, 0.189309)
2	9.91825×10^{-5}	(0.631376, 0.189413)
3	6.43373×10^{-6}	(0.631353, 0.189405)
4	4.19023×10^{-7}	(0.631354, 0.189406)

Table 2.1: Applying the fixed point correction procedure with the OGY method.

The refinement procedure can be adapted for use in the presence of small amplitude noise. We shall now study the noisy Hénon map, equation (1.4.12), with noise distributed as $\text{Normal}(0, 2.4 \times 10^{-9})$. With this level of noise, a regression on $N = 10$ pairs of iterates within a distance of 0.1 from an approximately found fixed point results in the following estimates for Jacobian and the fixed point

$$J(\mathbf{x}_R^*) \simeq \begin{pmatrix} -1.726507 & 0.991414 \\ 0.299720 & -0.000063 \end{pmatrix} \quad \text{and} \quad \mathbf{x}_R^* = \begin{pmatrix} 0.630828 \\ 0.188878 \end{pmatrix}.$$

Using a two sided approximation, $\mathbf{w}^T \simeq (-0.420496, 0.012232)$. Application of the OGY control algorithm results in convergence to the fixed point $(0.631, 0.189)$. Specification of further decimal places is not possible as they change at every iteration due to the noise signal. This ‘fixed point’ lies at a distance of 5.4×10^{-4} from the true fixed point. Thus neither \mathbf{x}_R^* nor the stabilised fixed point give a particularly accurate approximation to the true fixed point. However, applying the OGY algorithm for many iterates, it is possible to find the point to which the algorithm settles down to on average. If the algorithm is applied K times and the coordinates of the stabilised fixed point are (\hat{x}_k, \hat{y}_k) at the k th application then

$$\mathbf{x}_{\text{ave}}^+ := \left(\frac{1}{K} \sum_{k=1}^K \hat{x}_k, \frac{1}{K} \sum_{k=1}^K \hat{y}_k \right)$$

gives the average value of the stabilised fixed point. The average value of δp_n is also easily found as

$$\delta p_{\text{ave}} = \frac{1}{K} \sum_{k=1}^K \delta p_k.$$

Then for K sufficiently large, the refinement procedure is the same as that used in the absence of noise, but just replacing \mathbf{x}^+ and δp^+ with their averaged counterparts. By taking K such that the norm of the difference between the averages $\mathbf{x}_{\text{ave}}^+$ based on $K - 1$ and K iterates was less than 1×10^{-8} and applying the correction procedure four times, a value for the fixed point was found to be $\mathbf{x}^{*T} \simeq (0.631347, 0.189398)$, which lies within a distance of 1.1×10^{-5} of the true fixed point. Compare this with an estimate of $\mathbf{x}_R^{*T} = (0.631370, 0.189478)$ obtained

via a regression on 1000 pairs of iterates within a distance of 0.05 of the numerically found fixed point. This lies at a distance of 7.3×10^{-5} from the true fixed point which is over six times further away than the estimate obtained with the refinement procedure.

Such a refinement procedure has applications to the accurate numerical calculation of fixed points, or indeed, periodic orbits of a mapping when the specific form for the mapping \mathbf{F} is unknown. It may also be applied to the accurate determination of periodic orbits of differential equations which do not possess an analytic solution. In such a case a Poincaré surface of section can be employed to produce a map suitable for the application of control methods and hence the refinement procedures. The mapping or the solution to the differential equation must, of course, be chaotic to permit the application of these methods.

To investigate the effect of a bad estimate of \mathbf{w} , let us return to the Hénon map in the presence of small amplitude noise, equation (1.4.12). Suppose the noise is distributed as $\text{Normal}(0, 2.4 \times 10^{-9})$. Then a regression based upon ten pairs of iterates, but this time using a one sided estimate for \mathbf{w} , yields $\mathbf{w}^T \simeq (-0.398150, 0.813780)$. Clearly, the second entry of \mathbf{w} has been poorly estimated. The estimate to the Jacobian and the fixed point are still relatively good however, with

$$J(\mathbf{x}_R^*) \simeq \begin{pmatrix} -1.766248 & 1.001091 \\ 0.291694 & 0.001285 \end{pmatrix} \quad \text{and} \quad \mathbf{x}_R^* = \begin{pmatrix} 0.627297 \\ 0.178208 \end{pmatrix}. \quad (2.3.35)$$

Application of the OGY method results in the stabilisation of a period two orbit in the vicinity of \mathbf{x}_R^* . On average, iterates are mapped from $\mathbf{x}_1^{+T} = (0.618323, 0.192829)$ to $\mathbf{x}_2^{+T} = (0.642774, 0.185493)$, the average value being relevant due to the presence of noise. This would indicate that a bifurcation of fixed points has been encountered due to a value of α above the critical value α_{cu} . Denoting $\hat{\lambda}_u = -1.918365$ as the unstable eigenvalue of the approximated Jacobian

matrix in (2.3.35), then α_{cu} can be approximated as

$$\hat{\alpha}_{cu} \simeq \frac{\hat{\lambda}_u}{\hat{\lambda}_u + 1} = 2.089.$$

Then scaling the estimate of \mathbf{w} by the factor $\frac{1}{\hat{\alpha}_{cu}}$, convergence to the fixed point $\mathbf{x}^{+T} = (0.627306, 0.188188)$ is obtained. Again this is an averaged quantity. Since \mathbf{w} is precisely known in this example, the exact value of α resulting from the bad estimate to \mathbf{w} is found to be

$$\alpha = \frac{\mathbf{f}_u^T \hat{\mathbf{w}}}{\mathbf{f}_u^T \mathbf{w}} = 2.060.$$

Hence the scaling of $\hat{\mathbf{w}}$ by $\frac{1}{\hat{\alpha}_{cu}}$ turns out to be a very appropriate one and especially easy to obtain from observed data.

Chapter 3

Basins of Attraction

In this chapter we derive a method for widening the basin of attraction for the OGY method. We then derive a generalisation of this result applicable to any of the one-step linear methods discussed in Chapter 1. By ‘basin of attraction’ for a control method, we mean the set of iterates which asymptote to the fixed point \mathbf{x}^* , in the presence of parameter perturbations, in the limit as the number of iterations of the perturbed mapping tends to infinity. According to Ott, Grebogi and Yorke [53], convergence to the fixed point occurs when an iterate falls in a narrow strip within which control may be effected. We attempt to widen and possibly lengthen this strip by allowing parameter perturbations to be activated at their maximum permissible value within a region which maps into the region within which we know, at least to a linear approximation, convergence to the fixed point occurs. The analysis is motivated by the fact that size of the basin of attraction may be somewhat curtailed by the requirement that only small perturbations are permissible. We shall consider in some detail how a basin of attraction for a control method should be chosen and then investigate the consequences of this choice on the time it takes to achieve control of a system.

3.1 Extending the Basin of Attraction

It turns out that widening the basin of attraction for the OGY method is a special case of the more general problem of widening the basin of attraction for the one-step linear control methods discussed in Chapter 1. After careful investigation of the basin widening process for the OGY method, we shall formulate the general result, and in particular, apply the result to the ZSR method.

3.1.1 The OGY Method

In Section 0.3.2 it was stated that parameter perturbations can only be activated provided that $|\delta p_n| \leq \delta p_{\max}$. This consequently defines a strip about the fixed point within which control may be realised (Fig. 3.1). The size of δp_{\max} governs the width of this strip – the larger δp_{\max} , the wider the strip. The strip effectively defines a basin of attraction for the control method, since in the presence of parameter perturbations all iterates within it are attracted to the fixed point \mathbf{x}^* (in a linear sense), whilst those outside it are not. For the time being we shall assume, without loss of generality, that the strip is infinitely long. Of course, it is not, but we shall return to the problem of determining its length later.

Let us change coordinates from ordinary Cartesian coordinates (x, y) to the basis $\{\mathbf{e}_s, \mathbf{e}_u\}$. We may then write

$$\delta \mathbf{x}_n = \alpha_n \mathbf{e}_s + \beta_n \mathbf{e}_u \quad (3.1.1)$$

for scalars $\alpha_n = \mathbf{f}_s^T \delta \mathbf{x}_n$ and $\beta_n = \mathbf{f}_u^T \delta \mathbf{x}_n$. Let us also use the eigenvector form for \mathbf{w} , namely $\mathbf{w} = \eta \mathbf{e}_s + \xi \mathbf{e}_u$. Using the usual linearisation

$$\delta \mathbf{x}_{n+1} = M \delta \mathbf{x}_n + \mathbf{w} \delta p_n \quad (3.1.2)$$

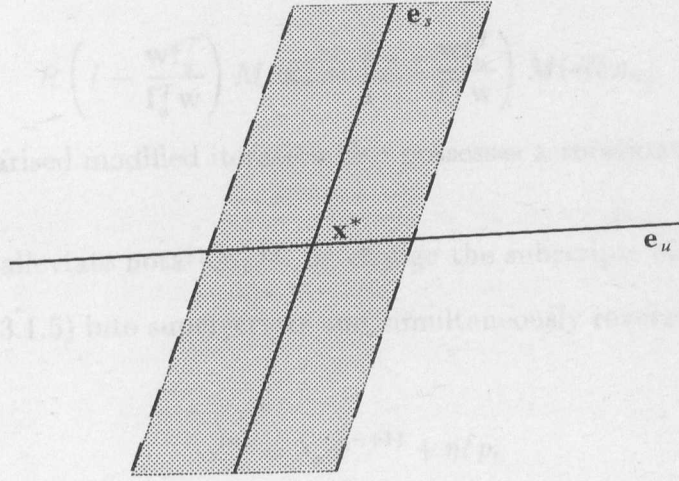


Figure 3.1: The region suitable for control activation.

and equation (3.1.1) we have that

$$\begin{aligned}\alpha_{n+1}\mathbf{e}_s + \beta_{n+1}\mathbf{e}_u &= M(\alpha_n\mathbf{e}_s + \beta_n\mathbf{e}_u) + (\eta\mathbf{e}_s + \xi\mathbf{e}_u)\delta p_n \\ &= (\lambda_s\alpha_n + \eta\delta p_n)\mathbf{e}_s + (\lambda_u\beta_n + \xi\delta p_n)\mathbf{e}_u.\end{aligned}\quad (3.1.3)$$

Then (3.1.3) decouples such that

$$\alpha_{n+1} = \lambda_s\alpha_n + \eta\delta p_n \quad (3.1.4)$$

and

$$\beta_{n+1} = \lambda_u\beta_n + \xi\delta p_n \quad (3.1.5)$$

which describe the dynamics in the \mathbf{e}_s and \mathbf{e}_u directions respectively.

Let $R = \begin{pmatrix} -x \\ -y \end{pmatrix}$ define a rotational symmetry in \mathbb{R}^2 . Then a (nonlinear) mapping $\mathbf{y} \mapsto \mathbf{g}(\mathbf{y})$ possesses a rotational symmetry if

$$R\mathbf{g}(\mathbf{y}) = \mathbf{g}(R\mathbf{y}).$$

The linearised map in the absence of parameter perturbations clearly has this symmetry since

$$RM\delta\mathbf{x}_n = -M\delta\mathbf{x}_n = M(-\delta\mathbf{x}_n) = M(R\delta\mathbf{x}_n).$$

Similarly,

$$R \left(I - \frac{\mathbf{w}\mathbf{f}_u^T}{\mathbf{f}_u^T\mathbf{w}} \right) M \delta \mathbf{x}_n = \left(I - \frac{\mathbf{w}\mathbf{f}_u^T}{\mathbf{f}_u^T\mathbf{w}} \right) M (R \delta \mathbf{x}_n)$$

and so the linearised modified iteration also possesses a rotational symmetry.

In order to alleviate notation, let us change the subscripts on the coordinates in (3.1.4) and (3.1.5) into superscripts and simultaneously reverse the iteration by writing

$$\alpha^{(n)} = \lambda_s \alpha^{(n+1)} + \eta \delta p_n \quad (3.1.6)$$

and

$$\beta^{(n)} = \lambda_u \beta^{(n+1)} + \xi \delta p_n. \quad (3.1.7)$$

That way, δp_n will be the perturbation that maps the $(n+1)$ th point onto the n th. The aim is to back iterate regions about the fixed point, with δp_{\max} set to its maximum permissible value, and hence find the sequence of regions which forward iterate to the linearised stable manifold. In order to do this we will back iterate lines representing the boundaries of these regions. Firstly, we shall look for lines which map, under an iteration of (3.1.3) with parameter perturbations set at their maximum value, onto the linearised stable manifold of \mathbf{x}^* . Note that these lines will be parallel to \mathbf{e}_s as a consequence of the decoupling in (3.1.3). We shall then look for further lines which map onto the lines mapping onto the stable manifold and so on, the process being repeated ad infinitum.

Let us now determine the lines defined by $\beta = \pm \beta^{(1)}$ which map, under an iteration of (3.1.3) with δp_n set at its maximum value, onto the linearised stable manifold of \mathbf{x}^* , defined by $\beta = \beta^{(0)} = 0$. From (3.1.7) we have that when δp_n is set to its maximum negative value, $-\delta p_{\max}$,

$$\beta^{(0)} = \lambda_u \beta^{(1)} - \delta p_{\max}$$

so that

$$\beta^{(1)} = \frac{\xi \delta p_{\max}}{\lambda_u}.$$

As a consequence of the rotational symmetry in the linearised problem, for each line $\beta = \beta^{(1)}$ lying to one side of the linearised stable manifold, there is an equivalent line given by $\beta = -\beta^{(1)}$ lying to the other side. This line is obtained from the line $\beta = \beta^{(1)}$ by a rotation about the fixed point \mathbf{x}^* . It can also be obtained by setting $\delta p_n = \delta p_{\max}$ in (3.1.7). In a linearised sense, any iterate (α_n, β_n) with $|\beta_n| \leq \beta^{(1)}$ will be mapped onto \mathbf{e}_s upon application of the OGY method. We shall term the region bounded by the lines $\beta = \pm\beta^{(1)}$ the *immediate basin of attraction* and denote it by B_1 . These lines define the width of the region in the \mathbf{e}_u direction suitable for control activation, or more precisely, iterates lying between these lines can be placed on \mathbf{e}_s in a linear sense by the application of a single parameter perturbation.

Having determined the immediate basin of attraction, we can look for further regions which map into B_1 when perturbations are set to their maximum value. The regions B_2 which map into B_1 when perturbations are activated at their maximum value are demarcated by the lines $\beta = \beta^{(1)}$ and $\beta = \beta^{(2)}$. Similarly, the regions B_n are demarcated by $\beta = \beta^{(n-1)}$ and $\beta = \beta^{(n)}$, the latter line being obtained from the former by an iteration of (3.1.7) with parameter perturbations set to their maximum value. Thus from equation (3.1.7),

$$\beta^{(n+1)} = \frac{\beta^{(n)} \pm \xi \delta p_{\max}}{\lambda_u}$$

when perturbations are set to their maximum value. We note here that if $\lambda_u > 0$ the lines defined by $\pm\beta^{(n+1)}$ are mapped onto the lines $\pm\beta^{(n)}$ under the action of the forward iterated map, whilst if $\lambda_u < 0$, they are mapped onto $\mp\beta^{(n)}$. This is easily seen since if an iterate we are attempting to control lies outside B_1 , it cannot be mapped directly onto \mathbf{e}_s . When $\lambda_u < 0$, the action of the map will take

it successively from one side of the stable manifold to the other until a control algorithm manages to place it within B_1 . In order to simplify the analysis we shall assume, without loss of generality, that $\lambda_u > 0$. Then as a direct consequence of the rotational symmetry of the linearised problem we can just consider the mapping

$$\beta^{(n+1)} = \frac{\beta^{(n)} + \xi \delta p_{\max}}{\lambda_u}$$

as defining the boundaries of the extended basins of attraction. In that case,

$$\begin{aligned} \beta^{(n)} &= \left(\frac{1}{\lambda_u^n} + \frac{1}{\lambda_u^{n-1}} + \cdots + \frac{1}{\lambda_u} \right) \xi \delta p_{\max} + \frac{1}{\lambda_u^{n+1}} \beta^{(0)} \\ &= \left(\frac{1 - \frac{1}{\lambda_u^n}}{\lambda_u - 1} \right) \xi \delta p_{\max}. \end{aligned}$$

We have that

$$\beta^{(\infty)} = \lim_{n \rightarrow \infty} \beta^{(n)} = \frac{1}{\lambda_u - 1} \xi \delta p_{\max}$$

for $\lambda_u > 0$. The general result, regardless of the sign of λ_u is

$$|\beta^{(\infty)}| = \lim_{n \rightarrow \infty} |\beta^{(n)}| = \frac{1}{|\lambda_u| - 1} |\xi| \delta p_{\max}.$$

The proportion by which, at best, the basin of attraction may be widened is given by the ratio $\left| \frac{\beta^{(\infty)}}{\beta^{(1)}} \right|$, and so B_1 may be widened by the factor

$$\frac{|\lambda_u|}{|\lambda_u| - 1}.$$

Consequently, if $|\lambda_u|$ is close to unity, the boundary may be pushed out a relatively long way. Conversely, for large $|\lambda_u|$ the boundary cannot be pushed out too far. This makes sense intuitively, since iterates are pushed rapidly away from the vicinity of \mathbf{x}^* when $|\lambda_u|$ is large.

We now consider the capping of the region B_1 in the \mathbf{e}_s direction. Suppose that the boundary of B_1 is capped by the lines $\pm \alpha^{(1)} \mathbf{e}_s + \beta \mathbf{e}_u$, $\beta \in [-\beta^{(1)}, \beta^{(1)}]$ for a suitable value of $\alpha^{(1)}$. We shall discuss precisely how $\alpha^{(1)}$ is determined later in this chapter, but for the time being it can be taken to be an arbitrary constant. Since

the linear dynamics in the \mathbf{e}_s and \mathbf{e}_u direction decouple, we can find the caps of the boundary of the regions B_{n+1} which map into B_n in an analogous way to that used for the \mathbf{e}_u direction. We now look for the lines $\pm\alpha^{(2)} + \beta\mathbf{e}_u$, $\beta \in [-\beta^{(2)}, \beta^{(2)}]$ mapping onto $\pm\alpha^{(1)}\mathbf{e}_s + \beta\mathbf{e}_u$, $\beta \in [-\beta^{(1)}, \beta^{(1)}]$ (for $\lambda_s > 0$). Again, considering just one of these lines and using (3.1.6) with δp_n set at its maximum negative value, we have

$$\alpha^{(1)} = \lambda_s \alpha^{(2)} - \eta \delta p_{\max}$$

which gives, upon rearrangement,

$$\alpha^{(2)} = \frac{\alpha^{(1)} + \eta \delta p_{\max}}{\lambda_s}.$$

Clearly, the general formula for $\alpha^{(n+1)}$ is

$$\alpha^{(n+1)} = \frac{\alpha^{(n)} + \eta \delta p_{\max}}{\lambda_s}$$

and so

$$\alpha^{(n)} = \frac{\alpha^{(1)}}{\lambda_s^{n-1}} + \left(\frac{1 - \frac{1}{\lambda_s^{n-1}}}{\lambda_s - 1} \right) \eta \delta p_{\max}.$$

This suffices to define the back iteration of the cap for the immediate basin for suitable $\alpha^{(1)}$. Since $|\lambda_s| < 1$, the sequence $\{\alpha^{(n)}\}$ diverges, rapidly for small $|\lambda_s|$.

The basin of attraction can thus be pushed out arbitrarily far in the \mathbf{e}_s direction, but nonlinearities soon take hold and so render the linear approximation to the boundary in the \mathbf{e}_s direction inaccurate. A similar phenomenon occurs in the \mathbf{e}_u direction, should the method described for extending the basin of attraction in this direction manage to push the boundary out a long way. If however we can define a region $\|\mathbf{x} - \mathbf{x}^*\| < \epsilon$ containing B_1 for some suitable ϵ within which the linear dynamics may be deemed appropriate, then it may be possible to extend the basin of attraction of the OGY method to all but fill this region by extending both in the \mathbf{e}_u and the \mathbf{e}_s directions (see Fig. 3.2).

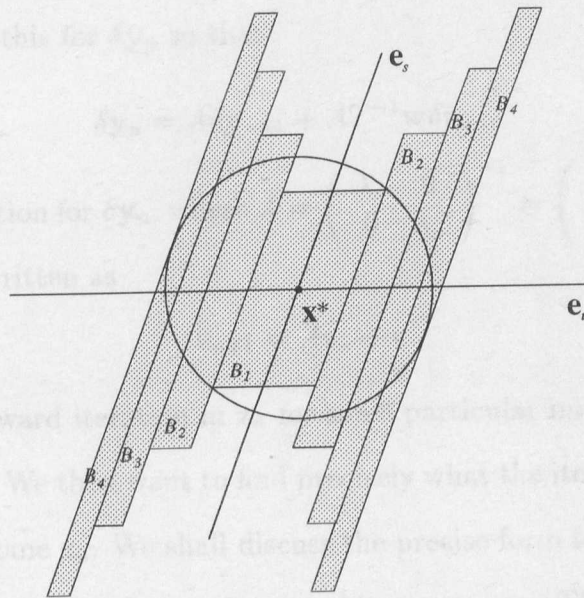


Figure 3.2: Example of an extended basin of attraction. The circle centred at \mathbf{x}^* denotes the region within which the linear dynamics are valid. The regions B_{n+1} are mapped into the regions B_n when parameter perturbations are set to their maximum value.

3.1.2 The General Result

Having dealt with extending the basin of attraction for the OGY method, we now move on to formulate a general result applicable to the one-step linear methods of Chapter 1. To begin with we shall assume that $\lambda_u > 0$. The sign of λ_s is irrelevant since we are only interested in widening the basin in the \mathbf{e}_u direction. Recall that, when perturbations are set to their maximum negative value, we have to a linear approximation,

$$\delta \mathbf{x}_{n+1} = M \delta \mathbf{x}_n - \mathbf{w} \delta p_{\max}. \quad (3.1.8)$$

Let $T = \begin{pmatrix} \mathbf{e}_s & \mathbf{e}_u \end{pmatrix}$ be the transformation matrix as defined in Section 3.1.1.

Writing $\mathbf{x} = T\mathbf{y}$, equation (3.1.8) may be written as

$$\begin{aligned} \delta \mathbf{y}_{n+1} &= T^{-1} M T \delta \mathbf{y}_n - T^{-1} \mathbf{w} \delta p_{\max} \\ &= \begin{pmatrix} \lambda_s & 0 \\ 0 & \lambda_u \end{pmatrix} \delta \mathbf{y}_n - T^{-1} \mathbf{w} \delta p_{\max}. \end{aligned}$$

We may rearrange this for $\delta \mathbf{y}_n$ so that

$$\delta \mathbf{y}_n = A \delta \mathbf{y}_{n+1} + AT^{-1} \mathbf{w} \delta p_{\max} \quad (3.1.9)$$

is a backward iteration for $\delta \mathbf{y}_n$, where $A = \begin{pmatrix} \lambda_s & 0 \\ 0 & \lambda_u \end{pmatrix}^{-1} = \begin{pmatrix} \frac{1}{\lambda_s} & 0 \\ 0 & \frac{1}{\lambda_u} \end{pmatrix}$. Equation (3.1.9) may be rewritten as

$$\mathbf{z}_{n+1} = A \mathbf{z}_n + \mathbf{c} \quad (3.1.10)$$

which is now a forward iteration in \mathbf{z}_n for some particular initial vector \mathbf{z}_0 , where $\mathbf{c} = AT^{-1} \mathbf{w} \delta p_{\max}$. We then want to find precisely what the iteration (3.1.10) tends to as $n \rightarrow \infty$ for some \mathbf{z}_0 . We shall discuss the precise form for \mathbf{z}_0 shortly, but for the time being it can be taken to be an arbitrary vector. Then as in the case of the OGY method discussed previously, this iteration will give rise to the extended basin of attraction. We have that

$$\begin{aligned} \mathbf{z}_{n+1} &= A \mathbf{z}_n + \mathbf{c} \\ &= A^{n+1} \mathbf{z}_0 + (A^n + A^{n-1} + \cdots + I) \mathbf{c} \\ &= A^{n+1} \mathbf{z}_0 + (I - A)^{-1} (I - A^{n+1}) \mathbf{c}. \end{aligned}$$

It is then easily verified that

$$\mathbf{z}_n = \begin{pmatrix} \frac{1}{\lambda_s^n} & 0 \\ 0 & \frac{1}{\lambda_u^n} \end{pmatrix} \mathbf{z}_0 + \begin{pmatrix} \frac{(\lambda_s^n - 1)}{\lambda_s^{n-1}(\lambda_s - 1)} & 0 \\ 0 & \frac{(\lambda_u^n - 1)}{\lambda_u^{n-1}(\lambda_u - 1)} \end{pmatrix} \mathbf{c}. \quad (3.1.11)$$

Letting $n \rightarrow \infty$ in (3.1.11) we see that

$$\lim_{n \rightarrow \infty} \mathbf{z}_n = \begin{pmatrix} \infty & 0 \\ 0 & 0 \end{pmatrix} \mathbf{z}_0 + \begin{pmatrix} \infty & 0 \\ 0 & \frac{\lambda_u}{\lambda_u - 1} \end{pmatrix} \mathbf{c}. \quad (3.1.12)$$

Suppose now that $\lambda_u < 0$. Then successive perturbations δp_n of the mapping will alternate in sign since iterates are successively mapped from one side of the linearised stable manifold to the other by the action of the map. In that case,

$$\begin{aligned} \mathbf{z}_n &= A \mathbf{z}_{n-1} + (-1)^n \mathbf{c} \\ &= A^{n+1} \mathbf{z}_0 + \left(\sum_{j=0}^n (-1)^{j+1} A^{j+1} \right) \mathbf{c} \\ &= A^{n+1} \mathbf{z}_0 + (I + A)^{-1} (I - (-1)^{n+1} A^{n+1}) \mathbf{c}. \end{aligned}$$

Then since

$$(I + A)^{-1} (I - (-1)^{n+1} A^{n+1}) = \begin{pmatrix} -\frac{\lambda_s((-1)^{n+1} - \lambda_s^{n+1})}{(\lambda_s + 1)\lambda_s^{n+1}} & 0 \\ 0 & -\frac{\lambda_u((-1)^{n+1} - \lambda_u^{n+1})}{(\lambda_u + 1)\lambda_u^{n+1}} \end{pmatrix},$$

we have that

$$\lim_{n \rightarrow \infty} \mathbf{z}_n = \begin{pmatrix} \infty & 0 \\ 0 & 0 \end{pmatrix} \mathbf{z}_0 + \begin{pmatrix} \infty & 0 \\ 0 & \frac{\lambda_u}{\lambda_u + 1} \end{pmatrix} \mathbf{c}.$$

Thus the general result regardless of the signs of λ_s and λ_u is then

$$\lim_{n \rightarrow \infty} \mathbf{z}_n = \begin{pmatrix} \infty & 0 \\ 0 & 0 \end{pmatrix} \mathbf{z}_0 + \begin{pmatrix} \infty & 0 \\ 0 & \frac{|\lambda_u|}{|\lambda_u| - 1} \end{pmatrix} \mathbf{c}. \quad (3.1.13)$$

For the OGY method, we simply take $\mathbf{z}_0 = \zeta \mathbf{e}_s$ for scalar ζ since this is the line upon which we aim to place iterates in order that they converge to the fixed point. For the ZSR method we aim to place iterates on $\zeta \mathbf{l}$ and so in this case $\mathbf{z}_0 = \zeta \mathbf{l}$. Recall that in Section 1.2.2 we were able to write \mathbf{l} in (α, β) coordinates as $\mathbf{l} = \eta \lambda_u \mathbf{e}_s + \xi \lambda_s \mathbf{e}_u$. We can thus substitute for $\mathbf{z}_0 = \zeta \begin{pmatrix} \eta \lambda_u \\ \xi \lambda_s \end{pmatrix}$ directly in (3.1.11). Note that, from (3.1.13), the width of the fully extended basin of attraction does not depend upon the choice of \mathbf{z}_0 .

3.1.3 Immediate Basin of Attraction for the ZSR Method

We now look for the immediate basin of attraction for the ZSR method. This is not as simple as for the OGY method, but nonetheless, we are able to gain some useful information on the performance of the method. We have, from (3.1.10), that

$$\mathbf{z}_1 = A\mathbf{z}_0 + \mathbf{c}_0$$

where $\mathbf{z}_0 = \zeta \mathbf{l}$ for scalar ζ . Then writing $\mathbf{l} = \eta \lambda_u \mathbf{e}_s + \xi \lambda_s \mathbf{e}_u$, from 3.1.10 we have

$$\begin{aligned} \mathbf{z}_1 &= \zeta \begin{pmatrix} \frac{1}{\lambda_s} & 0 \\ 0 & \frac{1}{\lambda_u} \end{pmatrix} \begin{pmatrix} \eta \lambda_u \\ \xi \lambda_s \end{pmatrix} \pm \begin{pmatrix} \frac{1}{\lambda_s} & 0 \\ 0 & \frac{1}{\lambda_u} \end{pmatrix} \begin{pmatrix} \mathbf{f}_s^T \mathbf{w} \\ \mathbf{f}_u^T \mathbf{w} \end{pmatrix} \delta p_{\max} \\ &= \zeta \begin{pmatrix} \frac{\lambda_u \eta}{\lambda_s \zeta} \\ \frac{\lambda_s \xi}{\lambda_u} \end{pmatrix} \pm \begin{pmatrix} \frac{\eta}{\lambda_s} \\ \frac{\xi}{\lambda_u} \end{pmatrix} \delta p_{\max}. \end{aligned}$$

So in the \mathbf{e}_s direction we have

$$\zeta \frac{\lambda_u \eta}{\lambda_s} \pm \frac{\eta}{\lambda_s} \delta p_{\max} \quad (3.1.14)$$

and in the \mathbf{e}_u direction,

$$\zeta \frac{\lambda_s \xi}{\lambda_u} \pm \frac{\xi}{\lambda_u} \delta p_{\max} \quad (3.1.15)$$

By setting $\zeta = 0$ in (3.1.14) and (3.1.15) we see that the lines defining the immediate basin of attraction pass through $(\pm \frac{\eta}{\lambda_s} \delta p_{\max}, \pm \frac{\xi}{\lambda_u} \delta p_{\max})$. Since we have a rotational symmetry about \mathbf{x}^* , the lines must be parallel.

To look at when the basin boundary crosses \mathbf{e}_u we can set (3.1.14) equal to zero. This gives

$$\zeta = \pm \frac{\xi}{\lambda_u} \delta p_{\max}$$

and substituting for ζ in (3.1.15) we obtain

$$\begin{aligned} \beta &= \pm \frac{\lambda_s \xi}{\lambda_u^2} \mp \frac{\xi}{\lambda_u} \delta p_{\max} \\ &= \pm \frac{\xi}{\lambda_u} \left(\frac{\lambda_s}{\lambda_u} - 1 \right) \delta p_{\max}. \end{aligned}$$

This suffices to define the width of the boundary in the \mathbf{e}_u direction. For the time being, we are not concerned with how the boundary will be capped.

Recalling that the width of the immediate basin of attraction for the OGY method was prescribed by $|\beta^{(1)}| = \left| \frac{\xi}{\lambda_u} \right| \delta p_{\max}$, the width of the basin for the ZSR method in the \mathbf{e}_u direction (with equivalent values of δp_{\max}) is larger than that for the OGY method if

$$\left| \frac{\lambda_s}{\lambda_u} - 1 \right| > 1.$$

Solving the inequality for $\frac{\lambda_s}{\lambda_u}$ and noting that $\left| \frac{\lambda_s}{\lambda_u} \right| < 1$ we find that if $\lambda_s \lambda_u < 0$, the basin stretches further in the \mathbf{e}_u direction. Clearly then, if λ_u and λ_s take on the opposite sign, the ZSR method possesses the wider immediate basin of attraction. This is another reason as to why the ZSR method out performed the

OGY method in the presence of noise in the numerical example of Chapter 1. Since the eigenvalues of the saddle fixed point of the Hénon are of opposite sign, the immediate basin of attraction for the ZSR method stretches further in the \mathbf{e}_u direction than that of the OGY method. Hence the region suitable for control is larger and once iterates are at the centre of that region (i.e. at the fixed point), they are less likely to be thrown from that region.

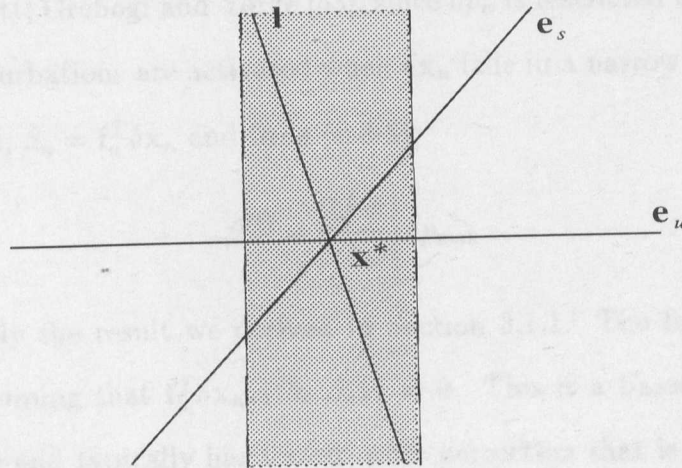


Figure 3.3: Example of a typical immediate basin of attraction for the ZSR method.

It is interesting to note that whilst the widened basins of attraction for the OGY and the ZSR methods are the same, they do not have the same immediate basin of attraction. The orientation of the lines defining the boundary for the ZSR method change with each iteration of the map (3.1.11) until, in the limit as $n \rightarrow \infty$, they lie parallel to \mathbf{e}_s . See Fig. 3.3 for a schematic representation of an immediate basin of attraction for the ZSR method.

3.2 Capping The Basin of Attraction

We now focus on the criteria which must be considered when deciding on the length of the immediate basin of attraction. Firstly, we shall review the criterion stated by Ott, Grebogi and Yorke [53] and then proceed to investigate other criteria which

take into account the one-dimensional dynamics of the map in the \mathbf{e}_s direction and the curvature of the stable manifold. This will lead a discussion of precisely how to choose a suitable basin of attraction.

3.2.1 The OGY Criterion

According to Ott, Grebogi and Yorke [53], since δp_n is restricted by $|\delta p_n| \leq \delta p_{\max}$, parameter perturbations are activated when $\delta \mathbf{x}_n$ falls in a narrow strip $|\beta_n| \leq \beta^{(1)}$ where we recall, $\beta_n = \mathbf{f}_u^T \delta \mathbf{x}_n$ and from (0.3.8),

$$\beta^{(1)} = \left| \frac{\mathbf{f}_u^T \mathbf{w}}{\lambda_u} \right| \delta p_{\max}$$

This is precisely the result we derived in Section 3.1.1. The formula for δp_n is derived by assuming that $\mathbf{f}_u^T \delta \mathbf{x}_{n+1} \equiv \beta_{n+1} = 0$. This is based upon a linearisation however and typically has lowest order correction that is quadratic. Now, $\alpha_n = \mathbf{f}_s^T \delta \mathbf{x}_n$ is not restricted by $|\alpha_n| \leq \beta^{(1)}$ and is not necessarily small when $|\beta_n| \leq \beta^{(1)}$. Thus the quadratic correction in α_n is the most significant correction term. Including such a correction, $\beta_{n+1} \simeq \kappa(\alpha_n)^2$ for some non-zero constant κ . Consequently if $|\kappa|(\alpha_n)^2 > \beta^{(1)}$ then $|\beta_{n+1}| > \beta^{(1)}$ and attraction to the fixed point will not occur even though $|\beta_n| \leq \beta^{(1)}$. Attraction to the fixed point is achieved when an iterate \mathbf{x}_n falls within the small parallelogram defined by $|\beta_n| \leq \beta^{(1)}$ and $|\alpha_n| \leq \left(\frac{\beta^{(1)}}{|\kappa|} \right)^{\frac{1}{2}}$. Thus we may take $\alpha^{(1)} = \left(\frac{\beta^{(1)}}{|\kappa|} \right)^{\frac{1}{2}}$ as defining the cap to the immediate basin of attraction for the OGY method.

3.2.2 Basin of Attraction for the One-dimensional Map

We may perform a change of coordinates on the map in the absence of perturbations,

$$\delta \mathbf{x}_{n+1} = \mathbf{F}(\delta \mathbf{x}_n) = M \delta \mathbf{x}_n + \frac{1}{2} F_{\mathbf{xx}}^* \delta \mathbf{x}_n \delta \mathbf{x}_n + \cdots \quad (3.2.1)$$

to transform to (α, β) coordinates (as defined in Section 3.1.1). It is easily shown that (3.2.1) may be written as

$$\begin{aligned}\alpha_{n+1} &= \lambda_s \alpha_n + d_1 \alpha_n^2 + d_3 \alpha_n \beta_n + d_5 \beta_n^2 + \dots \\ \beta_{n+1} &= \lambda_u \beta_n + d_2 \alpha_n^2 + d_4 \alpha_n \beta_n + d_6 \beta_n^2 + \dots\end{aligned}\quad (3.2.2)$$

where d_j , $j = 1, 2, \dots, 6$ are constants. Since we assume that β_n is small, higher order terms involving β_n in (3.2.2) may be neglected. Now, the first equation in (3.2.2) is an approximation to the one-dimensional dynamics in the \mathbf{e}_s direction in the absence of parameter perturbations. The constants d_1 and d_2 may be obtained by iterating the map and collecting pairs of iterates in a strip such that $|\alpha| < \alpha^s$, $|\beta| < \beta^s$ for suitable small scalars α^s and β^s . We then have that

$$\begin{aligned}d_1 \alpha_n^2 &\simeq \alpha_{n+1} - \lambda_s \alpha_n \\ d_2 \alpha_n^2 &\simeq \beta_{n+1} - \lambda_u \beta_n\end{aligned}$$

and so a regression may be performed to obtain estimates for d_1 and d_2 .

The map in the presence of parameter perturbations may be written as

$$\begin{aligned}\delta \mathbf{x}_{n+1} &= \mathbf{F}(\delta \mathbf{x}_n, p^* + \delta p_n(\mathbf{x}_n)) = \\ M \delta \mathbf{x}_n + \mathbf{w} \delta p_n + \frac{1}{2} &\left(\mathbf{F}_{\mathbf{x}\mathbf{x}}^* \delta \mathbf{x}_n \delta \mathbf{x}_n + \mathbf{F}_{\mathbf{x}p}^* \delta \mathbf{x}_n \delta p_n + \mathbf{F}_{pp}^* \delta p_n^2 \right) + \dots\end{aligned}\quad (3.2.3)$$

Now let $\delta \mathbf{x} = \alpha' \mathbf{e}_s + \beta' \mathbf{v}$, where $\mathbf{v} = \chi \mathbf{e}_s + \mathbf{e}_u$ is the right eigenvector of the linearised map in the presence of parameter perturbations corresponding to the zero eigenvalue (see Section 1.1). Then $\alpha \mathbf{e}_s + \beta \mathbf{e}_u = \alpha' \mathbf{e}_s + \beta' \mathbf{v}$ so that

$$\begin{pmatrix} \mathbf{e}_s & \mathbf{e}_u \end{pmatrix} \begin{pmatrix} \alpha \\ \beta \end{pmatrix} = \begin{pmatrix} \mathbf{e}_s & \mathbf{v} \end{pmatrix} \begin{pmatrix} \alpha' \\ \beta' \end{pmatrix}$$

and so

$$\begin{pmatrix} \alpha \\ \beta \end{pmatrix} = \begin{pmatrix} \mathbf{f}_s^T \\ \mathbf{f}_u^T \end{pmatrix} \begin{pmatrix} \mathbf{e}_s & \mathbf{v} \end{pmatrix} \begin{pmatrix} \alpha' \\ \beta' \end{pmatrix} = T_p \begin{pmatrix} \alpha' \\ \beta' \end{pmatrix}$$

where $T_p = \begin{pmatrix} 1 & \chi \\ 0 & 1 \end{pmatrix}$. Clearly $T_p^{-1} = \begin{pmatrix} 1 & -\chi \\ 0 & 1 \end{pmatrix}$ and $\beta = \beta'$ so that if β is small then β' can also be assumed small. Recalling that $\delta p_n = -\frac{\lambda_u \beta_n}{\mathbf{f}_u^T \mathbf{w}}$, the second order

terms in (3.2.3) involving δp_n may be neglected and thus (3.2.3) can be written as

$$\begin{aligned}\alpha'_{n+1} &\simeq \lambda_s \alpha'_n + D_1 \alpha_n'^2 \\ \beta'_{n+1} &\simeq 0 \times \beta'_n + D_2 \alpha_n'^2\end{aligned}\tag{3.2.4}$$

In (α, β) coordinates,

$$\mathbf{w} \delta p_n = -T_p^{-1} \mathbf{w} \frac{\lambda_u \beta_n}{\mathbf{f}_u^T \mathbf{w}}\tag{3.2.5}$$

So adding (3.2.5) to (3.2.2) and transforming to (α', β') coordinates will result in (3.2.4). It is then easily verified that

$$\begin{pmatrix} D_1 \\ D_2 \end{pmatrix} = T_p^{-1} \begin{pmatrix} d_1 \\ d_2 \end{pmatrix}$$

and so the most significant second order terms in the presence of parameter perturbations can be found from the second order terms of the unperturbed mapping.

We now concentrate on the dynamics of the perturbed mapping in the \mathbf{e}_s direction, that is, the one-dimensional dynamics along the direction of the linearised stable manifold. In this direction, the dynamics are approximated by

$$\alpha'_{n+1} = \lambda_s \alpha'_n + D_1 \alpha_n'^2.\tag{3.2.6}$$

Then for suitable initial conditions α_0 , the iteration (3.2.6) will converge to a fixed point of this mapping at $\alpha = 0$, corresponding to the fixed point \mathbf{x}^* .

According to Devaney [13], one endpoint of the immediate basin of attraction for (3.2.6) may be found by solving

$$\alpha = \lambda_s \alpha + D_1 \alpha^2$$

giving $\alpha = \frac{1-\lambda_s}{D_1}$. Note that this is an unstable fixed point of (3.2.6). The other endpoint, given by the solution of

$$\frac{1-\lambda_s}{D_1} = \lambda_s \alpha + D_1 \alpha^2$$

is $\alpha = -\frac{1}{D_1}$ and so the immediate basin of attraction of (3.2.4) is $\alpha \in \left(-\frac{1}{D_1}, \frac{1-\lambda_s}{D_1}\right)$ for $D_1 > 0$. If $D_1 < 0$ then the limits must be switched round. Note that the basin of attraction extends further to one side of \mathbf{x}^* than it does to the other, the difference in length depending on the size and sign of λ_s . For small D_1 the one-dimensional map will have a relatively wide basin of attraction, narrowing with increasing D_1 .

3.2.3 Curvature of the Stable Manifold

Let us write (3.2.2) as

$$\begin{aligned}\alpha_{n+1} &= f(\alpha_n, \beta_n) \\ \beta_{n+1} &= g(\alpha_n, \beta_n)\end{aligned}\tag{3.2.7}$$

for suitable scalar functions f and g . Let

$$\beta = h(\alpha)\tag{3.2.8}$$

be the equation of the local stable manifold, w_{loc}^s , of \mathbf{x}^* for some scalar function h . At the fixed point

$$\alpha = f(\alpha, \beta) \quad \text{and} \quad \beta = g(\alpha, \beta)$$

and so using (3.2.8) we have that

$$g(\alpha, h(\alpha)) = h(f(\alpha, h(\alpha))).\tag{3.2.9}$$

Since w_{loc}^s is invariant under the map \mathbf{F} and the fixed point lies on w_{loc}^s , equation (3.2.9) is valid at all points on the local stable manifold.

Letting $h(\alpha) = c_0 + c_1\alpha + c_2\alpha^2 + \dots$ we can equate coefficients in (3.2.9) for particular functions f and g to find h and hence an approximation to w_{loc}^s . In particular, we are interested in the curvature of w_{loc}^s near to \mathbf{x}^* . In general, since $h(\alpha)$ passes through \mathbf{x}^* and is tangent to \mathbf{e}_s at \mathbf{x}^* , the coefficients c_0 and c_1 will both be zero. The coefficient c_2 will then give a quadratic approximation to $h(\alpha)$.

We can in fact find the value of c_2 by using (3.2.2) including terms up to $O(\alpha_n^2)$ so that $f = \lambda_s \alpha_n + d_1 \alpha_n^2$ and $g = \lambda_u \beta_n + d_2 \alpha_n^2$. It can then be shown that

$$c_2 = \frac{d_2}{\lambda_s^2 - \lambda_u}.$$

Ascertaining the constant c_2 does not directly give a criterion for capping the basin of attraction. However, the larger c_2 , the more severe the curvature of the stable manifold. In such a case, we would not expect a stabilisation algorithm to work particularly well for larger values of α_n and so we may tend to cap the basin with a relatively small value of α^s .

3.2.4 Choosing a Basin of Attraction

So far we have discussed how to ascertain the width of the immediate basin of attraction (in a linearised sense) for the OGY and ZSR methods, how the immediate basin may be extended and various criteria that should be considered when choosing a cap for the immediate basin. We shall now combine these results in order to choose a basin of attraction for a particular control algorithm. The width of the immediate basin of attraction is primarily governed by the size of δp_{\max} , as is the size of the extended basin of attraction. If we extend the basin of attraction as far as possible to

$$|\beta^{(\infty)}| = \frac{|\lambda_u|}{|\lambda_u| - 1} |\xi| \delta p_{\max} \quad (3.2.10)$$

then applying a control algorithm when an iterate falls on, or just inside the boundary defined by (3.2.10) will take many steps of the perturbed map to reach the vicinity of the fixed point. Indeed, if \mathbf{x}_n lies on this boundary, infinitely many steps of the perturbed mapping will be required to achieve control, which is clearly unacceptable.

In fact, extending the basin of attraction to its full extent introduces two new

‘spurious’ fixed points. Consider the mapping when perturbations are set to their maximum value. From (3.1.4) and (3.1.5) we have that

$$\begin{aligned}\alpha_{n+1} &= \lambda_s \alpha_n \pm \eta \delta p_{\max} \\ \beta_{n+1} &= \lambda_u \beta_n \pm \xi \delta p_{\max}.\end{aligned}$$

Then fixed points of this mapping satisfy

$$\begin{aligned}\lambda_s \alpha \pm \eta \delta p_{\max} &= \alpha \\ \lambda_u \beta \pm \xi \delta p_{\max} &= \beta\end{aligned}$$

so that

$$\alpha = \pm \frac{\eta \delta p_{\max}}{1 - \lambda_s}$$

and

$$\beta = \pm \frac{\xi \delta p_{\max}}{1 - \lambda_u}.$$

Thus the two new spurious fixed points are created at $\left(\pm \frac{\eta \delta p_{\max}}{1 - \lambda_s}, \pm \frac{\xi \delta p_{\max}}{1 - \lambda_u}\right)$. See Fig.

3.4. The Jacobian of the modified mapping evaluated at these fixed points is

$$\begin{pmatrix} \lambda_s & 0 \\ 0 & \lambda_u \end{pmatrix}.$$

and so they are saddle fixed points. Note that they lie on the lines $\pm \beta^{(\infty)}$.

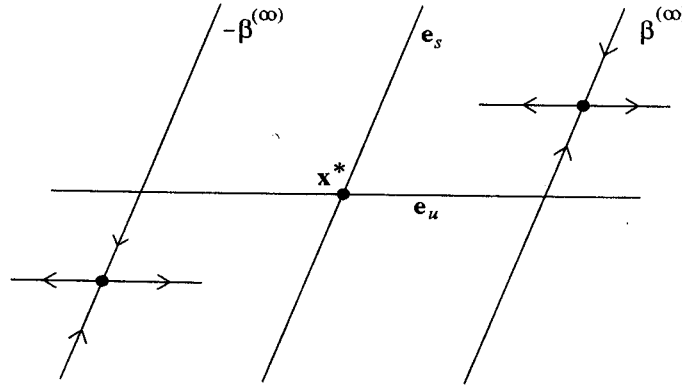


Figure 3.4: Spurious fixed points created when implementing a fully extended basin of attraction. In this case, λ_u and ξ are of opposite sign and $\eta > 0$.

It would thus be more sensible to let

$$|\beta^{(\infty)}| = \frac{|\lambda_u|}{|\lambda_u| - 1} |\xi| \delta p_{\max} - \epsilon_b \quad (3.2.11)$$

for some suitably chosen $\epsilon_b > 0$. That way, one can avoid having to make too many iterations of the perturbed mapping before the fixed point is stabilised. Alternatively, we could choose a boundary such that a maximum of k perturbations would have to be made in order to place an iterate in B_1 in a linearised sense. This can be done by only allowing perturbations to be activated when iterates fall with the lines defined by $\beta = \beta^{(k-1)}$.

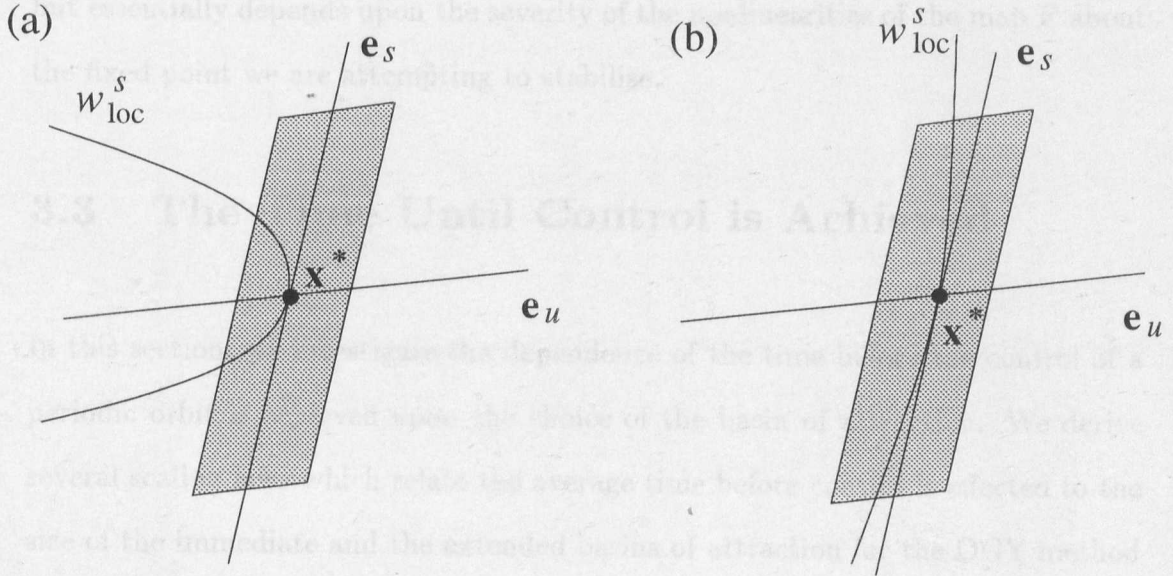


Figure 3.5: Situations where the local stable manifold leaves the strip (a) along its width and (b) along its length.

To choose the length of the immediate basin of attraction, we could use the OGY type criterion and the basin of attraction for the one-dimensional map to give us values for the maximum value of α for which convergence should occur, picking the minimum value from the two to define our cap. One should then consider whether this cap is appropriate by investigating the curvature of the stable manifold. Referring to Fig. 3.5, situation (b) is clearly preferential to (a) since w_{loc}^s stretches the full length of the immediate basin, whereas in (a), the

local stable manifold leaves the strip relatively close to the fixed point. Intuitively, one might not expect convergence to the fixed point to always occur in situations such as (a). We thus might want to cap the basin in such a way that the local stable manifold leaves the immediate basin passing through the line defining its cap, as in Fig. 3.5(b). Finally, one must always remember that the results we have discussed here are based upon linearisations of the dynamics about fixed points, as are the control algorithms themselves. Consequently, the basin of attraction we deem appropriate for a given control algorithm should not stretch outside an ϵ -neighbourhood of the fixed point. The particular choice for ϵ is somewhat arbitrary but essentially depends upon the severity of the nonlinearities of the map \mathbf{F} about the fixed point we are attempting to stabilise.

3.3 The Time Until Control is Achieved

In this section, we investigate the dependence of the time before the control of a periodic orbit is achieved upon the choice of the basin of attraction. We derive several scaling laws which relate the average time before control is effected to the size of the immediate and the extended basins of attraction for the OGY method and for the ZSR method. This gives some indication of the length of the chaotic transient likely to be observed before control is achieved.

When an iterate falls in the region within which control may be effected a stable orbit is created since the application of the control algorithm stabilises a previously unstable orbit. However, for a given initial condition, typically not within the control region, a system will exhibit a chaotic transient before settling into a stable behaviour. Iterates will bounce around the uncontrolled attractor until they land within the basin of attraction suitable for control. The length τ of such a transient depends sensitively upon the initial conditions and has exponential

probability distribution [30] $P(\tau) \sim \exp(-\tau/\bar{\tau})$. Here, $\bar{\tau}$ is the mean length of the chaotic transient, which increases with decreasing δp_{\max} and for small δp_{\max} follows a power law relationship, $\bar{\tau} \sim \delta p_{\max}^\gamma$ for some γ .

We may derive a formula for the exponent γ , but before we do so, we need to discuss some relevant theory. Firstly we define the pointwise dimension of a d -dimensional attractor [32]. Let S be a subset of the phasespace and \mathbf{x}_0 be an initial condition in the basin of attraction of the attractor. Define $\mu(\mathbf{x}_0, S)$ as the fraction of time the trajectory originating at \mathbf{x}_0 spends in S in the limit that the length of the trajectory goes to infinity. If $\mu(\mathbf{x}_0, S)$ is the same for almost every initial condition \mathbf{x}_0 then we denote this value $\mu(S)$ and say that μ is the natural measure of the attractor. We assume that this natural measure exists. This consequently means that the attractor is ergodic [32], which was one of our fundamental assumptions.

Now let $B(l, \mathbf{x})$ be a d -dimensional ball of radius l centered on \mathbf{x} embedded within the attractor. Then the pointwise dimension at the point \mathbf{x} on the attractor is defined to be

$$D_p(\mathbf{x}) := \lim_{l \rightarrow 0} \frac{\ln \mu(B(l, \mathbf{x}))}{\ln l}$$

so that in the limit as $l \rightarrow 0$,

$$\mu(B(l, \mathbf{x})) \sim l^{D_p(\mathbf{x})}. \quad (3.3.12)$$

Note that for almost every point with respect to the natural measure on the attractor, $D_p(\mathbf{x})$ takes on a common value.

Let $\mathbf{y}_{n+1} = A\mathbf{y}_n$ be the linearisation of the map (0.3.6) at any given point \mathbf{x} in the basin of attraction of the attractor. Let λ_1, λ_2 be the eigenvalues of A . If $\lambda_1, \lambda_2 \neq 0$ then we may split the vector space within which \mathbf{y} lies into subspaces E^s and E^u which are invariant under the map A [51]. The vectors \mathbf{y} are known as

tangent vectors and the space in which they lie the tangent space of the map at \mathbf{x} , denoted $T_{\mathbf{x}}$. The tangent space has a direct sum decomposition into subspaces E^s and E^u , $T_{\mathbf{x}} = E_{\mathbf{x}}^s \oplus E_{\mathbf{x}}^u$. We say that a point \mathbf{x} is hyperbolic if this direct sum $T_{\mathbf{x}} = E_{\mathbf{x}}^s \oplus E_{\mathbf{x}}^u$ exists at the point \mathbf{x} . A invariant set Σ is hyperbolic if all points $\mathbf{x} \in \Sigma$ are hyperbolic. We may then define the partial pointwise dimensions d_s and d_u at a point \mathbf{x} as the pointwise dimensions of the subspaces $E_{\mathbf{x}}^s$ and $E_{\mathbf{x}}^u$ respectively. In what follows we assume only that periodic points are hyperbolic and thus the partial pointwise dimensions exist at such points.

At any hyperbolic point \mathbf{x} , $D_p(\mathbf{x}) = d_s + d_u$. In the case of a two-dimensional map, it is easily shown [31] that for any point \mathbf{x} on the unstable manifold of a saddle periodic point,

$$D_p(\mathbf{x}) = 1 - \frac{\ln \lambda_u}{\ln \lambda_s}. \quad (3.3.13)$$

Note here that at different periodic points, λ_s and λ_u typically take on different values, $D_p(\mathbf{x})$ will not be the same at different periodic points. Indeed, periodic points and their stable manifolds form part of the set that $D_p(\mathbf{x})$ does not assume its common value upon. We make the assumption that the attractor is effectively smooth in the unstable direction so that $d_u = 1$; and so $d_s = -\frac{\ln \lambda_u}{\ln \lambda_s}$.

In the case of the OGY method, for small $\beta^{(1)}$, an initial condition bounces around the attractor for a long time before it falls within the immediate basin of attraction B_1 . Then at any given iterate, the probability of falling in B_1 is simply $\mu(B_1)$, the natural measure of the uncontrolled attractor contained in B_1 . Thus $\bar{\tau}^{-1} = \mu(B_1)$. The scaling of $\mu(B_1)$ with $\beta^{(1)}$ is

$$\mu(B_1) \sim (\beta^{(1)})^{d_u} \left[\left(\frac{\beta^{(1)}}{|\kappa|} \right)^{\frac{1}{2}} \right]^{d_s} \sim (\beta^{(1)})^{d_u + \frac{1}{2}d_s}$$

and so $\mu(B_1) = (\beta^{(1)})^\gamma$ where $\gamma d_u + \frac{1}{2}d_s$. Thus

$$\gamma = 1 - \frac{1}{2} \frac{\ln \lambda_u}{\ln \lambda_s}.$$

This result was obtained under the assumption that the basin was capped using the OGY criterion.

For the extended basin of attraction, we have shown that the basin may be stretched by the factor $\frac{|\lambda_u|}{1-|\lambda_u|}$ in the unstable direction in the case of the OGY method. Since $d_u = 1$, the average time until control may be achieved, $\bar{\tau}$, may be reduced by the factor $\frac{1-|\lambda_u|}{|\lambda_u|}$.

Extending the basin of attraction as far as possible is all very well, but we must always remember that all the results we have derived so far are based upon linearisations about the fixed point \mathbf{x}^* . We should thus only use the results within an ϵ -neighbourhood of \mathbf{x}^* for suitable ϵ . As we stated in Section 3.1.1, in many cases it is possible to extend the basin of attraction to all but fill such an ϵ -neighbourhood of \mathbf{x}^* . Certainly, it is possible to do this if the condition

$$\frac{|\lambda_u|}{|\lambda_u| - 1} > \epsilon$$

holds. In this case, to a good approximation, the time before control of a system is achieved depends directly upon the size of the ϵ -neighbourhood about the fixed point \mathbf{x}^* which, in two dimensions, is simply a circle of radius ϵ centred at \mathbf{x}^* . Let us denote such a circle by C . Using equation (3.3.12),

$$\mu(C) \sim \epsilon^{D_p}$$

for suitably small ϵ , where D_p is the pointwise dimension at the fixed point.

Summary

We have discussed a method here for extending the basin of attraction, which we have seen that in certain circumstances allows us to effect control anywhere within an ϵ -neighbourhood of the fixed point we are attempting to stabilise. Romeiras *et*

al. [67] state that before a system settles down onto a desired controlled state, the trajectory experiences a chaotic transient whose expected duration diverges as the maximum allowed perturbation approaches zero. Clearly, since δp_{\max} governs the size of the vicinity about the fixed point within which control may be effected, any enlargement of this vicinity is particularly helpful in reducing the average transient length experienced before control is achieved. We shall now consider a numerical example that clearly demonstrates the effect of widening the basin on the length of the experienced transient.

3.4 Numerical Example

Let us consider the control of the Hénon map with $\delta p_{\max} = 0.05$. Taking a grid of initial conditions about the fixed point $\mathbf{x}^{*T} = (0.631354, 0.189406)$ we are able to determine the actual immediate basin of attraction for the OGY method. Taking each initial condition in turn, the value of δp_n is calculated according to the OGY criterion. If $|\delta p_n| > \delta p_{\max}$, then parameter perturbations cannot be activated in order to effect control for that particular initial condition. Therefore, the initial condition does not lie within the immediate basin of attraction for the control method. If parameter perturbations can be activated for a particular initial condition, that initial condition may not converge to the fixed point because of the fact that the control formula is based upon a linearisation about the fixed point. To check that it does converge, we apply parameter perturbations to the map until the initial condition is forward iterated to an ϵ -neighbourhood of the fixed point. Thus only initial conditions that converge to the fixed point are deemed to lie within the actual immediate basin of attraction for the OGY method. The long thin shaded region of Fig. 3.6 emanating from the fixed point shows the actual immediate basin of attraction for the Hénon map, calculated as described above.

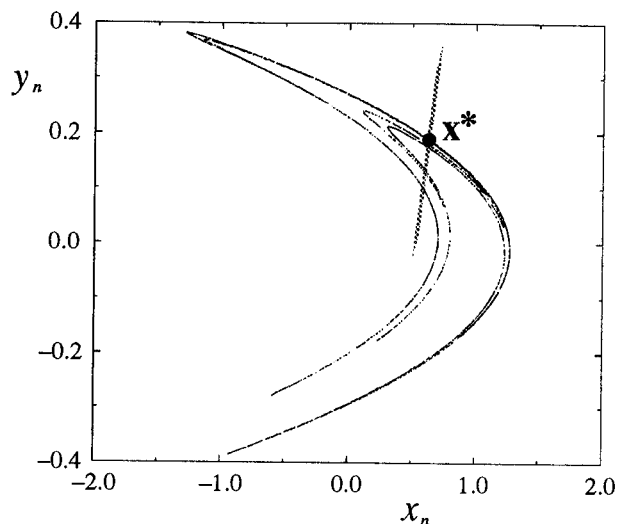


Figure 3.6: The actual basin of attraction for the OGY method with $\delta p_{\max} = 0.05$ applied to the Hénon map.

The numerically calculated measure of the attractor lying within the shaded region of Fig. 3.6 is $\mu = 9.50 \times 10^{-3}$. This gives the probability that a randomly chosen iterate on the attractor of the map lies within the actual immediate basin of attraction for the OGY method. We can thus estimate the average transient length, $\bar{\tau}$, for randomly chosen initial conditions lying on the attractor. This estimate is simply $\bar{\tau} = \frac{1}{\mu} \simeq 105$. Thus, on average, randomly chosen initial conditions lying on the attractor will need to be iterated 105 times before they can be controlled.

The factor by which the basin can be widened was shown to be $\frac{|\lambda_u|}{|\lambda_u|-1}$ and for the fixed point of the Hénon map this turns out to be approximately 1.52. We would expect that when the basin of attraction is extended, the average transient time is reduced. Calculating the measure, μ_e , of the attractor lying within the extended basin of attraction, we find that $\mu_e = 1.412 \times 10^{-2}$. Thus average transient times should be reduced to $\bar{\tau} \simeq 71$. Taking 500 randomly chosen initial conditions lying on the attractor of the Hénon map, the observed average transient times were 103 for the OGY method without the extended basin and 74 with an extended basin

whose extent was defined by the line $\beta = \beta^{(20)}$.

One of the problems involved in using the OGY method we mentioned in Chapter 1 was the sometimes long transient seen before control. The extended basins approach can often be used to significantly cut the transient time down, as demonstrated here. Recall that the other problem was that of noise. Even small amplitude noise was seen to have a detrimental effect on the use of the OGY method in Section 1.4, where control of the noisy Hénon map could not be fully effected. Interestingly, with the same level of noise and the same value of $\delta p_{\max} = 0.05$, the map can be fully controlled using the extended basins approach. Control can be achieved for long periods of time, in excess of 10,000 iterations. The explanation for this lies in the measure of the attractor within the immediate and the extended basins of attraction. As we saw in Section 1.4, intermittent bursting away from the control region frequently occurred. Noise throwing iterates from the region suitable for control (the immediate basin of attraction for the method, B_1) was the initiation of a burst. If we extend the basin of attraction and apply the same control method, noise will still occasionally throw iterates from B_1 . However, they may land in B_2 , for example, whereby control is not lost. Perturbations can be activated at their maximum value within that region (and the other parts of the extended basin) to push iterates back towards B_1 , and hence control can still be maintained. There is a larger measure of the attractor lying within the extended basin as compared to the immediate basin and so noise has to be at such a level to throw iterates from an area with larger measure and extent in order to disrupt control. Thus the problem of noise can also be addressed by using an extended basin of attraction.

Chapter 4

Targeting

It is well known [71, 72, 70, 69, 85] that trajectories can be directed towards specific targets by the application of small, discerningly chosen perturbations of an available system parameter. The trajectory directing technique provides us with a valuable tool for changing the state of an ergodic process from an initial state to some desired target state in a much shorter time than if no perturbation were applied to the system. Consequently, for example, this gives us the potential to proficiently trim the average length of the chaotic transient typically experienced before a system can be brought under control via the application of control methods such as those discussed in Chapter 1. The targeting technique could also provide us with an efficient means of switching from one desired behaviour to another, e.g. switching from a controlled periodic point to a period-2 point. With precisely these applications in mind, we investigate targeting algorithms that will provide us with a vehicle to both control a system more rapidly (that is, trim the average transient length before control is achieved) and efficiently switch between two controlled states.

Provided that the dynamical equations of the system are known, or a good (global) approximation to them can be procured, the method of Shinbrot *et al.*

[70] can be used to achieve both of the goals discussed above. We shall review this algorithm here and then derive a new algorithm which, in contrast to that of Shinbrot *et al.*, requires neither any knowledge of the underlying dynamical equations describing the behaviour of the system, nor any global approximation to them. All that is required is the availability of a system parameter p , adjustable by a small amount such that $|\delta p| \leq \delta p_{\max}$. We will show, by means of a numerical example, that the new method is not necessarily robust in the presence of even small amplitude noise, but that it may be adapted to cope with noise.

In what proceeds, we assume that the system under consideration is describable by the map

$$\mathbf{x}_{n+1} = \mathbf{F}(\mathbf{x}_n, p_n) \quad (4.0.1)$$

where $\mathbf{F} : \mathbb{R}^2 \times \mathbb{R} \mapsto \mathbb{R}^2$ and p_n is our system parameter, available for tuning at each iteration of (4.0.1). The methods discussed here are easily generalised to higher dimensional systems.

4.1 Targeting in Systems Where \mathbf{F} is Known

We shall now review the method proposed by Shinbrot *et al.* [70] for targeting in systems where the precise form of the mapping \mathbf{F} is known. Suppose we are presented with a chaotic system described by (4.0.1) in which we wish to proceed from an initial state \mathbf{x}_s to the vicinity of some target state \mathbf{x}_t in a ^{small}~~short~~ number of steps. We allow the parameter p_n to be varied at each step about its nominal value p^* by an amount δp_n such that $|\delta p_n| \leq \delta p_{\max}$. After one iteration of the map (4.0.1), beginning with the initial condition $\mathbf{x}_0 = \mathbf{x}_s$, the change in the state of the system due to a perturbation of δp_0 applied at the first step may be described via

the Taylor expansion

$$\mathbf{F}(\mathbf{x}_s, p^* + \delta p_0) = \mathbf{F}(\mathbf{x}_s, p^*) + \mathbf{F}_p(\mathbf{x}_s, p^*) \delta p_0 + O(\delta p_0^2),$$

where we have expanded about the unperturbed position (\mathbf{x}_s, p^*) . Thus the change in state $\delta \mathbf{x}$, relative to the point $\mathbf{F}(\mathbf{x}_s, p^*)$ due to a small perturbation δp_0 is

$$\delta \mathbf{x} := \mathbf{F}(\mathbf{x}_s, p^* + \delta p_0) - \mathbf{F}(\mathbf{x}_s, p^*) \simeq \mathbf{F}_p(\mathbf{x}_s, p^*) \delta p_0 \quad (4.1.2)$$

ignoring terms of $O(\delta p_0^2)$. We emphasise here that \mathbf{F} must be known, or that some global approximation to \mathbf{F} can be formed and is assumed to be necessarily invertible. Letting δp_0 vary through its permissible range of values $-\delta p_{\max} \leq \delta p_0 \leq \delta p_{\max}$, equation (4.1.2) defines a small line segment through $\mathbf{F}(\mathbf{x}_s, p^*)$. Denote this line segment by $\overline{\delta x}$ and its length by δx .

With each successive iteration of the map (4.0.1), the line segment will grow in length approximately geometrically at a rate governed by the positive Lyapunov exponent of the system, denoted by λ_1 . We let n_1 be the number of iterations of (4.0.1) required for the line segment to grow to a length of order 1, which typically happens when $\delta x \exp(n_1 \lambda_1) \sim 1$ for small δx . Without loss of generality, we may take the size of the relevant ergodic region (i.e. the region in which the natural measure of the attractor is defined) to be of the order of 1 so that n_1 is the number of iterations of (4.0.1) such that $\overline{\delta x}$ spans the ergodic region.

Define λ_2 to be the negative Lyapunov exponent of the system \mathbf{F} and let $\bar{\epsilon}_t$ be the region about \mathbf{x}_t that we are targeting and denote the negative Lyapunov exponent of the system by λ_2 . Mapping this region backwards in time, its n_2 th preimage will span the ergodic region when $n_2 \sim \frac{1}{|\lambda_2|} \ln\left(\frac{1}{\epsilon_t}\right)$ where ϵ_t (assumed small) is a measure of the linear size of $\bar{\epsilon}_t$. For example, $\bar{\epsilon}_t$ may be a box of side length ϵ_t . We now look for an intersection of the forward iterated line segment and the backward iterated region. Taking a point on the middle of this intersection

and iterating it backward in time n_1 steps, we find a point on the line segment $\overline{\delta x}$ from which we may determine a value of δp_0 which, if applied to the system, beginning with the initial point \mathbf{x}_s , should take us to the vicinity of \mathbf{x}_t in $n_1 + n_2$ further steps of the map (4.0.1). In the absence of noise, no further perturbations of the map are necessary.

In practice, we cannot iterate a line or a region, so we iterate discrete approximations to them, joining the points with a straight line. Once an intersection is detected, its accuracy may be refined by repeatedly halving the intersecting forward and backward line segments and determining which of these halves actually contains the intersection. In the presence of noise, a perturbation is applied at each step to keep the trajectory ‘on target’. See [70] for more details.

4.2 Targeting in Systems With \mathbf{F} Unknown

The targeting algorithm outlined above has been shown to work well if the dynamical equations are known, or if the system is described reasonably accurately by a one-dimensional map [72, 69]. A variation on their approach is considered by Xu and Bishop [85], where parameter perturbations are chosen in an optimal way to steer trajectories swiftly to their targets. Again though, the precise form of the dynamical equations must be known. If the dynamics are complicated, or if say, \mathbf{F} is non-invertible, then a different approach is called for. We describe now a targeting algorithm for directing trajectories where the underlying dynamical equations are unknown and are not easily estimated.

Suppose, as before, we wish to proceed from some initial state \mathbf{x}_s to the vicinity of the target \mathbf{x}_t , but this time \mathbf{F} is unknown. We cannot iterate a region about the target backward in time without knowledge of \mathbf{F} . Instead we let our system run,

unperturbed, collecting iterates which we shall label \mathbf{x}^i in an ϵ_t -neighbourhood of \mathbf{x}_t . Such collected points satisfy

$$\|\mathbf{x}^i - \mathbf{x}_t\| < \epsilon_t \quad (4.2.3)$$

for small ϵ . Let there be N_b such points \mathbf{x}^i . We then form the $2 \times (n_b + 1)$ matrices

$$\mathbf{y}^i = \begin{pmatrix} \mathbf{x}_n^i & \mathbf{x}_{n-1}^i & \cdots & \mathbf{x}_{n-n_b}^i \end{pmatrix}$$

for $i = 1, 2, \dots, N_b$, where \mathbf{x}_{k-1}^i is the preimage of \mathbf{x}_k^i , $k = n - n_b + 1, \dots, n$ for some $n_b > 1$. We shall term such matrices *history matrices*. Thus, as well as collecting points satisfying (4.2.3) we have also collected their preimages to form their history going back n_b steps. Each \mathbf{y}^i is a $2 \times (n_b + 1)$ matrix whose first column defines a point lying in an ϵ -neighbourhood of \mathbf{x}_t and whose remaining columns define a short ‘history’ of that point. We then start our system running, many times, beginning with the initial condition \mathbf{x}_s , each time with a different perturbation at the first step, and allow the system to run for at least another n_f steps. We shall indicate how to determine n_b and n_f presently.

Suppose that the applied perturbations are spaced evenly in the interval $[-\delta p_{\max}, \delta p_{\max}]$ (though this is not a necessary requirement) and let there be N_f such perturbations. Then we can form the approximation to the line segment $\overline{\delta x}$ as given by equation (4.1.2), together with its n_f forward images, by simply joining neighbouring points with straight line segments. We then look for ‘backward iterated’ points lying on, or at least very close to, the forward iterated line segment $\overline{\delta x}$. Labelling the perturbations as $-\delta p_{\max} \leq \delta p_0^1 < \delta p_0^2 < \cdots < \delta p_0^{N_f} \leq \delta p_{\max}$, we may say that an intersection between the j th forward iterated line segment (corresponding to the forward iterated points with first step perturbations of δp_0^j and δp_0^{j+1}) and a ‘backward iterated’ trajectory has occurred if $\mathbf{x}_{n-n_b}^i$ approximately lies on this line for some i .

Let $A = \mathbf{x}_{n_f}(\delta p_0^j)$ be the n_f th point on the j th forward trajectory corresponding to a first step perturbation of δp_0^j . Let $B = \mathbf{x}_{n_f}(\delta p_0^{j+1})$ be similarly defined, and P be the point between A and B of the (approximately) intersecting history matrix, $P = \mathbf{x}_{n-n_b}^i$. An intersection is determined as follows. Form the vector

$$\mathbf{d}_j = \vec{AB} = (\mathbf{x}_{n_f}(\delta p_0^j) - \mathbf{x}_{n_f}(\delta p_0^{j+1}))$$

and the perpendicular to this vector, \mathbf{d}_j^\perp , passing through the point P . Standard coordinate geometry techniques can be used here. Let Q be the point where \mathbf{d}_j meets \mathbf{d}_j^\perp . Then an intersection is deemed to have occurred when

$$\|\vec{PQ}\| < \epsilon$$

for some suitably small $\epsilon > 0$. By linear interpolation,

$$\delta p_0 \simeq \delta p_0^j + \frac{\|\vec{AP}\|}{\|\vec{AB}\|} (\delta p_0^{j+1} - \delta p_0^j). \quad (4.2.4)$$

Thus, given \mathbf{x}_s and a first step perturbation of δp_0 defined by equation (4.2.4), we can form the trajectory

$$\mathbf{Y}_I = \begin{pmatrix} \mathbf{x}_1 & \mathbf{x}_2 & \dots & \mathbf{x}_{n_f+n_b} \end{pmatrix}$$

where $\mathbf{x}_1 = \mathbf{F}(\mathbf{x}_s, \delta p_0)$, $\mathbf{x}_k = \mathbf{F}(\mathbf{x}_{k-1}, p^*)$, $k = 2, 3, \dots, n_f + n_b$ which we shall call the *idealised trajectory* from \mathbf{x}_s to the vicinity of \mathbf{x}_t . So if we start at \mathbf{x}_s , make a small perturbation of δp_0 to the system at the first step, we will then follow the idealised trajectory to the vicinity of \mathbf{x}_t in $n_f + n_b$ further steps.

We remark that the targets we aim for using this algorithm must necessarily lie on the attractor and consequently if n_f is not to be too large, \mathbf{x}_s should also lie on or near the attractor. The algorithm is thus particularly well suited to switching between different states lying on the attractor.

4.3 The Effect of Noise

The algorithm described in the previous section is not robust, since even very small amplitude noise can cause an observed trajectory to wander far from the idealised trajectory during the targeting process (see the example at the end of the chapter). This is clearly due to the extreme sensitivity of chaotic systems to small perturbations. In this section we propose a method which helps combat the detrimental effect of small amplitude noise on our algorithm. The method consists of firstly finding an *averaged idealised trajectory* from \mathbf{x}_s to the vicinity of \mathbf{x}_t . That is, we determine a trajectory that takes us from \mathbf{x}_s to \mathbf{x}_t which is an average of several forward and several ‘backward iterated’ trajectories that approximately intersect at some point on the attractor. We then estimate the linearised maps at each point on the averaged idealised trajectory and use these estimates to apply a perturbation at each step such that the observed trajectory approximately follows the averaged idealised trajectory from \mathbf{x}_s to the vicinity of \mathbf{x}_t .

The first step is the same as before. We determine an intersection of a forward iterated line segment and a ‘backward iterated’ point and estimate δp_0 . Denote the point at which the intersection occurs by \mathbf{x}_{int} . We then take an ϵ -neighbourhood about \mathbf{x}_{int} and determine the m_f forward (almost) intersecting trajectories whose n_f th point lies within this neighbourhood. Numerically, one determines m_f points (and their histories) on the trajectories emanating from \mathbf{x}_s such that

$$\|\mathbf{x}_{n_f} - \mathbf{x}_{\text{int}}\| < \epsilon.$$

Denote these m_f trajectories by

$$\mathbf{X}_f^k = \begin{pmatrix} \mathbf{x}_{1f}^k & \mathbf{x}_{2f}^k & \dots & \mathbf{x}_{n_f}^k \end{pmatrix}$$

$k = 1, 2, \dots, m_f$, where $(\mathbf{x}_j^k)^T = (x_j^k, y_j^k)$ are the Cartesian coordinates of the j th point on the k th trajectory. We average these trajectories to form the approximate

forward part of the idealised trajectory so that

$$\bar{\mathbf{x}}_{jf} = \begin{pmatrix} \bar{x}_j \\ \bar{y}_j \end{pmatrix} = \frac{1}{m_f} \begin{pmatrix} \sum_{k=1}^{m_f} x_j^k \\ \sum_{k=1}^{m_f} y_j^k \end{pmatrix} \quad (4.3.5)$$

for $j = 1, 2, \dots, n_f$. In doing so we hope to average out the noise. Similarly averaging the first step perturbations gives

$$\overline{\delta p_0} = \frac{1}{m_f} \sum_{k=1}^{m_f} \delta p_0^k.$$

As before, we collect iterates in the neighbourhood of the target point \mathbf{x}_t together with their ‘histories’. We then average the m_b backward trajectories whose n_b th point lies in an ϵ -neighbourhood of \mathbf{x}_{int} so that

$$\bar{\mathbf{x}}_{lb} = \begin{pmatrix} \bar{x}_l \\ \bar{y}_l \end{pmatrix} = \frac{1}{m_b} \begin{pmatrix} \sum_{k=1}^{m_b} x_l^k \\ \sum_{k=1}^{m_b} y_l^k \end{pmatrix} \quad (4.3.6)$$

where $l = 1, 2, \dots, n_b$. We can then form the approximate idealised trajectory from \mathbf{x}_s to the vicinity of \mathbf{x}_t by concatenating the $\bar{\mathbf{x}}_{jf}$, $j = 1, 2, \dots, n_f$ of equation (4.3.5) with the $\bar{\mathbf{x}}_{lb}$, $l = n_b, n_b - 1, \dots, 1$ of (4.3.6) giving the averaged idealised trajectory, $\bar{\mathbf{Y}}_I$, as

$$\bar{\mathbf{Y}}_I = \begin{pmatrix} \bar{\mathbf{x}}_{1f} & \bar{\mathbf{x}}_{2f} & \dots & \bar{\mathbf{x}}_{m_{ff}} & \bar{\mathbf{x}}_{(m_b-1)b} & \dots & \bar{\mathbf{x}}_{1b} \end{pmatrix}.$$

Let $\bar{\mathbf{Y}}_{Ii}$ denote the i th point on this trajectory, $i = 1, 2, \dots, n_f + n_b$. Returning to (4.0.1) we have

$$\begin{aligned} \mathbf{x}_{n+1} &= \mathbf{F}(\bar{\mathbf{Y}}_{Ii} + (\mathbf{x}_n - \bar{\mathbf{Y}}_{Ii}), p^* + (p_n - p^*)) \\ &= \mathbf{F}(\bar{\mathbf{Y}}_{Ii}, p^*) + D_{\mathbf{x}}\mathbf{F}(\bar{\mathbf{Y}}_{Ii}, p^*)(\mathbf{x}_n - \bar{\mathbf{Y}}_{Ii}) + D_p\mathbf{F}(\bar{\mathbf{Y}}_{Ii}, p^*)(p_n - p^*) + \dots \\ &\simeq \bar{\mathbf{Y}}_{I(i+1)} + A_i\delta\mathbf{x}_n + \mathbf{w}_i\delta p_n \end{aligned}$$

where $\delta\mathbf{x}_n = \mathbf{x}_n - \bar{\mathbf{Y}}_{Ii}$, by a Taylor expansion about $(\bar{\mathbf{Y}}_{Ii}, p^*)$. This result assumes that $\bar{\mathbf{Y}}_{I(i+1)} \simeq \mathbf{F}(\bar{\mathbf{Y}}_{Ii}, p^*)$, which is not unreasonable. Thus the linearised maps about each point $\bar{\mathbf{Y}}_{Ii}$ on the approximate idealised trajectory take the form

$$\mathbf{x}_{n+1} = A_i\mathbf{x}_n + \mathbf{b}_i + \mathbf{w}_i\delta p_n$$

where $\mathbf{b}_i = \bar{\mathbf{Y}}_{I(i+1)} - A_i \bar{\mathbf{Y}}_{Ii}$. The A_i and \mathbf{b}_i can be experimentally obtained by setting $\delta p_n = 0$ and letting the system run, collecting data about each point of the approximate idealised trajectory and performing a regression as described in Section 0.3.3. Of course, one could use all the trajectories which were used to find the averaged idealised trajectory in the regression process.

The \mathbf{w}_i can be estimated by allowing the system to run, unperturbed, waiting until the state of the system falls within an ϵ -neighbourhood of the i th point on the approximate idealised trajectory, then perturbing the parameter by some small prescribed value δp_w and finding where the next point $\mathbf{Y}_{I(i+1)}(\delta p_w)$ lies on the attractor. Doing this many times for each point i of the trajectory and averaging to obtain $\bar{\mathbf{Y}}_{I(i+1)}(\delta p_w)$, \mathbf{w}_i is given by

$$\mathbf{w}_i \simeq \frac{\bar{\mathbf{Y}}_{I(i+1)}(\delta p_w) - \bar{\mathbf{Y}}_{I(i+1)}}{\delta p_w}.$$

Alternatively, one could use a central difference approximation here. Calculating the $n_f + n_b$ \mathbf{w}_i derivative vectors requires a considerable amount of computation.

Our targeting algorithm then consists of applying a perturbation of $\bar{\delta p}_0$ at the first step and applying perturbations δp_n at subsequent steps such that

$$\|\mathbf{x}_{n+1} - \bar{\mathbf{Y}}_{I(i+1)}\|_2$$

is a minimum. We thus choose δp_n to minimise

$$\|A_i \mathbf{x}_n + \mathbf{b}_i + \mathbf{w}_i \delta p_n - \bar{\mathbf{Y}}_{I(i+1)}\|_2$$

giving

$$\delta p_n = \frac{\mathbf{w}_i^T (A_i \mathbf{x}_n + \mathbf{b}_i - \bar{\mathbf{Y}}_{I(i+1)})}{\mathbf{w}_i^T \mathbf{w}_i} \quad (4.3.7)$$

Compare this with the shortest distance method of Section 1.2.1.

One possibility for the determination of n_f and n_b is to use the same criterion as used to determine n_1 and n_2 in the targeting method of Shinbrot *et al.* [72].

However, numerical simulations suggest that these estimates can be too large since it is often the case that we do not need to iterate the line segment and ‘back iterate’ the target region until they are of order one to find an intersection. The intersection often happens before the iterated regions reach order one. In the numerical example below, we have chosen n_f and n_b in an ad hoc fashion, trying many combinations for which we chose a combination giving the smallest value of $n_f + n_b$, and hence the shortest targeting time. However, n_f and n_b are always chosen such that $n_f \leq n_1$ and $n_b \leq n_2$.

Remarks

The targeting methods discussed here are for targeting in two-dimensional systems. Targeting is also possible in higher dimensional systems. See, for example, Kostelich *et al.* [37] and Barreto *et al.* [7]. The new targeting algorithms described here are easily generalised to the higher dimensional problem, but much more computation is involved in implementing the methods.

4.4 Numerical Example

Consider the Hénon map of equation (1.4.11) in which we wish to progress from the initial state $\mathbf{x}_s = (0.9758, -0.1427)$ (very close to a period-2 point) to the vicinity of $\mathbf{x}_t = (0.6313, 0.1894)$ (a fixed point). We shall say that an iterate \mathbf{x}_n is in the vicinity of \mathbf{x}_t when $\|\mathbf{x}_n - \mathbf{x}_t\| < 5 \times 10^{-3}$. Then without applying the targeting algorithm, 4440 iterations of the Hénon map are required to reach \mathbf{x}_t . Letting $\delta p_{\max} = 0.05$ and applying our algorithm, we find that with a first step perturbation of $\delta p_0 = 0.03247$ \mathbf{x}_t can be targeted in only eleven steps. We now

add some noise to the system such that the equations become

$$\begin{aligned}x_{n+1} &= 1 - (1.4 + \delta p_n)x_n^2 + y_n + \xi_n \\y_{n+1} &= 0.3x_n + \eta_n\end{aligned}$$

where the ξ_n and η_n are noise terms, the noise being uniformly distributed in the interval $[-4 \times 10^{-3}, 4 \times 10^{-3}]$. The resulting chaotic attractor is shown in Fig. 4.1. Applying the new algorithm to find the averaged idealised trajectory we find that it should be possible to reach \mathbf{x}_t in eleven steps with a first step perturbation of $\delta p_0 = -0.04716$. If we apply this perturbation at the first step, and no further perturbations, the trajectory ends up at the point denoted by $\tilde{\mathbf{x}}_t$ shown in Fig. 4.1 after eleven steps. Estimating the linearised maps at each point on the idealised trajectory and applying a perturbation as prescribed by (4.3.7) at each step after the first, we end up at the point $\mathbf{x} = (0.6313, 0.1843)$ after eleven iterations of the map, which is indeed in the vicinity of \mathbf{x}_t . In producing these results, the Hénon map has only been used to create data. It has not been used explicitly in the targeting process.

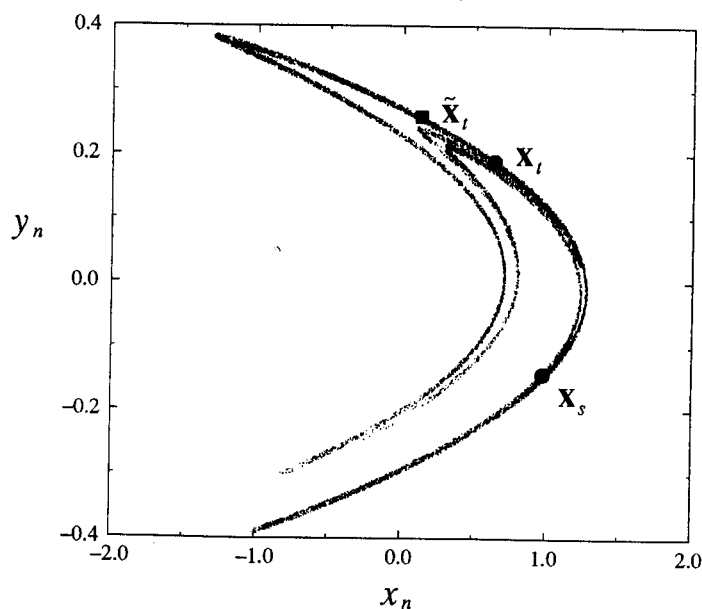


Figure 4.1: Targeting in the Hénon map with added noise.

To demonstrate the speed at which switching between different controlled states can be effected, we attempt to repeatedly switch between a fixed point and period-2 points. Using $\delta p_{\max} = 0.02$ we apply the control alternately in the vicinities of the fixed point and period-2 points, applying this control every 3000 iterations of the map. We then repeat the process, but this time using the targeting algorithm between successive switches. The length of the chaotic transients exhibited before periodic motion is achieved can be seen to be significantly reduced (Fig. 4.2). Similar results can be achieved in the presence of small amplitude noise. Note that the ‘windows’ of chaotic transients seen in Fig. 4.2 are either approximately 200 or 2000 iterations in length without applying targeting, whilst with targeting they are either 10 or 12 iterations long.

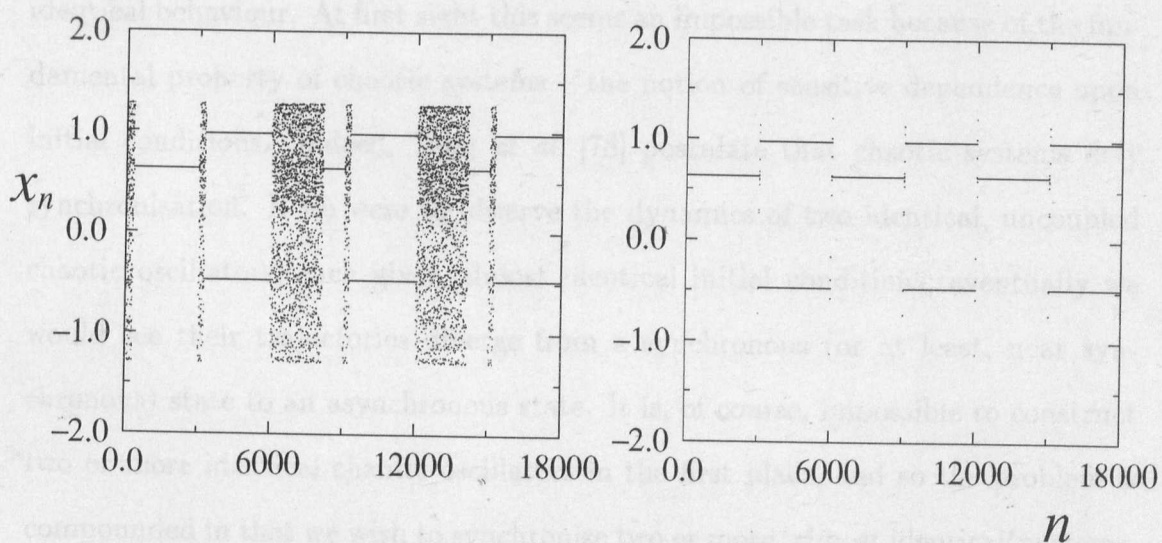


Figure 4.2: Switching between controlled states without (left) and with (right) the targeting process.

Chapter 5

Synchronisation

The synchronisation of chaotic systems, along with the control of chaos, has been a popular focus for recent research. The problem consists of the synchronisation of two or more identical coupled chaotic oscillators such that they both exhibit identical behaviour. At first sight this seems an impossible task because of the fundamental property of chaotic systems – the notion of sensitive dependence upon initial conditions. Indeed, Tang *et al.* [78] postulate that chaotic systems defy synchronisation. If we were to observe the dynamics of two identical, uncoupled chaotic oscillators, each given almost identical initial conditions, eventually we would see their trajectories diverge from a synchronous (or at least, near synchronous) state to an asynchronous state. It is, of course, impossible to construct two or more identical chaotic oscillators in the first place, and so the problem is compounded in that we wish to synchronise two or more ‘almost identical’ systems.

Much of the interest in this area was initiated by Pecora and Carroll [60], who demonstrated that, under certain circumstances, it is possible to synchronise the behaviour of two systems which do not have to be identical, only ‘similar’. This is achieved by ‘linking’ the chaotic systems with a common signal or signals. Provided that these signals are appropriately chosen, synchronisation of the systems will

occur spontaneously as the time development of the coupled system progresses. Yamada and Fujisaka [88] use a simple coupling technique in order to achieve synchronisation of two independent oscillators. The strength of the coupling signal or signals must be above a certain threshold for synchronisation to naturally occur.

The synchronisation of chaotic oscillators has applications in the field of secure communication. Hayes *et al.* [33] first looked at transmitting data securely by using a pair of coupled oscillators. Kocarev and Stojanovski [36] have also investigated the application of chaotic synchronisation to secure communications. Roy and Thornburg [66] have looked at the experimental synchronisation of chaotic lasers. Further recent work in this area can be found in the papers of Yu *et al.* [89, 90] and Coumo *et al.* [12]. For an excellent summary of some of the earlier work on synchronisation, see Ogorzalek [49].

The aim of this chapter is to demonstrate that synchronisation can be achieved in low-dimensional systems, when it would not naturally occur, via the application of small parameter perturbations. In certain circumstances, for example when the coupling is not at or above the required threshold, systems may not automatically synchronise. The application of parameter perturbations can sometimes be used to induce synchronisation under these circumstances. This is easily accomplished if the systems under consideration can be adequately modelled, but proves a little more difficult if they cannot. Close investigation of the structure of coupled systems reveals particular regions where control via parametric perturbations can result in synchronous behaviour.

We shall begin with a brief review of the the method proposed by Pecora and Carroll [60]. Consider an N -dimensional autonomous dynamical system

$$\dot{\mathbf{X}} = \Phi(\mathbf{X}).$$

Divide the system arbitrarily into two subsystems such that $\mathbf{X} = (\mathbf{Y}, \mathbf{Z})$, giving

$$\dot{\mathbf{Y}} = \mathbf{g}(\mathbf{Y}, \mathbf{Z}), \quad \dot{\mathbf{Z}} = \mathbf{h}(\mathbf{Y}, \mathbf{Z}). \quad (5.0.1)$$

Now duplicate the \mathbf{Z} subsystem, call it \mathbf{Z}' , and substitute the set of variables \mathbf{Y} for the corresponding \mathbf{Y}' in the function \mathbf{h} . Then augmenting the new system with (5.0.1) we have

$$\dot{\mathbf{Y}} = \mathbf{g}(\mathbf{Y}, \mathbf{Z}), \quad \dot{\mathbf{Z}} = \mathbf{h}(\mathbf{Y}, \mathbf{Z}), \quad \dot{\mathbf{Z}}' = \mathbf{h}(\mathbf{Y}, \mathbf{Z}').$$

Define a transformation of variables given by

$$\mathbf{u} = \mathbf{Y}, \quad \mathbf{v} = \frac{\mathbf{Z} + \mathbf{Z}'}{2}, \quad \mathbf{y} = \frac{\mathbf{Z} - \mathbf{Z}'}{2}.$$

Then the system becomes

$$\begin{aligned} \dot{\mathbf{u}} &= \mathbf{g}(\mathbf{u}, \mathbf{v} + \mathbf{y}) \\ \dot{\mathbf{v}} &= \frac{1}{2}\{\mathbf{h}(\mathbf{u}, \mathbf{v} + \mathbf{y}) + \mathbf{h}(\mathbf{u}, \mathbf{v} - \mathbf{y})\} \\ \dot{\mathbf{y}} &= \frac{1}{2}\{\mathbf{h}(\mathbf{u}, \mathbf{v} + \mathbf{y}) - \mathbf{h}(\mathbf{u}, \mathbf{v} - \mathbf{y})\} \end{aligned}$$

in the new coordinates. Linearising about $\mathbf{y} = 0$ we have

$$\begin{pmatrix} \dot{\mathbf{u}} \\ \dot{\mathbf{v}} \\ \dot{\mathbf{y}} \end{pmatrix} = \begin{pmatrix} \mathbf{g}_{\mathbf{Y}}(\mathbf{u}, \mathbf{v}) & \mathbf{g}_{\mathbf{Z}}(\mathbf{u}, \mathbf{v}) & \mathbf{g}_{\mathbf{Z}'}(\mathbf{u}, \mathbf{v}) \\ \mathbf{h}_{\mathbf{Y}}(\mathbf{u}, \mathbf{v}) & \mathbf{h}_{\mathbf{Z}}(\mathbf{u}, \mathbf{v}) & 0 \\ 0 & 0 & \mathbf{h}_{\mathbf{Z}'}(\mathbf{u}, \mathbf{v}) \end{pmatrix} \begin{pmatrix} \mathbf{u} \\ \mathbf{v} \\ \mathbf{y} \end{pmatrix}.$$

Then a necessary condition for the systems \mathbf{Z} and \mathbf{Z}' to synchronise is that the sub-Lyapunov exponents (i.e. the Lyapunov exponents of the \mathbf{y} subsystem) are all negative. This says nothing about the set of initial conditions that will lead to synchronisation. Note that synchronisation occurs when $\mathbf{y} = 0$. One can think of the \mathbf{Y} variables as being the driving variables and the \mathbf{Z}' variables as being the response. See Fig. 5.1 for a representation of the coupling.

Another interesting problem is the synchronisation of a system of two coupled units describable by an equation of the form

$$\begin{aligned} \dot{\mathbf{X}} &= \mathbf{g}(\mathbf{X}) + c(\mathbf{Y} - \mathbf{X}) \\ \dot{\mathbf{Y}} &= \mathbf{g}(\mathbf{Y}) + c(\mathbf{X} - \mathbf{Y}) \end{aligned} \quad (5.0.2)$$

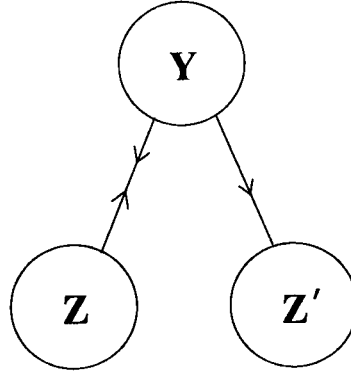


Figure 5.1: Schematic representation of the coupling of the \mathbf{Y} , \mathbf{Z} and \mathbf{Z}' subsystems of the Pecora and Carroll method.

where $\mathbf{X} \in \mathbb{R}^N$, $c \in \mathbb{R}$ and such that the system $\dot{\mathbf{X}} = \mathbf{g}(\mathbf{X})$ possesses a chaotic attractor. Yamada and Fujisaka [88] show that the synchronous state $\mathbf{X}(t) = \mathbf{Y}(t)$ is stable if $c > \frac{\lambda}{2}$ where λ is the leading Lyapunov exponent of the system. Note that the coupled system in (5.0.2) possesses a \mathbf{Z}_2 symmetry defined by

$$S \begin{pmatrix} \mathbf{X} \\ \mathbf{Y} \end{pmatrix} = \begin{pmatrix} \mathbf{Y} \\ \mathbf{X} \end{pmatrix}.$$

The coupling is represented in Fig. 5.2. We will look at a similar type of linear coupling again later.

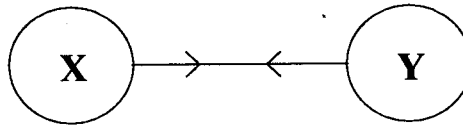


Figure 5.2: Schematic representation of the coupling between the \mathbf{x} and \mathbf{y} systems considered by Yamada and Fujisaka.

Ashwin *et al.* [2] note that the problem of the synchronisation of identical systems is just one example of a very general situation in which the same issues arise. The essential ingredients are a dynamical system whose dynamics evolve on some manifold \mathcal{M} possessing a dynamically invariant subspace \mathcal{N} . If the restriction of the system to \mathcal{N} has an attractor \mathcal{A} then the behaviour of the system near \mathcal{A} is a combination of the dynamics on \mathcal{A} and the dynamics transverse to \mathcal{N} . The attractor \mathcal{A} is stable with respect to perturbations within \mathcal{N} , but the effect of

perturbations transverse to \mathcal{N} has a global nature, more especially when \mathcal{A} is chaotic.

Symmetry provides a natural setting for the existence of invariant subspaces and invariant submanifolds. Let $\mathbf{f} : \mathcal{M} \mapsto \mathcal{M}$ be a smooth map leaving a lower dimensional submanifold \mathcal{N} invariant. Then the restriction $\mathbf{g} = \mathbf{f}|_{\mathcal{N}} : \mathcal{N} \mapsto \mathcal{N}$ defines a dynamical system in its own right. To define this more precisely, suppose that \mathbf{f} commutes with the smooth action of a compact Lie group of symmetries Γ on \mathcal{M} . Let $\Sigma \leq \Gamma$ be a subgroup of the group of symmetries. Then the fixed point submanifold

$$\mathcal{N} = \text{Fix}(\Sigma) = \{\mathbf{x} \in \mathcal{M} : \sigma(\mathbf{x}) = \mathbf{x} \text{ for all } \sigma \in \Sigma\}$$

is invariant under the action of \mathbf{f} . See [3] for more details. Systems such as (5.0.2) possess such fixed point submanifolds precisely at the synchronous state $\mathbf{X} = \mathbf{Y}$.

5.1 Coupled One-dimensional Systems

The problem we shall begin with here is the synchronisation of one-dimensional parameter dependent maps of the form $X_{n+1} = f(X_n, p)$. In particular, we will concentrate on problems that currently defy synchronisation. To begin with, the problem on which we shall focus will be the synchronisation of systems of maps of the form

$$\begin{aligned} X_{n+1} &= f(X_n, p^* + \delta q_n) + c(Y_n - X_n) \\ Y_{n+1} &= f(Y_n, p^* + \delta p_n) + c(X_n - Y_n). \end{aligned} \quad (5.1.3)$$

where $f : \mathbb{R} \times \mathbb{R} \mapsto \mathbb{R}$ and $c \in \mathbb{R}$. When $\delta p_n = \delta q_n$, equation (5.1.3) possesses a \mathbf{Z}_2 symmetry defined by the symmetry operator

$$S \begin{pmatrix} X_n \\ Y_n \end{pmatrix} = \begin{pmatrix} Y_n \\ X_n \end{pmatrix}.$$

The approach to the problem follows the same direction of that of controlling chaos. We shall attempt to determine parameter perturbations, which when carefully

applied to (5.1.3), results in synchronous behaviour. We shall also consider how to synchronise higher dimensional systems later.

5.1.1 Simultaneously Perturbing Both Equations

Let us consider the effect of perturbing both systems in (5.1.3) in an identical manner by setting $\delta q_n \equiv \delta p_n$. Define a transformation of coordinates given by

$$x_n = \frac{X_n + Y_n}{2}, \quad y_n = \frac{X_n - Y_n}{2}. \quad (5.1.4)$$

Then the system (5.1.3) becomes

$$\begin{aligned} x_{n+1} &= \frac{1}{2} \{ \tilde{f}(x_n + y_n, p^* + \delta p_n) + f(x_n - y_n, p^* + \delta p_n) \} \\ y_{n+1} &= \frac{1}{2} \{ f(x_n + y_n, p^* + \delta p_n) - \tilde{f}(x_n - y_n, p^* + \delta p_n) \} - 2cy_n. \end{aligned} \quad (5.1.5)$$

This new system possesses a \mathbf{Z}_2 symmetry defined by

$$S \begin{pmatrix} x \\ y \end{pmatrix} = \begin{pmatrix} x \\ -y \end{pmatrix}.$$

It also possesses a one-dimensional invariant subspace given by $y_n = 0$. The first equation in (5.1.5) describes the dynamics within the subspace and the second the transverse dynamics. Many maps possess an invariant subspace and we shall now take a closer look at the complex structures such maps can possess. We will diverge slightly from the synchronisation problem in what follows, but the proceeding discussion greatly aids the understanding of synchronisation via control methods.

The results of Ashwin [1] will be used as the archetypal example exhibiting the qualitative behaviours necessary to observe synchronisation via parametric perturbation. We shall begin by exploring the rich structure of systems possessing an invariant subspace and identify the situations in which a control algorithm can be applied in order to induce synchronisation of coupled maps. We shall be particularly interested in the case where an attractor \mathcal{A} is a *Milnor attractor*, that is if $\mathcal{B}(\mathcal{A})$ has non-zero Lebesgue measure and there is no compact proper subset

\mathcal{A}' of \mathcal{A} whose basin coincides with $\mathcal{B}(\mathcal{A})$ up to a set of zero measure [40]. Let $B_\delta(\mathcal{A})$ denote a δ -neighbourhood of \mathcal{A} in \mathcal{M} . Then a Milnor attractor \mathcal{A} has a *riddled basin* if for all $x \in \mathcal{B}(\mathcal{A})$ and $\delta > 0$ we have

$$\ell(B_\delta(x) \cap \mathcal{B}(\mathcal{A})^c) > 0$$

where $\mathcal{B}(\mathcal{A})^c$ denotes the complement of $\mathcal{B}(\mathcal{A})$ and $\ell(\cdot)$ the ordinary Lebesgue measure on \mathcal{M} . A Milnor attractor has a *locally riddled basin* if there exists a neighbourhood V of \mathcal{A} such that for all $x \in A$ and $\delta > 0$,

$$\ell(B_\delta(x) \cap U(V)^c) > 0$$

where $U(V)$ is the set of points in V whose iterates always remain in V , i.e. $U(V) = \cap_{n \geq 0} \mathbf{f}^{-n}(V)$. Note that the existence of a locally riddled basin permits the set which is locally repelled from \mathcal{A} to later ‘fold back’ onto \mathcal{A} . Nusse and Yorke [45] define a chaotic invariant set to be a *chaotic saddle* if there exists a neighbourhood U of \mathcal{A} such that $\mathcal{B}(\mathcal{A}) \cap U \neq \mathcal{A}$ but $\ell(\mathcal{B}(\mathcal{A})) = 0$. Riddled basins are closely related to the notion of ‘on-off intermittency’ whereby a system exhibits large deviations away from an invariant subspace (see [62]). The so-called blowout bifurcation is the connecting factor (Ott and Sommerer [54]) whereby an attractor with an invariant subspace loses its transverse stability and becomes a chaotic saddle.

Ashwin [1] introduces the concept of a ‘stuck on’ attractor. He considers the mapping

$$\begin{aligned} x_{n+1} &= g(x_n) + \epsilon x_n y_n^2 \\ y_{n+1} &= \tau y_n e^{-(x_n^2 + y_n^2)} + \frac{1}{2} y_n (1 - e^{-y_n^2}). \end{aligned} \quad (5.1.6)$$

The map g is the cubic logistic map, given by

$$g(x) = \frac{3\sqrt{3}}{2} x(x^2 - 1),$$

which has a unique attractor $\mathcal{A} = [-1, 1]$. The system (5.1.6) has the following relevant properties:

- (i) There is a chaotic invariant set \mathcal{A} in the invariant subspace.
- (ii) For $1 < \tau < 1.430$, \mathcal{A} has an open basin of attraction. Moreover, this basin is locally riddled.
- (iii) For $1.430 < \tau < 1.850$, \mathcal{A} is a chaotic saddle.

We shall consider the case where $\epsilon = 0$ and $\tau = 1.5$ for which \mathcal{A} is a chaotic saddle. The phase portrait (Fig. 5.3) shows an attractor stuck on to its invariant subspace $y = 0$. This is precisely the setting we require in order to apply the OGY control algorithm. By definition, there is a set of points of non-zero Lebesgue measure in the invariant subspace that are attracting in the transverse direction (if not, the attractor would not, and could not be stuck on to its invariant subspace). Moreover, these points must be saddles for they are unstable within the invariant subspace.

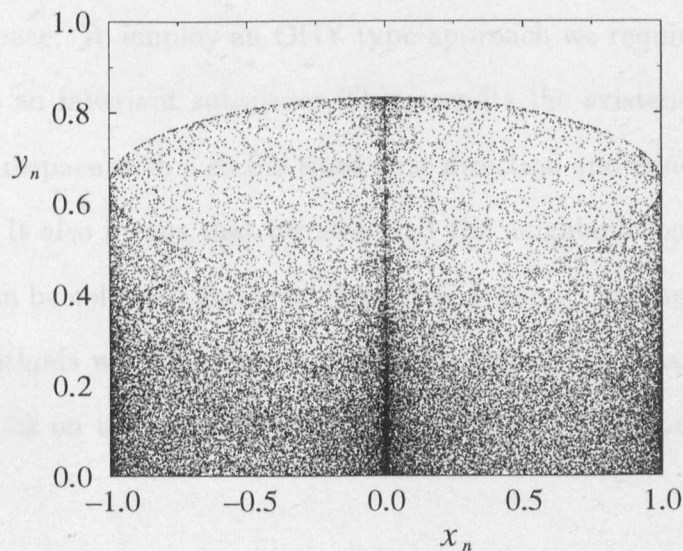


Figure 5.3: The stuck on attractor of Ashwin.

One can easily find periodic points of (5.1.6) in the invariant subspace which are saddles in the whole space and can thus be stabilised by a control method. To

find a period- n point one solves the fixed point equation

$$x^* = g^n(x^*)$$

for x^* . Then a check of the Jacobian evaluated at $(x^*, 0)$ suffices to confirm the nature of the fixed point. For example, the twice iterated map $g^2(x)$ has fixed points at $(0.905065, 0)$ and $(-0.425274, 0)$ and the Jacobian of the twice iterated map of (5.1.6) evaluated at these points is

$$\begin{pmatrix} -4.500000 & 0 \\ 0 & 0.827729 \end{pmatrix}.$$

The fixed points of $g^2(x)$ constitute a period-2 orbit of $g(x)$ and one can easily apply the OGY method to stabilise this orbit which lies in the invariant subspace.

The theory and approach discussed above relates to the problem of synchronising chaotic oscillators in the following sense. In order to observe synchronous behaviour in a system such as (5.1.3), the dynamics must be confined to a synchronous subspace. To employ an OGY type approach we require an attractor to be stuck on to an invariant subspace. This permits the existence of saddle fixed points in the subspace with a stable transverse direction and hence opportunity to apply control. It also means that iterates visit the neighbourhood of these points so that data can be collected and local linearised dynamics can be estimated. Thus the control methods we shall discuss in this chapter are applicable only when an attractor is stuck on to an invariant subspace, the subspace of synchronous solutions.

Returning to the original problem, suppose that (5.1.5) possesses a saddle fixed point at $(x, y) = (x^*, 0)$ lying in the invariant subspace for $\delta p_n = 0$. Consider the first order Taylor expansion of (5.1.5) about that fixed point,

$$\begin{pmatrix} \delta x_{n+1} \\ \delta y_{n+1} \end{pmatrix} = \begin{pmatrix} M_w & 0 \\ 0 & M_t \end{pmatrix} \begin{pmatrix} \delta x_n \\ \delta y_n \end{pmatrix} + \begin{pmatrix} f_p^* \\ 0 \end{pmatrix} \delta p_n \quad (5.1.7)$$

where $M_w = f_X(x^*, p^*)$, $M_t = f_X(x^*, p^*) - 2c$ and $f_p^* = f_p(x^*, p^*)$. Since the fixed point is a saddle, $|M_t| < 1 < |M_w|$. Equation (5.1.7) clearly has the form

$$\delta \mathbf{x}_{n+1} = M \delta \mathbf{x}_n + \mathbf{w} \delta p_n$$

where $M = \begin{pmatrix} M_w & 0 \\ 0 & M_t \end{pmatrix}$ and $\mathbf{w} = \begin{pmatrix} f_p^* \\ 0 \end{pmatrix}$ and so an OGY type approach could be used to stabilise the fixed point. Note that in (5.1.7) the linear dynamics within the synchronous subspace decouple from the transverse linear dynamics. Thus we can decompose the tangent space at $y = 0$ into the direct sum of the subspaces X_w and X_t , where X_w represents the linearised synchronous subspace and X_t the transverse linearised subspace. Since \mathbf{w} lies parallel to the synchronous subspace, parameter perturbations will only have an effect on the x variable. The existence of the linearised stable manifold of the fixed point in X_t provides the necessary mechanism stabilising the fixed point and thus producing synchronous behaviour. Using a perturbation of

$$\delta p_n = -\frac{M_w \delta x_n}{f_p^*}$$

provided that $|\delta p_n| \leq \delta p_{\max}$, we can place iterates on the stable manifold of the fixed point whereby they will converge to the fixed point within X_w .

The OGY criterion is not the only criterion we could use to produce dynamics within an invariant subspace. We could simply keep the x -coordinate fixed in the vicinity of a fixed point and allow the dynamics in the y direction to naturally contract (see Fig. 5.4). Note that we cannot use the ZSR method since \mathbf{w} is an eigenvector of M . An SD approach would be identical to using the OGY method since the stable and unstable eigenvectors are orthogonal (due to the diagonal form of M). Whilst control is being effected there is a transformation in the behaviour of the system from a chaotic regime to an orderly one. As soon as control is turned off, chaotic behaviour is restored. However, since we have effectively stabilised a fixed point, the dynamics will remain in the vicinity of that point for quite some

time before eventually being pushed away along the unstable direction (in the invariant subspace). Thus chaotic dynamics will not be immediately realised after the termination of control. If this were undesirable, we could apply a parameter perturbation to nudge the state of the system away from the fixed point and hence rapidly restore chaotic behaviour within the synchronous subspace. Alternatively, using the method depicted in Fig. 5.4, the fixed point is never actually stabilised and so iterates would naturally leave the vicinity of the fixed point upon the cessation of parameter perturbations.

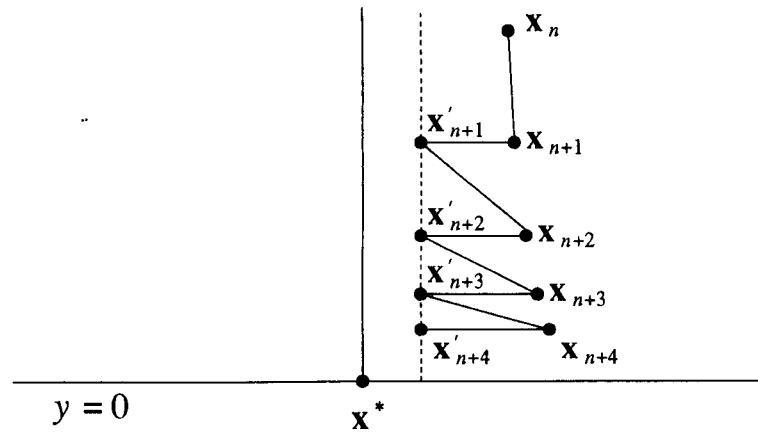


Figure 5.4: Keeping the x -coordinate fixed in the vicinity of the fixed point where $\mathbf{x}_k = \mathbf{x}_k(p^*)$ and $\mathbf{x}'_k = \mathbf{x}_k(p^* + \delta p_{k-1})$.

The problem then is how to maintain the dynamics close to the invariant subspace. Since the control is unlikely to place the state of the system precisely in the invariant subspace, iteration of the unperturbed mapping will eventually result in behaviour far from that subspace. Hence control must be periodically reapplied in order to maintain the dynamics close to the invariant subspace. The control procedure then consists of the following steps:

- (i) Find the (low order) saddle periodic orbits of the system and approximate the local dynamics;
- (ii) Wait until the state of the system falls close to one of these periodic orbits and apply control;

- (iii) Turn off control once the state of the system lies within an ϵ -neighbourhood of the fixed point and hence the invariant subspace;
- (iv) Arbitrarily nudge the system away from the periodic orbit to restore chaos;
- (v) Repeat the procedure from step (ii) onwards.

One could envisage encountering problems with the above procedure. Provided that there were enough saddle periodic orbits around, it would not be long before an iterate initially close to one orbit is nudged away and quickly comes close to another orbit where control can be applied again in order to maintain the dynamics close to the invariant subspace. However, if the time spent wandering chaotically between control applications were long, the state of the system could quite conceivably be pushed far from the invariant subspace and hence the one-dimensional dynamics would be lost. Instead of simply arbitrarily nudging the system as in step (iv) above, one could carefully choose the value of the perturbation to be applied at this step. In doing so, one of the targeting algorithms discussed in Chapter 4 could then be applied. The specific value of the nudging perturbation could be chosen such that the state of the system is pushed rapidly from one periodic orbit to the vicinity of another orbit. That way, the system can be controlled again and hence large excursions away from the invariant subspace can be avoided.

5.1.2 Perturbing One Equation

Perturbing both equations as in (5.1.3) gives rise to a derivative vector which lies parallel to the synchronous subspace. The alternative is to perturb just one equation by setting $\delta q_n \equiv 0$ so that the system under consideration becomes

$$\begin{aligned} X_{n+1} &= f(X_n, p^*) + c(Y_n - X_n) \\ Y_{n+1} &= f(Y_n, p^* + \delta p_n) + c(X_n - Y_n). \end{aligned} \tag{5.1.8}$$

Using the transformation of coordinates defined by (5.1.4), the system (5.1.8) can be written as

$$\begin{aligned}x_{n+1} &= \frac{1}{2}\{f(x_n + y_n, 0) + f(x_n - y_n, \delta p_n)\} \\y_{n+1} &= \frac{1}{2}\{f(x_n + y_n, 0) - f(x_n - y_n, \delta p_n)\} - 2cy_n\end{aligned}$$

and by a Taylor expansion about the point $x = x^*$, $y = y^*$, $p = p^*$ we have

$$\begin{pmatrix} \delta x_{n+1} \\ \delta y_{n+1} \end{pmatrix} = \begin{pmatrix} M_w & 0 \\ 0 & M_t \end{pmatrix} \begin{pmatrix} \delta x_n \\ \delta y_n \end{pmatrix} + \begin{pmatrix} f_p^* \\ -f_p^* \end{pmatrix} \delta p_n + \dots$$

In this case, the derivative vector no longer lies parallel to the synchronous subspace, but rather, it passes through it. It is then possible to formulate many different control methods to induce synchronous behaviour in coupled systems. The standard OGY method can still be applied, but as was shown in Chapter 1, there are many other methods that result in faster convergence, for example the ZSR method. If the goal is to produce synchronous behaviour as quickly as possible, then one of the faster converging methods would be more appropriate. Alternatively, an iterate can be easily placed directly on the synchronous subspace, by virtue of the direction of the derivative vector, if that iterate lies sufficiently close. If not, a control method could be used in order to bring it sufficiently close and then place it within the synchronous subspace. Now the dynamics in the transverse direction are given by

$$\delta y_{n+1} = M_t \delta y_n - f_p^* \delta p_n.$$

We require that $\delta y_{n+1} = 0$ so that the value of the required perturbation is

$$\delta p_n = \frac{M_t \delta y_n}{f_p^*}$$

provided that $f_p^* \neq 0$. A chaos restoring perturbation is not then required since no fixed point has been stabilised.

Remarks

We have seen that there are ways to induce synchronisation in coupled maps where it would not naturally occur via the application of small parameter perturbations in the vicinity of a synchronous subspace. An attractor stuck on to an invariant manifold was the essential ingredient required to effect the control methods of Chapter 1. In practice it is difficult to find one-dimensional chaotic maps which can be synchronised. However, the methods discussed above can be used on maps such as (5.1.6) in order to collapse system dynamics onto one-dimensional submanifolds. The theory does however serve as a useful precursor to the more interesting problem of synchronising higher dimensional systems, of which there are many examples of systems which can be synchronised via parametric perturbations. We shall now generalise the synchronisation theory and methods discussed here to such problems.

5.2 Higher Dimensional Systems

In order to extend the synchronisation methods for use on the general N -dimensional problem, we shall consider how to synchronise two-dimensional systems. The extension to higher dimensions should then be apparent. Firstly, we shall consider the coupling of a pair of two-dimensional maps, whereby the theory of Section 5.1 is easily generalised to the slightly more complicated problem. We shall then investigate the coupling of continuous time systems, in particular, a pair of Duffing oscillators. The approach there will be to synchronise the corresponding Poincaré sections.

The general problem of the linear coupling of dynamical systems is considered

by Aston and Dellnitz [4]. They investigate systems of the form

$$\dot{\mathbf{x}} = \mathbf{f}(\mathbf{x})$$

where $\mathbf{f} : \mathbb{R}^N \mapsto \mathbb{R}^N$. Coupling r such systems using a linear coupling gives rise to the system

$$\dot{\mathbf{x}}_i = \mathbf{f}(\mathbf{x}_i) + \sum_{j=1}^k \beta_{i,j} \mathbf{x}_j \quad i = 1, \dots, k$$

where $\beta_{i,j}$ are constant $N \times N$ matrices. The system can be written as

$$\dot{\mathbf{x}} = \mathbf{F}(\mathbf{x}) + B\mathbf{x}$$

where $\mathbf{x}^T = \begin{pmatrix} \mathbf{x}_1 & \mathbf{x}_2 & \cdots & \mathbf{x}_k \end{pmatrix}$ and $\mathbf{F}(\mathbf{x})^T = \begin{pmatrix} \mathbf{f}(\mathbf{x}_1) & \mathbf{f}(\mathbf{x}_2) & \cdots & \mathbf{f}(\mathbf{x}_k) \end{pmatrix}$, $\mathbf{F} : \mathbb{R}^{kN} \mapsto \mathbb{R}^{kN}$. B is a $kN \times kN$ block matrix consisting of the $\beta_{i,j}$ blocks. The coupling matrix can be expressed as

$$B = C \otimes D$$

where the $N \times N$ matrix D (non-null) describes the coupling between the oscillators and the $k \times k$ matrix C describes the strength and directions of the coupling. The coupling is assumed not to be directed and so C is symmetric. The theory applies equally well to maps by replacing $\dot{\mathbf{x}}$ and \mathbf{x} with \mathbf{x}_{n+1} and \mathbf{x}_n respectively. Of course, a parameter dependence can also be introduced into the system equations, so that \mathbf{f} not only depends upon \mathbf{x} , but upon some parameter p also.

5.2.1 Iterated Maps

Consider a pair of coupled two-dimensional iterated maps

$$\begin{pmatrix} \mathbf{X}_{n+1} \\ \mathbf{Y}_{n+1} \end{pmatrix} = \begin{pmatrix} \mathbf{f}(\mathbf{X}_n, p^* + \delta p_n) \\ \mathbf{f}(\mathbf{Y}_n, p^* + \delta q_n) \end{pmatrix} + B \begin{pmatrix} \mathbf{X}_n \\ \mathbf{Y}_n \end{pmatrix} \quad (5.2.9)$$

where $\mathbf{f} : \mathbb{R}^2 \times \mathbb{R} \mapsto \mathbb{R}^2$ and B is a 4×4 non-null matrix as defined previously. Writing $B = C \otimes D$ where $C = \begin{pmatrix} -c & c \\ c & -c \end{pmatrix}$ and $D = \begin{pmatrix} d_{11} & d_{12} \\ d_{21} & d_{22} \end{pmatrix}$ we shall be

considering an undirected coupling as before. Each of the d_{ij} are either 0 or 1. Using the transformation of variables

$$\mathbf{x}_n = \frac{\mathbf{X}_n + \mathbf{Y}_n}{2} \quad \text{and} \quad \mathbf{y}_n = \frac{\mathbf{X}_n - \mathbf{Y}_n}{2}$$

in (5.2.9) yields the system

$$\begin{pmatrix} \mathbf{x}_{n+1} \\ \mathbf{y}_{n+1} \end{pmatrix} = \frac{1}{2} \begin{pmatrix} \mathbf{f}(\mathbf{x}_n + \mathbf{y}_n, p^* + \delta p_n) + \mathbf{f}(\mathbf{x}_n - \mathbf{y}_n, p^* + \delta q_n) \\ \mathbf{f}(\mathbf{x}_n + \mathbf{y}_n, p^* + \delta p_n) - \mathbf{f}(\mathbf{x}_n - \mathbf{y}_n, p^* + \delta q_n) \end{pmatrix} + C' \otimes D \begin{pmatrix} \mathbf{x}_n \\ \mathbf{y}_n \end{pmatrix} \quad (5.2.10)$$

where $C' = \begin{pmatrix} 0 & 0 \\ 0 & -2c \end{pmatrix}$.

We shall now investigate the effects of parameter perturbations in (5.2.10) and seek forms for the parameters δp_n and δq_n that result in synchronous behaviour. Synchronisation occurs when $\mathbf{y}_n = 0$ and the dynamics of (5.2.10) collapse onto the now two-dimensional synchronous subspace. In what follows, we shall assume that a fixed point exists within the synchronous subspace and that the fixed point is a saddle when the dynamics are restricted to this subspace.

Perturbing Both Systems Simultaneously

Let us begin by setting $\delta q_n \equiv \delta p_n$, so that both systems are perturbed in an identical manner. Consider a Taylor expansion of (5.2.10) about the fixed point lying within the synchronous subspace,

$$\begin{pmatrix} \delta \mathbf{x}_{n+1} \\ \delta \mathbf{y}_{n+1} \end{pmatrix} = M \begin{pmatrix} \delta \mathbf{x}_n \\ \delta \mathbf{y}_n \end{pmatrix} + \mathbf{w} \delta p_n + \dots$$

where

$$M = \begin{pmatrix} M_w & 0 \\ 0 & M_t \end{pmatrix},$$

and

$$\mathbf{w} = \begin{pmatrix} \mathbf{w}_w \\ \mathbf{0} \end{pmatrix}.$$

This time M_w and M_t are 2×2 matrices and \mathbf{w}_w is a two dimensional derivative vector. Clearly, \mathbf{w} lies parallel to the synchronous subspace. In order to apply the OGY method to stabilise the fixed point, we require that \mathbf{x}^* possesses a two-dimensional linearised stable manifold in X_t . Iterates can be placed on that part of the stable manifold lying in X_t where they will converge to the fixed point in X_w and hence the two maps will synchronise. Let λ_{wu} denote the unstable eigenvalue of the submatrix M_w with corresponding left eigenvector \mathbf{f}_{wu}^T . Then the control formula is simply

$$\delta p_n = -\frac{\mathbf{f}_{wu}^T M_w \delta \mathbf{x}_n}{\mathbf{f}_{wu}^T \mathbf{w}_w}$$

provided that $\mathbf{f}_{wu}^T \mathbf{w}_w \neq 0$. As usual, perturbations are only activated when $|\delta p_n| \leq \delta p_{\max}$ for suitable $\delta p_{\max} > 0$. Once the fixed point has been stabilised, a chaos restoring perturbation can be applied if synchronous chaotic behaviour is required.

Since the transverse dynamics are globally unstable, control may have to be reapplied when the dynamics begin to stray from the vicinity of the synchronous subspace. In practice it may prove more effective to control fixed points which are visited most frequently by iterates of the map. The stabilisation of higher period orbits may also be more effective since control could be initiated when the state of the system falls close to any point of the orbit, thus allowing greater opportunity to apply control.

Clearly this method is a little restrictive in that a fixed point with three contracting directions is necessary in order to apply control. Such points may be uncommon or may not even exist within a particular system. The following two sections give methods that can be used to induce synchronisation without the necessity for such points.

Perturbing One System

Suppose that perturbations are made only to one system so that $\delta q_n \equiv 0$. In that case, the derivative vector \mathbf{w} will no longer lie parallel to the synchronous subspace, and in particular

$$\mathbf{w} = \begin{pmatrix} \mathbf{w}_w \\ -\mathbf{w}_w \end{pmatrix}.$$

The restriction of requiring a three-dimensional stable manifold of a fixed point can now be lifted. Suppose that M_t has eigenvalues λ_{tu} and λ_{ts} where $|\lambda_{ts}| < 1 < |\lambda_{tu}|$ so that the fixed point has a two-dimensional stable manifold. Then it is possible to place an iterate onto the stable manifold of the fixed point in the full four-dimensional space. Let $\begin{pmatrix} \mathbf{0} \\ \mathbf{f}_{tu}^T \end{pmatrix}$ and $\begin{pmatrix} \mathbf{f}_{wu}^T \\ \mathbf{0} \end{pmatrix}$ be the left eigenvectors of M with corresponding eigenvalues λ_{tu} and λ_{wu} respectively. Consider the twice iterated linearised map

$$\begin{pmatrix} \delta \mathbf{x}_{n+2} \\ \delta \mathbf{y}_{n+2} \end{pmatrix} = M^2 \begin{pmatrix} \delta \mathbf{x}_n \\ \delta \mathbf{y}_n \end{pmatrix} + M \mathbf{w} \delta p_n + \mathbf{w} \delta p_{n+1}. \quad (5.2.11)$$

The condition that $\begin{pmatrix} \delta \mathbf{x}_{n+2} \\ \delta \mathbf{y}_{n+2} \end{pmatrix}$ lies on the linearised stable manifold of the fixed point is $\mathbf{f}_{tu}^T \delta \mathbf{y}_{n+2} = \mathbf{f}_{wu}^T \delta \mathbf{x}_{n+2} = 0$. Thus, using (5.2.11) we have

$$\mathbf{f}_{tu}^T M_t^2 \delta \mathbf{y}_n - \mathbf{f}_{tu}^T M_a \mathbf{w}_w \delta p_n - \mathbf{f}_{tu}^T \mathbf{w}_w \delta p_{n+1} = \lambda_{tu}^2 \mathbf{f}_{tu}^T \delta \mathbf{y}_n - \lambda_{tu} \mathbf{f}_{tu}^T \mathbf{w}_w \delta p_n - \mathbf{f}_{tu}^T \mathbf{w}_w \delta p_{n+1} = 0$$

and

$$\begin{aligned} & \mathbf{f}_{wu}^T M_w^2 \delta \mathbf{x}_n + \mathbf{f}_{wu}^T M_w \mathbf{w}_w \delta p_n + \mathbf{f}_{wu}^T \mathbf{w}_w \delta p_{n+1} \\ &= \lambda_{wu}^2 \mathbf{f}_{wu}^T \delta \mathbf{x}_n + \lambda_{wu} \mathbf{f}_{wu}^T \mathbf{w}_w \delta p_n + \mathbf{f}_{wu}^T \mathbf{w}_w \delta p_{n+1} = 0. \end{aligned}$$

Then solving simultaneously for δp_n and δp_{n+1} we obtain

$$\delta p_n = \frac{\lambda_{wu}^2 \mathbf{f}_{tu}^T \mathbf{w}_w \mathbf{f}_{wu}^T \delta \mathbf{y}_n - \lambda_{tu}^2 \mathbf{f}_{wu}^T \mathbf{w}_w \mathbf{f}_{tu}^T \delta \mathbf{x}_n}{(\lambda_{wu} - \lambda_{tu}) \mathbf{f}_{wu}^T \mathbf{w}_w \mathbf{f}_{tu}^T \mathbf{w}_w}$$

and

$$\delta p_{n+1} = \lambda_{tu} \left(\frac{\lambda_{tu} \mathbf{f}_{tu}^T \delta \mathbf{y}_n}{\mathbf{f}_{tu}^T \mathbf{w}} - \delta p_n \right)$$

provided that $\mathbf{f}_{wu}^T \mathbf{w}_w \neq 0$, $\mathbf{f}_{tu}^T \mathbf{w}_w \neq 0$ and $\lambda_{tu} \neq \lambda_{wu}$. Perturbations are only activated when $|\delta p_n| \leq \delta p_{\max}$ and $|\delta p_{n+1}| \leq \delta p_{\max}$.

In order to restore chaotic behaviour, we can apply the stabilisation algorithm until convergence to within a given neighbourhood of the fixed point is attained. Once within that neighbourhood, we aim directly for X_w . Suppose that the application of control results in placing an iterate at $(\mathbf{x}^+, \mathbf{y}^+)$, a distance ϵ from the fixed point. The twice iterated map in the transverse direction is

$$\delta \mathbf{y}_{n+2} = M_t^2 \delta \mathbf{y}_n - M_t \mathbf{w}_w \delta p_n - \mathbf{w}_w \delta p_{n+1}. \quad (5.2.12)$$

To place an iterate within X_w we require that $\delta \mathbf{y}_{n+2} = 0$ which is equivalent to requiring that $\mathbf{f}_{tu}^T \delta \mathbf{y}_{n+2} = 0$ and $\mathbf{f}_{ts}^T \delta \mathbf{y}_{n+2} = 0$. Thus using (5.2.12), and solving for the parameters δp_n and δp_{n+1} , we have

$$\delta p_n = \frac{(\lambda_{tu}^2 \mathbf{f}_{ts}^T \mathbf{w}_w \mathbf{f}_{tu}^T - \lambda_{ts}^2 \mathbf{f}_{tu}^T \mathbf{w}_w \mathbf{f}_{ts}^T) \mathbf{y}^+}{(\lambda_{tu} - \lambda_{ts}) \mathbf{f}_{ts}^T \mathbf{w}_w \mathbf{f}_{tu}^T \mathbf{w}_w}$$

and

$$\delta p_{n+1} = \frac{\lambda_{tu}^2 \mathbf{f}_{tu}^T \mathbf{y}^+ - \lambda_{ts} \mathbf{f}_{tu}^T \mathbf{w}_w \delta p_n}{\mathbf{f}_{tu}^T \mathbf{w}_w}$$

as the parameter perturbations required to produce synchronous chaotic behaviour provided that $\mathbf{f}_{ts}^T \mathbf{w}_w \neq 0$, $\mathbf{f}_{tu}^T \mathbf{w}_w \neq 0$ and $\lambda_{ts} \neq \lambda_{tu}$.

Perturbing Both Systems Independently

Suppose that δp_n and δq_n are both available for independent external adjustment.

Then a first order Taylor expansion of (5.2.10) gives

$$\begin{pmatrix} \delta \mathbf{x}_{n+1} \\ \delta \mathbf{y}_{n+1} \end{pmatrix} = M \begin{pmatrix} \delta \mathbf{x}_n \\ \delta \mathbf{y}_n \end{pmatrix} + \mathbf{w}_p \delta p_n + \mathbf{w}_q \delta q_n \quad (5.2.13)$$

where $\mathbf{w}_p = \begin{pmatrix} \mathbf{f}_p^* \\ \mathbf{f}_p^* \end{pmatrix}$ and $\mathbf{w}_q = \begin{pmatrix} \mathbf{f}_p^* \\ -\mathbf{f}_p^* \end{pmatrix}$ and the Jacobian M is as before. With the availability of two parameters, iterates can be placed on the two-dimensional

stable manifold of the fixed point in one iteration of the map. The criterion for placing an iterate on the stable manifold is $\mathbf{f}_{wu}^T \delta \mathbf{x}_{n+1} = \mathbf{f}_{tu}^T \delta \mathbf{y}_{n+1} = 0$. Thus using (5.2.13) we have

$$\lambda_{tu} \mathbf{f}_{tu}^T \delta \mathbf{y}_n + \mathbf{f}_{tu}^T \mathbf{f}_p^* (\delta p_n - \delta q_n) = 0$$

and

$$\lambda_{wu} \mathbf{f}_{wu}^T \delta \mathbf{x}_n + \mathbf{f}_{wu}^T \mathbf{f}_p^* (\delta p_n + \delta q_n) = 0.$$

This gives the required values of the perturbation parameters as

$$\delta p_n = \frac{\lambda_{wu} \mathbf{f}_{tu}^T \mathbf{f}_p^* \mathbf{f}_{wu}^T \delta \mathbf{x}_n + \lambda_{tu} \mathbf{f}_{wu}^T \mathbf{f}_p^* \mathbf{f}_{tu}^T \delta \mathbf{y}_n}{2 \mathbf{f}_{wu}^T \mathbf{f}_p^* \mathbf{f}_{tu}^T \mathbf{f}_p^*}$$

and

$$\delta q_n = \frac{\lambda_{wu} \mathbf{f}_{tu}^T \mathbf{f}_p^* \mathbf{f}_{wu}^T \delta \mathbf{x}_n - \lambda_{tu} \mathbf{f}_{wu}^T \mathbf{f}_p^* \mathbf{f}_{tu}^T \delta \mathbf{y}_n}{2 \mathbf{f}_{wu}^T \mathbf{f}_p^* \mathbf{f}_{tu}^T \mathbf{f}_p^*}$$

provided the denominators are non-zero and subject to the usual constraints $|\delta p_n| \leq \delta p_{\max}$ and $|\delta q_n| \leq \delta p_{\max}$. A pair of chaos restoring perturbations can be applied by aiming for the synchronous subspace once stabilisation has been achieved in a similar way to that discussed in the previous section.

5.2.2 Continuous Time Systems

The theory discussed in Section 5.2.1 can be adapted for the synchronisation of continuous time systems by considering a Poincaré surface of section. A two-dimensional map can easily be generated from an autonomous three-dimensional continuous time system. Thus one might expect that the results given above would naturally be appropriate for synchronising continuous systems. Synchronising the Poincaré sections would lead to the full systems synchronising. Indeed this turns out to be the case apart from the fact that the Jacobian takes on a slightly different form from that seen previously. Whereas with the coupled maps we had a relationship between the block matrices M_w and M_t in that $M_t = M_w - 2C'$, with a Poincaré section, this relationship will no longer be satisfied.

Let us now consider the synchronisation of a pair of Duffing oscillators. Duffings equation may be written as

$$\frac{d^2 X}{dt^2} + K \frac{dX}{dt} + X^3 - X = A \cos \omega t \quad (5.2.14)$$

The solution of (5.2.14) is sampled once per period of the forcing term, i.e. at $t_n = \frac{2\pi n}{\omega}$ for $n = 1, 2, \dots$, beginning with the initial conditions $\frac{dx}{dt} = x = 0.3$ at time $t = 0$ resulting in a two dimensional Poincaré section. Suppose we have a simple linear coupling of two such oscillators with the coupling defined by

$$C = \begin{pmatrix} -c & c \\ c & -c \end{pmatrix} \quad \text{and} \quad D = \begin{pmatrix} 0 & 0 \\ 0 & 1 \end{pmatrix}.$$

This gives the system

$$\begin{aligned} \dot{X}_1 &= Y_1 \\ \dot{Y}_1 &= -K_1 Y_1 - X_1^3 + X_1 + A \cos \omega t + c(Y_2 - Y_1) \\ \dot{X}_2 &= Y_2 \\ \dot{Y}_2 &= -K_2 Y_2 - X_2^3 + X_2 + A \cos \omega t + c(Y_1 - Y_2). \end{aligned} \quad (5.2.15)$$

Then writing

$$\begin{aligned} x_1 &= \frac{X_1 + X_2}{2}, & x_2 &= \frac{Y_1 + Y_2}{2}, \\ y_1 &= \frac{X_1 - X_2}{2}, & y_2 &= \frac{Y_1 - Y_2}{2} \end{aligned}$$

gives rise to the transformed system

$$\begin{aligned} \dot{x}_1 &= x_2 \\ \dot{x}_2 &= -\frac{1}{2}K_1(x_2 + y_2) - \frac{1}{2}K_2(x_2 - y_2) - (x_1^3 + 3x_1y_1^2) + x_1 + A \cos \omega t \\ \dot{y}_1 &= y_2 \\ \dot{y}_2 &= -\frac{1}{2}K_1(x_2 + y_2) + \frac{1}{2}K_2(x_2 - y_2) - (y_1^3 + 3x_1^2y_1) + y_1 - 2cy_1. \end{aligned} \quad (5.2.16)$$

The coupling only appears in the equation for \dot{y}_2 and the forcing term only in the equation for \dot{x}_2 . If we were to take a Poincaré Section of the orbits of this system, a four dimensional map would result. The addition of the coupling term in the \dot{y}_2 equation will generically have an effect on all of the variables of the corresponding Poincaré Section.

The only significant effect, however, would be on the estimation of the derivative terms in the Taylor expansion, namely M and \mathbf{w} . The Jacobian would still

take on a block diagonal structure since the linearised dynamics in X_w will remain independent of those in X_t . However, two separate regressions are required to obtain M_w and M_t since they are no longer bound by a linear relationship due to the coupling having an effect upon all the variables. We will discuss this in the next section.

5.2.3 Calculating the Required Quantities

If the map is unknown, the calculation of M , \mathbf{w} and \mathbf{x}^* must be done via a regression procedure. In order to obtain reliable results, one has to carry out this regression procedure with some care. Firstly, since the linear dynamics near to the fixed point within X_w decouple with those in X_t , the Jacobian takes on a block diagonal form. Since we are attempting to obtain the Jacobian of a fixed point within the synchronous subspace, the data collected generally consists of small \mathbf{y} values and somewhat larger \mathbf{x} values. In order to avoid an ill-conditioned set of normal equations in the regression (see [37] for example), it is preferable to perform a regression on the \mathbf{x} and \mathbf{y} data separately in order to obtain M_t and M_w . Whilst calculating M_w , an estimate for the \mathbf{x} coordinates of the fixed point can be procured, as per the method described in the Introduction. There is no need to do this when calculating M_t , since the \mathbf{y} coordinates of the fixed point are known to be zero.

One has to be even more careful when calculating \mathbf{w} since different control methods require different approaches. Note that from equation (0.3.14), M is required when calculating \mathbf{w} . If the synchronous subspace is not destroyed under parametric perturbations (i.e. when calculating \mathbf{w}) then calculation of M is as described previously. If it is, for example when perturbing only one system, then M is no longer block diagonal when the parameter p is perturbed from its nominal

value p^* . Thus a separate regression on the \mathbf{x} and \mathbf{y} data is no longer acceptable, as there is no longer an invariant subspace $\mathbf{y} = 0$.

5.3 Numerical Example

We shall consider the example of the coupled Duffing oscillators (5.2.15) with parameter values of $K_1 = K_2 = 0.1$, $A = 3.0$ and $\omega = 0.2$. Using a coupling strength of $c = 0.68$, the oscillators will not readily synchronise. In fact, synchronisation occurs when $c > 0.715$, as can be seen from the bifurcation diagram of Fig. 5.5. Here the Poincaré map (produced by sampling the solution once per period of the forcing term) is pre-iterated 10,000 times to eliminate transient effects. Then an average of the distance (in terms of the two-norm) iterates spend away from the synchronous subspace is calculated over a further 40,000 iterates of the Poincaré map for various values of c . When $c \simeq 0.715$, a blowout bifurcation occurs and the dynamics are no longer confined to the synchronous subspace. As one might expect, this is not a ‘smooth’ bifurcation, since the Lyapunov exponents of the system are likely to be affected in a non-smooth way when c is varied.

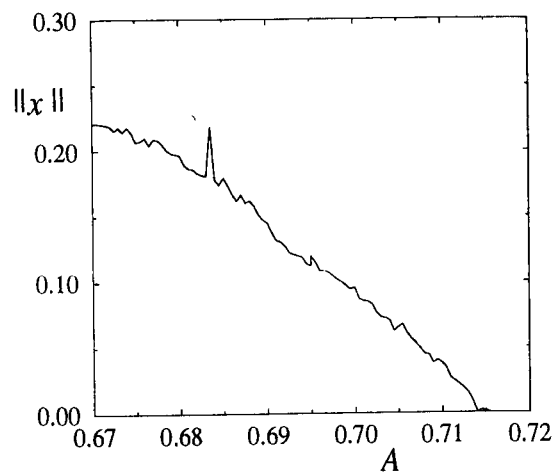


Figure 5.5: The average distance iterates spend from the synchronous subspace for a pair of coupled Duffing oscillators with $K_1 = K_2 = 0.1$, $A = 0.3$ and $\omega = 0.2$.

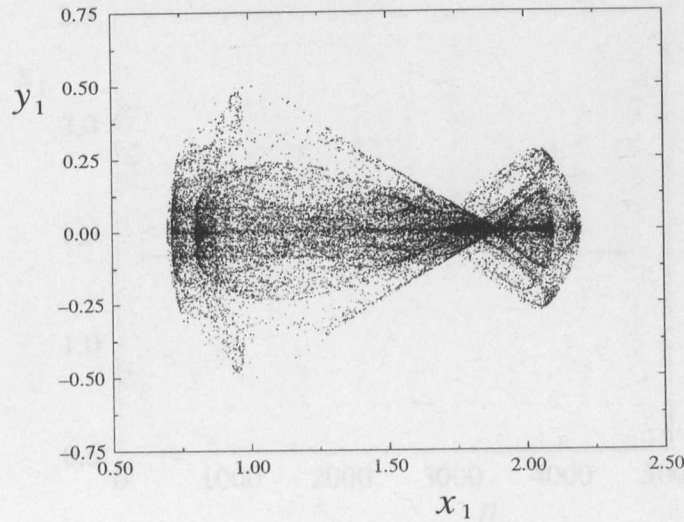


Figure 5.6: Poincaré section of the coupled Duffing system where $K_1 = K_2 = 0.1$, $\gamma = 0.3$, $\omega = 0.2$ and $c = 0.68$.

A projection of the Poincaré section where y_1 is plotted against x_1 is shown in Fig. 5.6. A saddle fixed point is located at $(1.401, 1.668, 0.0, 0.0)$ and at that point

$$M \simeq \begin{pmatrix} -5.250 & 3.947 & 0 & 0 \\ -3.014 & 2.244 & 0 & 0 \\ 0 & 0 & -1.379 & -0.314 \\ 0 & 0 & 1.856 & 0.386 \end{pmatrix} \quad \text{and} \quad \mathbf{w} = \begin{pmatrix} -21.759 \\ -18.748 \\ 0 \\ 0 \end{pmatrix}.$$

The eigenvalues of M within X_w are -2.967 and -0.039 whilst those within X_t are -0.939 and -0.054 . Thus the fixed point has a three-dimensional stable manifold. This permits the use of the OGY method to stabilise the fixed point and hence to induce synchronous behaviour. Convergence will be relatively slow, governed by the largest (in absolute value) of the stable eigenvalues in X_t . Parameter perturbations are activated when iterates fall within a distance of 0.1 of the fixed point. With a randomly chosen initial condition, a short transient is seen before the system is brought under control. Perturbations are applied until iterates lie within a distance of 1×10^{-8} of the fixed point and then turned off, with the exception of a randomly chosen chaos restoring perturbation. The iterates then wander chaotically close to the synchronous subspace for a while before they begin to wander away from the vicinity of the synchronous subspace. Control is then

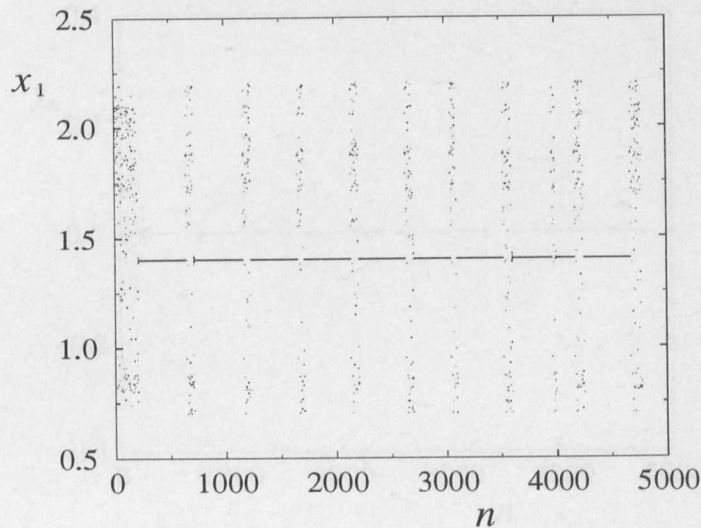


Figure 5.7: A projection of the dynamics in the invariant subspace when a periodic point with two stable directions is stabilised.

reapplied when iterates fall close to the fixed point to maintain the dynamics close to that subspace. However, chaotic behaviour can be lost for quite some time whilst control is reapplied, as can be seen from Fig. 5.7, due to the slow convergence of the method. Fig. 5.8 shows a projection of the dynamics in the transverse direction. The dynamics remain close to the synchronous subspace for over four thousand iterations of the Poincaré map.

Fixed points with a three-dimensional stable manifold prove difficult to find within the coupled Duffing system. Saddles with two stable directions are far more numerous thus suggesting that the perturbation of one system would be more preferable. Now consider (5.2.15) with parameter values of $K_1 = K_2 = 0.5$, $A = 2.5$ and $\omega = 2.6$ together with a coupling constant of 0.13. A projection of the phase portrait is shown in Fig. 5.9. For these parameter values, no low order periodic points lying within the synchronous subspace with a three dimensional stable manifold could be found. Thus the method of the simultaneous perturbation of both systems cannot be implemented on this system. A saddle fixed point was

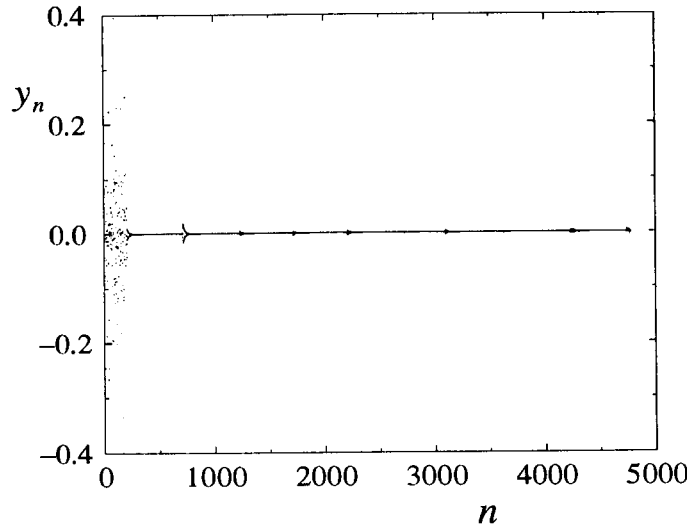


Figure 5.8: A projection of the transverse dynamics when control is repeatedly applied.

located at $(0.174, -0.052, 0, 0)$. The Jacobian at that point is

$$M \simeq \begin{pmatrix} -1.013 & -1.524 & 0 & 0 \\ -0.826 & -1.336 & 0 & 0 \\ 0 & 0 & -0.823 & -0.934 \\ 0 & 0 & -0.627 & -0.743 \end{pmatrix}$$

and $\mathbf{w}^T \simeq (1.562, 1.738, -1.482, -1.565)$. The eigenvalues of the Jacobian are -0.041 and -2.308 , within X_s , and those within X_t are -0.017 and -1.549 . Since the stable eigenvalues are small, convergence to the fixed point will occur relatively rapidly. Again, perturbations are activated when iterates are within a distance of 0.1 of the fixed point. A pair of perturbations are applied to the system when an iterate is placed within a distance of 0.01 of the period two point in order to place the iterate within X_w , thereby restoring chaotic behaviour. Since iterates will never be placed precisely within the synchronous subspace, the state of the system will move away from a synchronous behaviour and when it does so, parameter perturbations are applied at the earliest opportunity in order to retain synchronous behaviour. Fig. 5.10 shows the transverse dynamics and Fig. 5.11 the dynamics within the invariant subspace when parameter perturbations are activated and the system brought to a synchronous behaviour. Thereafter, perturbations are applied

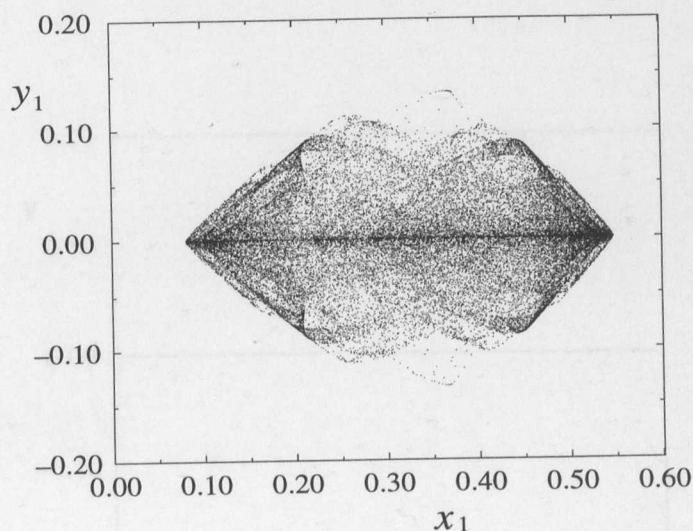


Figure 5.9: Poincaré section of the coupled Duffing system where $K_1 = K_2 = 0.5$, $A = 2.5$, $\omega = 2.6$ and $c = 0.13$.

when the dynamics begin to stray from the vicinity of the synchronous subspace and iterates fall within the vicinity of the period two orbit suitable for control.

5.4 Remarks

The OGY and related methods are specifically developed with the control of chaos in mind. In turn, this control can be used to achieve many desired system behaviours. In this chapter it has been demonstrated that synchronous behaviour in coupled systems can be produced via the application of a control method. By closely looking at the structure of coupled systems when they are in a synchronous or near synchronous state, we can exploit the existence of saddle fixed points within the synchronous subspace in order to produce the desired type of behaviour. The synchronisation of higher dimensional systems should be possible via a control method, though this has yet to be considered. It might also be useful to extend the synchronisation technique for use on multiple coupled systems such as coupled map lattices, for example.

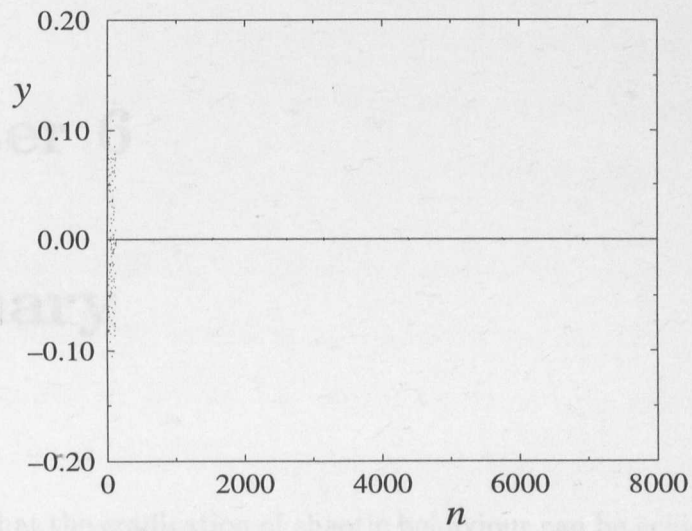


Figure 5.10: Projection of the controlled transverse dynamics for a periodic point possessing two stable directions.

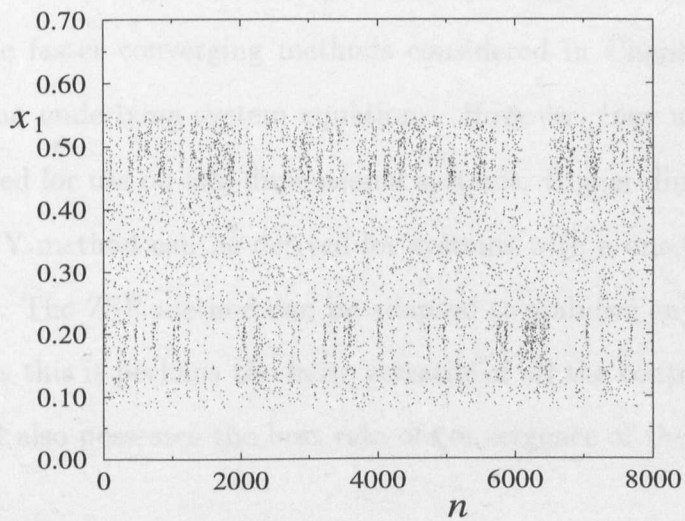


Figure 5.11: The corresponding chaotic dynamics within the invariant subspace.

Chapter 6

Summary

We have seen that the eradication of chaotic behaviour can be achieved in a variety of manners, control being just one option. The OGY method exploits the complicated structure exhibited within chaotic attractors by stabilising just one of the unstable periodic orbits embedded within the attractor. The restriction of allowing only small parameter perturbations consequently means that only diminutive changes are made to the dynamical system. Indeed, if control is achieved and $\delta p_n \rightarrow 0$, then in the long term, the system is unchanged. Moreover, the OGY method and the faster converging methods considered in Chapter 1 require no knowledge of the underlying system equations. However, they are limited since they were derived for use on two-dimensional systems. Higher dimensional analogies for the OGY method can be derived for systems with a one-dimensional unstable manifold. The ZSR method can be adapted to stabilise any type of saddle fixed point, thus this is perhaps the most versatile of all the control methods discussed here and also possesses the best rate of convergence of the one-step linear methods.

We have seen that long transients and noise can be detrimental to the goal of achieving control. To a certain degree, stronger control methods such as the ZSR

**PAGE
NUMBERING
AS
ORIGINAL**

method of Chapter 1 can be used to overcome the problems associated with noise. Though noise is always a problem in chaotic dynamical systems as it destroys any small scale structure seen in such systems, it is encouraging that more robust methods that are better able to cope with noise can be developed. Realistically, one could hope to control systems with only a minimal amount of noise.

The versatility of the control methods discussed here comes from the fact that system equations are not needed in their implementation. Only estimates to local linearised dynamics are needed. In many cases, these estimates do not have to be particularly accurate thus allowing great flexibility in implementation. In Chapter 2 we attempted to quantify just how bad the estimates to system dynamics had to be before control of particular methods broke down. This led to methods of improving estimates to the fixed point and the derivative vector \mathbf{w} without performing a further regression.

The aim of the analysis in Chapter 3 was to extend the region within which control can be effected. Not only does this reduce transient times, but also helps to further combat the effect of system noise. Firstly, control can be achieved more quickly since the measure of the attractor lying within the control region is increased when using the extended basin approach. Secondly, control can be achieved in the presence of larger amplitude noise as compared with the standard OGY or ZSR approach. Hence an extended basin approach addresses both of the problems associated with the control of chaotic dynamical systems.

Targeting in systems is a useful way of rapidly changing the state of a system from one desired behaviour to another. Most notably in Chapter 4, we derived a method to target states in systems where the underlying dynamical equations are not known. This method can also be easily adapted to cope with small amplitude noise. It can thus be used in conjunction with the control methods discussed

herein to reduce transient times quite drastically. This, combined with the use of extended basins, comes a good way to addressing the problems associated with the control of chaotic systems.

The versatility of control methods lends itself to the synchronisation of identical chaotic systems. The existence of saddle fixed points in an invariant (synchronous) subspace permits the use of methods such as the OGY method to stabilise these points. In doing so, synchronous behaviour is simultaneously produced. Thus systems that do not naturally synchronise can be forced into a synchronous behaviour via the application of control.

We have shown here that the application of small parameter perturbations can produce varied and drastic effects in chaotic systems. This is mainly due to the sensitive dependence upon initial conditions exhibited by such systems. It thus turns out that this sensitivity can prove extremely useful, in contradiction to earlier premises that it was a problem. Such sensitivity endows systems with an inbuilt flexibility that would not otherwise be there in a non-chaotic system.

The systems considered in this thesis are essentially of low order. One has to understand these relatively simple systems well before attempting to look at higher dimensional problems. Hopefully a greater understanding has been developed here. Further research into understanding the effects of small parameter perturbations in higher dimensional systems is needed in order to generalise the ideas proposed here. It would be greatly beneficial to be able to control such systems in the efficient way we are able to control low dimensional systems. There may also be many other uses for the application of parametric perturbations to systems than those previously indicated.

Bibliography

- [1] Ashwin, P., Attractors stuck on to invariant subspaces, *Phys. Lett. A* **209** (5), 1995, pp. 338–344.
- [2] Ashwin, P. Buescu, J. and Stewart, I., Bubbling of attractors and synchronisation of chaotic oscillators, *Phys. Lett. A* **193** (2), 1994, pp. 126–139.
- [3] Ashwin, P. Buescu, J. and Stewart, I., From attractor to chaotic saddle: a tale of transverse instability, *Nonlinearity* **9**, 1996, pp. 703–737.
- [4] Aston, P. J. and Dellnitz, M., Symmetry-breaking bifurcations of chaotic attractors, *Int. J. Bif. Chaos* **5** (6), 1995, pp. 1643–1676.
- [5] Auerbach, D., Grebogi, C., Ott, O. and Yorke, J. A., Controlling chaos in high dimensional systems, *Phys. Rev. Lett.* **69** (24), 1992, pp. 3479–3482.
- [6] Azevedo, A. and Rezende, S.M., Controlling chaos in spin wave instabilities, *Phys. Rev. Lett.* **66** (10), 1991, pp. 1342–1345.
- [7] Barreto, E., Kostelich, E. J., Grebogi, C., Ott, E. and Yorke, J. A., Efficient switching between controlled unstable periodic-orbits in higher-dimensional chaotic systems, *Phys. Rev. E* **51** (5), 1995, pp. 4169–4172.
- [8] Braiman, Y. and Goldhirsch, I., Taming chaotic dynamics with weak periodic perturbations, *Phys. Rev. Lett.* **66** (20), 1991, pp. 2545–2548.

- [9] Burden, R. L. and Faires, J. D., *Numerical Analysis, Fifth Edition*, Boston: PWS-Kent.
- [10] Chen, G. and Dong, X., From chaos to order — perspectives and methodologies in controlling chaotic nonlinear dynamical systems, *Int. J. Bif. Chaos*, **3** (6), 1993, pp. 1363–1409.
- [11] Cliffe, K. A. and Spence, A., The calculation of high order singularities in the finite Taylor problem, in *Numerical Methods for Bifurcation Problems*, ed. by Küpper, T., Mittelman, H. D. and Weber, H., Basel; Boston; Stuttgart: Birkhäuser, 1984, pp. 129–144.
- [12] Cuomo, K. M., Oppenheim, A. V. and Strogatz S. H., Synchronization of lorenz-based chaotic circuits with applications to communications *IEEE Trans Circ and Systems II-Analog and Digital Signal Processing*, **40** (10), 1993, pp. 626–633.
- [13] Devaney, R., *An Introduction to Chaotic Dynamical Systems* Reading Mass.; Wokingham: Addison-Wesley, 1989.
- [14] Ding, M. and Kelso, J. A. S., in *Measuring Chaos in the Human Brain*, Singapore: World Scientific, 1991.
- [15] Ditto, W. L., Rauser, S. N. and Spano, M. L., Experimental control of chaos, *Phys. Rev. Lett.* **65** (26), 1990, pp. 3211–3214.
- [16] Doedel, E. J., AUTO: A program for the automatic bifurcation analysis of autonomous systems, *Congressus Numerantium* **30**, 1981, pp. 265–284.
- [17] Dressler, U. and Nitsche, G., Controlling chaos using time delay coordinates, *Phys. Rev. Lett.* **68** (1), 1991, pp. 1–4.
- [18] Dressler, U. and Nitsche, G., Controlling chaotic dynamical systems using time delay coordinates, *Physica D* **58**, 1992, pp. 153–164.

- [19] Eckmann, J. -P. and Ruelle, D., Ergodic theory of strange attractors, *Rev. Mod. Phys.* **57** (3), 1985, pp. 617–656.
- [20] Efron, L., Yeomans, D. K. and Schanzie, A. F., ISEE-3/ICE navigation analysis, *J. astronaut. Sci* **33** (3), 1985, pp. 301–323.
- [21] Farquhar, R., Muhonen, D. and Church, L. C., Trajectories and orbital manouvers for the ISEE-3/ICE comet mission, *J. astronaut. Sci* **33** (3), 1985, pp. 235–254.
- [22] Freeman, W. J., Strange attractors that govern mammalian brain dynamics shown by trajectories of electroencephalographic (EEG) potential, *IEEE Trans. Circuits Syst.* **35**, 1988, pp. 781–783.
- [23] Galias, Z., New method for stabilisation of unstable periodic orbits in chaotic systems, *Int. J. Bif. Chaos* **5** (1), 1995, pp. 281–295.
- [24] Garfinkel, A., Spano, M. L., Ditto, W. L. and Weiss, J. N., Controlling cardiac chaos, *Science* **257**, 1992, pp. 1230–1235.
- [25] Gills, Z., Iwata, C., Roy, R., Schwartz. I. B. and Triandaf, I., Tracking unstable steady-states – extending the stability regime of a multimode laser system *Phys Rev Lett* **69** (22), 1992, pp. 3169–3172.
- [26] Goldberger, A. L., Nonlinear dynamics, fractals and chaos. Applications to cardiac electrophysiology, *Ann. Biomed. Eng.* **18** (2), pp. 195–198, 1990.
- [27] Golubitsky, M. and Schaefer, D. G., *Singularities and Groups in Bifurcation Theory*, New York: Springer Verlag, 1985.
- [28] Grassberger, P. and Procaccia, I., Estimating the Kolmogorov entropy from a chaotic signal, *Phys. Rev. A* **28** (4), 1983, pp. 2591–2593.

- [29] Grassberger, P. and Procaccia, I., Measuring the strangeness of strange attractors, *Physica D* **9** (1-2), 1983, pp. 189-208.
- [30] Grebogi, C., Ott, E. and Yorke, J. A., Critical exponents of chaotic transients in nonlinear dynamical systems, *Physica D* **7**, 1983, pp. 181-200.
- [31] Grebogi, C., Ott, E. and Yorke, J. A., Unstable periodic orbits and the dimension of chaotic attractors, *Phys. Rev. A* **36** (7), 1987, pp. 3522-3524.
- [32] Grebogi, C., Ott, E. and Yorke, J. A., Unstable periodic orbits and the dimensions of multifractal chaotic attractors, *Phys. Rev. A* **37** (5), 1988, pp. 1711-1724.
- [33] Hayes, S., Grebogi, C. and Ott, E., Communicating with chaos, *Phys. Rev. Lett.* **70** (20), 1993, pp. 3031-3034.
- [34] Huberman, B. A. and Lumer, E., Dynamics of adaptive systems, *IEEE Trans. Circ. and Systems*, **37** (4), 1990, pp. 547-550.
- [35] Hunt E. R., Stabilising high period orbits in a chaotic system: the diode resonator, *Phys. Rev. Lett.* **67** (15), 1991, pp. 1953-1955.
- [36] Kocarev, L. M and Stojanovski, T. D., On chaotic synchronization and secure communications, *IEICE Transactions on Fundamentals of Electronics Communications and Computer Sciences* **78** (9), 1995 pp. 1142-1147.
- [37] Kostelich, E. J., Problems in estimating dynamics from data, *Physica D* **58**, 1992, pp. 138-152.
- [38] Kostelich, E. J., Grebogi, C. Ott, E. and Yorke, J. A., Higher dimensional targeting, *Phys. Rev. E* **47** (1), 1993, pp. 305-310.
- [39] Kostelich, E. J. and Yorke, J. A., Noise reduction in dynamical systems, *Phys. Rev. A* **38** (3), 1988, pp. 1649-1652.

- [40] Milnor, J., On the concept of attractor, *Commun. Math. Phys.* **99**, 1985, pp. 177–195.
- [41] Mpitsos, G. J. and Burton, R. M., Convergence and divergence in neural networks: Pprocessing of chaos and biological analogy, *Neural Networks* **5**, 1992, pp. 605–625.
- [42] Muhonen, D. Davis, S. and Dunham, D., Alternative gravity-assist sequences for the ISEE-3 escape trajectory, *J. astronaut. Sci* **33** (3), 1985, pp. 255–273.
- [43] Muhonen, D. and Folta, D. J., Accelerator enhanced trajectory control for the ISEE-3 halo orbit, *J. astronaut. Sci* **33** (3), 1985, pp. 289–300.
- [44] Nicolis, J. S., Chaotic dynamics in biological information processing: A heuristic outline, in *Chaos in Biological Systems*, ed. by Degn, H., Holden, A. V. and Olsen, L. F., New York: Plenum, 1987, pp. 221–232.
- [45] Nusse, H. and Yorke, J. A., Analysis of a procedure for finding numerical trajectories close to chaotic saddle hyperbolic sets, *Ergod. Th. Dynam. Sys.* **11**, 1991, pp. 189–208.
- [46] Ogata, H., *Modern Control Engineering 2E*, New Jersey: Prentice Hall, 1990.
- [47] Ogorzalek, M. J., Remerging bifurcation sequences in an autonomous electric circuit, in *Proc. 1989 Euro. Conf. Circuit Theory Design* (Brighton), 1989, pp. 142–146.
- [48] Ogorzalek, M. J., Ordering and chaos in RC-ladder network with nonlinear feedback, *IEEE Trans. Circuits Syst.* **36**, 1989, pp. 1221–1230.
- [49] Ogorzalek, M..J., Taming chaos – Part I: synchronisation, *IEEE Trans. Circ. Syst. I (Fundamental Theory and Applications)* **40** (10), 1993, pp. 693–699.

- [50] Ogorzalek, M. J., Taming chaos – Part II: Control, *IEEE Trans. Circ. Syst. I (Fundamental Theory and Applications)* **40** (10), 1993, pp. 700–706.
- [51] Ott, E., *Chaos in Dynamical Systems*, Cambridge: Cambridge University Press, 1993.
- [52] Ott, E., Grebogi, C. and Yorke, J. A., unstable periodic orbits and the dimension of chaotic attractors, *Phys. Rev. A* **36** (7), 1987, pp. 3522–3524.
- [53] Ott, E., Grebogi, C. and Yorke, J. A., Controlling chaos, *Phys. Rev. Lett.* **64** (11), 1990, pp. 1196–1199.
- [54] Ott, E. and Sommerer, J. C., Blowout bifurcations: the occurrence of riddled basins and on-off intermittency, *Phys. Lett. A* **188** (1), 1994, pp. 39–47.
- [55] Ottino, J. M., The mixing of fluids, *Sci. Am.* **260** (1), 1989, pp. 40–56.
- [56] Ottino, J. M., Muzzio, F. J., Tjahjadi, M., Franjione, J. G., Jana, S. C. and Kusch, H. A., Chaos, symmetry and self-similarity – exploiting order and disorder in mixing processes, *Science* **257**, 1992, pp. 754–760.
- [57] Packard, N. H., Crutchfield, J. P., Farmer, J. D. and Shaw R. S., Geometry from a time series, *Phys. Rev. Lett.* **45** (9), 1980, pp. 712–716.
- [58] Paskota, M., Mees, A. I. and Teo, K. I., Stabilising higher period orbits, *Int. Jnl. Bif. Chaos* **4** (2), 1994, pp. 457–460.
- [59] Paskota, M., Mees, A. I. and Teo, K. I., On control of chaos: higher period orbits, *Dynamics and Control* **5** (4), 1995, pp. 365–387.
- [60] Pecora, L. M. and Carroll, T. C., Synchronisation in chaotic oscillators, *Phys. Rev. Lett.* **64** (8), 1990, pp. 821–824.
- [61] Peng, B., Petrov, V. and Showalter, K., Controlling chemical chaos, *J. Phys. Chem.* **95**, 1991, pp. 4957–4959.

- [62] Platt, N. Spiegel, E. A. and Tresser, C., On-off intermittency: a mechanism for bursting, *Phys. Rev. Lett.* **70**, 1993, pp. 279–282.
- [63] Rajasekar, S. and Lakshmanan, M., Period-doubling route to chaos for a BVP oscillator with periodic external force, *J. Theoret. Biol.* **133**, 1988, pp. 4473–4477.
- [64] Rajasekar, S. and Lakshmanan, M., Controlling of chaos in bonhoeffer van der pol oscillator, *Int. Jnl. Bif. and Chaos* **2** (1), 1992, pp. 201–204.
- [65] Roy, R., Murphy Jr., T. W., Maier, T. D., Gills, Z and Hunt E. R., Dynamical control of a chaotic laser: experimental stabilisation of a globally coupled system, *Phys. Rev. Lett.* **68** (9), 1992, pp. 1259–1262.
- [66] Roy, R. and Thornburg, K. S., Experimental synchronization of chaotic lasers *Phys. Rev. Lett.* **72** (13), 1994, pp. 2009–2012.
- [67] Romeiras, F. J., Grebogi, C., Ott, E. and Dayawansa, W. P., Controlling chaotic dynamic-systems, *Physica D* **58** (1-4), 1992, pp. 165–192.
- [68] Schiff, S. J., Jerger, K., Duong, D. H., Chang, T., Spano, M. L. and Ditto, W. L., Controlling chaos in the brain, *Nature* (London) **370**, 1994, pp. 615–620.
- [69] Shinbrot, T., Ditto, W., Grebogi, C., Ott, E., Spano, M. and Yorke, J. A., Using sensitive dependence of chaos (the ‘butterfly effect’) to direct trajectories in an experimental chaotic system, *Phys. Rev. Lett.* **68** (19), 1992, pp. 2863–2866.
- [70] Shinbrot, T., Ott, E., Grebogi, C. and Yorke, J. A., Using chaos to direct trajectories to targets, *Phys. Rev. Lett.* **65** (26), 1990, pp. 3215–3218.
- [71] Shinbrot, T., Gregogi, C., Ott, E. and Yorke, J. A., Using chaos to target stationary states of flows, *Phys. Lett. A* **169**, 1992, pp. 349–354.

- [72] Shinbrot, T., Ott, E., Grebogi, C. and Yorke, J. A., Using chaos to direct orbits to targets in systems describable by a one-dimensional map, *Phys. Rev. A* **45**, (6), 1992, pp. 4165–4168.
- [73] Shinbrot, T., Ott, E., Grebogi, C. and Yorke, J. A., Using small perturbations to control chaos, *Nature* **363**, 1993, pp. 411–417.
- [74] Shroff, G. M. and Keller, H. B., Stabilisation of unstable procedures: the recursive projection method, *SIAM J. Num. Anal.* **30**, 1993, p. 1099–1120.
- [75] Singer, J., Wang Y-Z. and Bau, H. H., Controlling a chaotic system, *Phys. Rev. Lett.* **66** (9), 1991, pp. 1123–1125.
- [76] Sinha, S., Rāmaswamy, R. and Subba Rao, J., Adaptive control in nonlinear dynamics, *Physica D* **43**, 1990, pp. 118–128.
- [77] Takens, F., in *Dynamical Systems and Turbulence* ed. by Rand, D. A. and Young L-S., Lecture Notes in Mathematics, Berlin: Springer Verlag, 1981.
- [78] Tang, Y. S., Mees, A. I. and Chua, L. O., Synchronisation and chaos, *IEEE Trans. Circuits* **30**, 1983, pp. 620–626.
- [79] Tél, T., Controlling transient chaos, *J. Phys. A: Math. Gen.* **24**, 1991, pp. 1359–1368.
- [80] Ushio, T., Chaotic synchronization and controlling chaos based on contraction-mappings, *Phys. Lett. A* **198**, (1), 1995, pp. 14–22.
- [81] Voigt, R. G., Orders of convergence for iterative procedures, *SIAM J. Numer. Anal.* **8** (2), 1971, pp. 222–243.
- [82] Wang, W., Bifurcations and chaos of the Bonhoeffer-van der Pol model, *J. Phys.* **A22** pp. 672–632.

- [83] Wilkinson, J. H., *The Algebraic Eigenvalue Problem* New York: Oxford University Press, 1988.
- [84] Woo, M. A., Stevenson, W. G., Moser, D. K., Harper, R. M. and Trealease, R., Patterns of beat-to-beat heart-rate-variability in advanced heart failure, *Am. Heart J.* **123**, 1992, pp. 704–710.
- [85] Xu, D. and Bishop, S. R., Steering dynamical trajectories to target a desired state, *Chaos, Solitons Fractal* **4** (10), 1994, pp. 1931–1942.
- [86] Xu, D. and Bishop, S. R., A contraction-mapping-based control approach to stabilize chaotic systems, *Int. J. Bif. Chaos* **5** (6), 1995, pp. 1741–1748.
- [87] Xu, D. and Bishop, S. R., Self-locating control of chaotic systems using Newton Algorithm, *Phys. Lett. A* **210**, 1996, pp. 273–278.
- [88] Yamada, T. and Fujisaka, H., Stability theory of synchronised motion in coupled oscillator systems II, *Prog. Theor. Phys.* **70**, 1993, pp. 1240–1248.
- [89] Yu, Y. H., Kwak, K. and Lim, T. K., Secure communication through synchronization of 2 chaotic systems with continuous feedback method. *Optical and Quantum Electronics* **27**, (5), 1995, pp. 535–540.
- [90] Yu, Y. H., Kwak, K. and Lim, T. K., Transmission of digital signals via synchronization of chaotic signals, *Journal of the Korean Physical Society* **28**, (1), 1995, pp. 109–112.